

Δr in the Two-Higgs-Doublet Model at full one loop level – and beyond

David López-Val¹ and Joan Solà²

¹ Institut für Theoretische Physik, Universität Heidelberg
Philosophenweg 16, D-69120 Heidelberg, Germany.
e-mail: lopez@thphys.uni-heidelberg.de

² Dept. Estructura i Constituents de la Matèria, Universitat de Barcelona, and Institut de Ciències del Cosmos
Av. Diagonal 647, E-08028 Barcelona, Catalonia, Spain.
e-mail: sola@ecm.ub.edu

Received: date / Revised version: date

Abstract. After the recent discovery of a Higgs-like boson particle at the CERN LHC-collider, it becomes more necessary than ever to prepare ourselves for identifying its standard or non-standard nature. The fundamental parameter Δr , relating the values of the electroweak gauge boson masses and the Fermi constant, is the traditional observable encoding high precision information of the quantum effects. In this work we present a complete quantitative study of Δr in the framework of the general Two-Higgs-Doublet Model (2HDM). While the one-loop analysis of Δr in this model was carried out long ago, in the first part of our work we consistently incorporate the higher order effects that have been computed since then for the SM part of Δr . Within the on-shell scheme, we find typical corrections leading to shifts of $\sim 20-40$ MeV on the W mass, resulting in a better agreement with its experimentally measured value and in a degree no less significant than in the MSSM case. In the second part of our study we devise a set of effective couplings that capture the dominant higher order genuine 2HDM quantum effects on the $\delta\rho$ part of Δr in the limit of large Higgs boson self-interactions. This limit constitutes a telltale property of the general 2HDM which is unmatched by e.g. the MSSM.

1 Introduction

After the recent announcement of the discovery of a Higgs-like boson candidate at the CERN LHC-collider [1–4], we might be closer than ever at unveiling the ultimate architecture of the Electroweak Symmetry Breaking (EWSB) mechanism. Since the idea of spontaneous symmetry breaking (SSB) was incorporated in the structure of the Standard Model (SM), it remained a most pressing and unsettled conundrum in our understanding of High Energy Physics. The ideas pioneered by Higgs [5, 6], Englert and Brout [7], and Guralnik and Kibble [8] crystallized into the present-day paradigm, in which we assume the existence of one fundamental scalar $SU_L(2)$ doublet whose particle remnant after SSB of the gauge symmetry corresponds to the physical Higgs boson of the SM. The quest for an experimental confirmation of this picture has hitherto ranked very high in the wishing list of the experimental efforts first conducted at LEP, and later on at the Tevatron and the LHC. The tantalizing Higgs-event candidates reported by the ATLAS and CMS collaborations during the last year have apparently been confirmed by the recent analysis of the new data [1–4], which have led them to conclude (at a $\sim 5\sigma$ confidence level) that a new particle has been discovered carrying most of the ingredients to be expected from a Higgs-like boson with a mass close to 125 – 126 GeV. The high evidence has been gathered by both the ATLAS and CMS collaborations from the detected signals in the diphoton ($\gamma\gamma$) and weak gauge boson ($Z^0 Z^{0*}$ and WW^*) decay modes [1–4]. If confirmed by subsequent searches and final identification, this could be the greatest achievement of Particle Physics since the discovery of the top quark 17 years ago at Fermilab. And in that case it would represent the most impressive and significant success of Particle Physics ever, since it would constitute the confirmation of the physical reality of the SSB, i.e. of the most subtle and far reaching quantum field theoretical (QFT) structure of the SM. Not surprisingly it would at the same time raise many other problems, even outside the strict domain of Particle Physics, such as for example in cosmology through the certified existence of the huge electroweak vacuum energy. However, we understand that obtaining a consistent overall picture of our world may still take quite some more time.

In the meanwhile, even after that phenomenal discovery, it is difficult to ascertain the nature of the found Higgs-like particle, whether it is the SM Higgs boson or a member of an extended Higgs sector whose remaining constituents are yet to be found, among other possibilities. There is no reason *a priori* for scalar particles not to appear within multiple families, as fermions or gauge bosons do. Both theoretically and phenomenologically there are many motivations for Higgs physics beyond the SM. For example, the Vacuum Expectation Value (VEV) of the Higgs field, $v \simeq 246$ GeV, is well known to be unstable under radiative corrections as ultraviolet (UV) contributions to this VEV must be fine-tuned to insure its stability at low energies. This naturalness puzzle has constituted a primary driving force for the study of extensions

of the Standard Model (SM), and of the Higgs sector in particular. As a simple, yet very attractive example of such an extension, we find the Two-Higgs-Doublet Model (2HDM) [9, 10]. Here, by introducing a second $SU_L(2)$ scalar doublet Φ_2 we meet a compelling phenomenological profile [9]–[13]. On a theoretical basis, there is indeed strong support for a multi-Higgs doublet structure. To begin with, a generic 2HDM furnishes a suitable low-energy description of multifarious EWSB models, such as the Minimal Supersymmetric Standard Model (MSSM) [14], Composite Higgs [15] and Little Higgs models [16]. Despite its simplicity, it may accommodate a plethora of new mechanisms either for spontaneous or explicit \mathcal{CP} -violation as well as a rich vacuum structure [17]. This sets the ground for novel scenarios in which to address a wide variety of unsolved riddles in very different areas, from neutrino mass generation [18] to Electroweak Baryogenesis [19]. In particular, we cannot exclude more exotic possibilities in the framework of Grand Unified Theories, which could also adapt to the properties of the purportedly found Higgs boson [20].

The simplicity and nevertheless very rich potentiality of the 2HDM qualifies as an excellent starting point for a broad class of model-building studies. For instance, if one posits additional discrete symmetries in the scalar potential, the generic 2HDM structure becomes further restricted and may lead to the so-called Inert Doublet Models (IDM) [21], in which at least one of the scalar degrees of freedom becomes a stable WIMP, and thus provides a natural candidate for Dark Matter. These models have been portrayed at length in the literature, both from the perspective of collider observables (cf. e.g. [22]) and astrophysics [23]. A 2HDM structure can also realize a *Higgs portal* scenario [24]. Here, one entertains the possibility of an additional Higgs field in a hidden sector, with no couplings to the SM particles – with the exception of the standard Higgs boson. The Higgs self-interactions thus constitute the only link (the “portal”) between the visible and the hidden domains, with a dramatic impact on the expected Higgs boson widths – and so on their foreseeable collider signatures [25]. Further extensions of the minimal 2HDM include vectorphobic [26] and scale-invariant formulations [27]; or combinations with additional gauge bosons [28], fermionic generations [29] or heavy neutrinos [30], among others.

Numerous studies have scrutinized the prospects for pinning down evidences of 2HDM physics at the LHC, see. e.g. Refs. [31]. In this vein, the potential Higgs-like candidates identified by ATLAS and CMS have already endorsed respective analyses on the corresponding implications for the model [32–34]. This task is certainly not easy, as long as the studies are restricted to direct collider observables. But the situation can improve when counting also on the information conveyed by EW precision analyses. In this respect it is fair to say that the LHC will soon be able to broaden its capabilities from direct discovery to precision physics measurements. This is of foremost importance since it may provide virtual access to possible new degrees of freedom coupled to the SM, and hence to

new – or modified – interaction patterns which can induce departures of the EW precision observables from the pure SM expectations¹.

A most important example of precision observable sensitive to virtual effects from new physics is the mass of the charged EW gauge boson [M_{W^\pm}]. The current uncertainty in its theoretical determination within the SM is estimated to be $\Delta M_W^{\text{th}} \simeq 4$ MeV [40]. On the other hand the present world-average of the experimental measurements renders the value $M_W^{\text{exp}} = 80.385 \pm 0.015$ GeV [41], thus carrying an accuracy at a remarkable level $\lesssim 0.02\%$, i.e. better than 2 parts in ten thousand. But not less remarkable is the fact that the experimental error still gives room for non-negligible non-SM contributions. Indeed, for a SM Higgs boson mass of $M_H = 125$ GeV (cf. the forthcoming discussions in Section 3), the corresponding prediction for the mass of the W-boson renders $M_W^{\text{SM}} = 80.363$ GeV. Despite the current discrepancy $|M_W^{\text{SM}} - M_W^{\text{exp}}| \simeq 20$ MeV lies to within one-sigma level of the experimental measurement, it is as big as five times the estimated theoretical error in the SM. Since the latter falls within the reach of the most accurate planned measurements of the W-mass in the future there is little doubt that a deviation from the SM of that sort should eventually be accessible to observation. This is strongly hinted by the expectation that with the upcoming LHC data the uncertainty on the W-boson mass can be narrowed down to $\Delta M_W^{\text{exp}} \simeq 10$ MeV [42], while a high-luminosity linear collider running in a low-energy mode at the W^+W^- threshold should be able to reduce it even further, namely at the $\Delta M_W^{\text{exp}} \simeq 6$ MeV level or less. The profound impact that a high precision measurement of M_W as well as its correlation to the Z-mass, M_Z , could have both as a precision test of the SM and as a probe of new physics should not be underestimated. This is not new of course, what is new is the fact that we are now much closer than ever to exploit this feature at the LHC. Let us recall that the $M_W - M_Z$ correlation is usually parameterized in terms of the quantity Δr , defined as $G_F/\sqrt{2} = (g^2/8 M_W^2)(1 + \Delta r)$ where G_F is Fermi’s constant and g is the weak $SU(2)$ gauge coupling – see Sec. 2.3 for a more detailed definition in the on-shell scheme. It suffices to say here that g^2 in this scheme is to be replaced by $e^2/s_W^2 \equiv 4\pi\alpha/(1 - M_W^2/M_Z^2)$, where α is the e.m. fine structure constant.

The history of Δr and its companion parameter $\delta\rho$ (i.e. that part of Δr which parametrizes the breaking of custodial symmetry) is extensive and already quite old [35–39]; it has at present more than thirty years. Let us recall that Δr was first computed in the SM context in 1980 by A. Sirlin and coworkers [43, 44], whereas the $\delta\rho$ parameter was defined earlier by Veltmann and collaborators [45–48]. Since then the calculations of these parameters in the SM became improved over the last three decades by important QCD and electroweak higher order effects, hence establishing a powerful relation which allows to perform accurate predictions of the W-boson mass in high-precision

¹ Cf. for instance [35–39] for a comprehensive exposition of the method.

tests of the standard model. Not only so, the calculations were soon extended to physics beyond the SM, mainly from Supersymmetry (SUSY). In this regard, an exhaustive coverage of Δr and $\delta\rho$ within the MSSM is available in the literature. The first preliminary calculations (including only the so-called oblique contributions) within the MSSM were presented some twenty years ago in [49], and then shortly afterwards at full one-loop level in [50] and [51] – see also [52], [53]². Subsequently a lot of refinements which include higher order effects have been performed up to the present days, see the comprehensive studies [56], including dedicated work e.g. on two-loop effects [57] or flavor violation [58].

In spite of the generous literature on the Δr parameter in various contexts of physics beyond the SM – mainly focused on the MSSM, as we have just seen – it is a bit surprising the scarce attention that has been paid to this topic from the viewpoint of the general 2HDM, except for some works presented long ago [59–64]. In these old papers the one-loop calculation of Δr was first presented. However, for a modern numerical prediction of the W -mass within the 2HDM at a level comparable to the SM, a consistent estimate of the higher order effects in the 2HDM is necessary. Filling such gap in the literature is our main task herewith. To that aim we provide a fully-fledged updated analysis of the 2HDM contributions to the parameter Δr by consistently including the known higher order effects from the SM as a part of the full 2HDM contribution in the currently allowed region of the parameter space. From here we obtain a theoretical determination of M_W in the 2HDM at a level comparable to the SM, taking G_F , α and M_Z as experimental inputs. In addition to that, we extend the previous analyses in an attempt to estimate the maximum impact on $\delta\rho$ from the genuine 2HDM higher order corrections associated to the Higgs boson self-interactions, namely in the limit where these self-interactions become very large (bordering the perturbative unitarity bounds). It is known that these scenarios can strongly modify the Higgs/gauge boson couplings, owing to the enhanced quantum effects driven by the Higgs self-interactions. Interestingly, multi-Higgs doublet structures with strongly coupled Higgs particles are well motivated from the theory side, in particular in view of strongly-interacting realizations of the EWSB. Our main focus in this second part of the paper will be to determine whether such augmented Higgs self-couplings may be able to stamp any sensible fingerprint on the EW precision observables under scope.

² Let us point out that to the best of our knowledge the oldest full one-loop MSSM calculation of the electroweak gauge boson masses existing in the literature was provided quite earlier in references [54] and [55]. Although it was presented in a renormalization framework slightly different from the usual one, it was later adapted to the standard on-shell scheme and this resulted in the first full one-loop MSSM calculation of Δr reported in the literature [50], followed shortly after by the similar analysis of [51].

The paper is organized as follows. In Section 2 we succinctly review the 2HDM setup and relevant constraints; we also consider a preview of the EW precision observables to be examined in detail thereafter, and set our definitions and notation. Section 3 is devoted to present the results of our detailed analysis of the predictions for Δr and M_W at full one loop level in the 2HDM in which the known higher order SM effects are consistently incorporated. In Section 4 we explore the maximum size of the genuine 2HDM contributions beyond one-loop level by introducing a set of effective couplings or form factors for the Higgs-gauge boson interactions that enable us to estimate the leading higher order effects on $\delta\rho$ in the large Higgs self-coupling limit. Conclusions and closing remarks are finally delivered in Section 5. Additional analytical details of the calculation are quoted in the Appendix.

2 Theoretical setup

2.1 The general Two-Higgs-Doublet-Model in a nutshell

The 2HDM [9] canonically extends the SM Higgs sector with a second $SU_L(2)$ doublet of weak hypercharge $Y = +1$, so that it contains 4 complex scalar fields. The most general form of a gauge invariant, renormalizable, \mathcal{CP} -conserving potential that one may construct out of two doublets Φ_i ($i = 1, 2$) can be cast as follows

$$\begin{aligned} V(\Phi) = & \lambda_1 \left(\Phi_1^\dagger \Phi_1 - \frac{v_1^2}{2} \right)^2 + \lambda_2 \left(\Phi_2^\dagger \Phi_2 - \frac{v_2^2}{2} \right)^2 \\ & + \lambda_3 \left(\Phi_1^\dagger \Phi_1 - \frac{v_1^2}{2} + \Phi_2^\dagger \Phi_2 - \frac{v_2^2}{2} \right)^2 + \\ & + \lambda_4 \left[(\Phi_1^\dagger \Phi_1)(\Phi_2^\dagger \Phi_2) - (\Phi_1^\dagger \Phi_2)(\Phi_2^\dagger \Phi_1) \right] \\ & + \lambda_5 \left[\Re e(\Phi_1^\dagger \Phi_2) - \frac{v_1 v_2}{2} \right]^2 + \lambda_6 \left[\Im m(\Phi_1^\dagger \Phi_2) \right]^2 \end{aligned} \quad (1)$$

where the self-couplings λ_i may be rewritten in terms of the masses of the physical Higgs particles (M_{h^0} , M_{H^0} , M_{A^0} , M_{H^\pm}); $\tan\beta = v_2/v_1$ (the ratio of the two VEV's $\langle\phi_i^0\rangle$ giving masses to the up- and down-like quarks); the mixing angle α between the two \mathcal{CP} -even states; and, last but not least, the self-coupling λ_5 , which cannot be absorbed in the previous quantities. Therefore we end up with a 7-parameter set: (M_{h^0} , M_{H^0} , M_{A^0} , M_{H^\pm} , $\sin\alpha$, $\tan\beta$, λ_5). An additional discrete symmetry $\Phi_i \rightarrow (-1)^i \Phi_i$ ($i = 1, 2$) – which is exact up to soft-breaking terms of dimension 2 – is canonically assumed as a warrant of Flavor-Changing Neutral-Current (FCNC) suppression³. Alternative constructions with no explicit Z_2 symmetry are described e.g. in [65] and references therein.

As for the Yukawa sector involving the Higgs/quark interactions, the absence of tree-level flavor changing neutral currents (FCNC) leads to two main canonical realizations: 1) type-I 2HDM, in which just one Higgs doublet couples

³ Let us note in passing that such a symmetry is automatically preserved in the MSSM.

to all quarks, whereas the other doublet does not; 2) type-II 2HDM, where one doublet couples only to down-like quarks and the other doublet just to up-like quarks. Other flavor structures are also conceivable and have indeed attracted a growing attention in the recent years [33, 66]. That said, we will see that the evaluation of Δr is barely influenced by the particular form of the Yukawa couplings after we impose the various phenomenological and theoretical restrictions. For a more comprehensive exposition within our notation, including a detailed list of Higgs boson couplings to fermions and bosons, and a discussion of the on-shell renormalization of the unconstrained 2HDM Higgs sector, see Ref. [67].

It is also worth recalling that the Higgs sector of the MSSM corresponds to a particular (constrained) realization of the general two-Higgs doublet structure. The underlying SUSY invariance restricts the form of the potential (1) in a way that has far-reaching phenomenological implications. While in the MSSM the Higgs self-interactions, and thereby also the Higgs mass spectrum, are dictated by the EW gauge couplings, in the 2HDM we no longer have such a dynamical restriction *a priori*. This implies that the triple, as well as the quartic, 2HDM Higgs self-interactions are fundamentally unconstrained – the influence of the latter being comparatively milder. In practice, they can be boosted as much as permitted by perturbative unitarity and vacuum stability, giving rise to trademark signatures which are completely foreign to the MSSM ⁴.

A rather extensive set of bounds restricts the regions of the 2HDM parameter space with potential significance to Phenomenology. Dedicated accounts on these topics can be found e.g. in Refs. [65, 72–74], and in particular also in Section II of Ref. [67], which very closely follows the notation and conventions employed herewith. It goes without saying that the recent identification of a ~ 125 GeV SM-like Higgs boson candidate by ATLAS and CMS raises a number of very significant implications, which we must take into account for realistic studies. A comprehensive updated analysis of the 2HDM parameter space constraints in the light of these novel results is not yet available. Nevertheless, we can rely on model-independent approaches [75] that spell out the general conditions to be satisfied by phenomenologically viable extensions of the standard Higgs sector.

2.2 Phenomenological restrictions

The basic restrictions to be imposed on the 2HDM parameter space can be outlined as follows: i) first, we need to

⁴ In contrast, the core of the enhancement capabilities of the MSSM Lagrangian resides in the richer pattern of Yukawa-like couplings between the Higgs bosons and the quarks, as well as between quarks, squarks and charginos/neutralinos. Their implications for collider and EW precision physics have been object of dedicated attention in the past for a plethora of varied processes, see e.g. [68]. For reviews on the subject, see e.g. [9, 69–71].

account for an upper limit on the loop-induced breaking of the (approximate) $SU(2)$ custodial symmetry, which one can precisely trade through $\delta\rho$, that is, one of the EW precision quantities under scrutiny in this paper. Its numerical value should lie below $|\delta\rho_{2\text{HDM}}| \lesssim \mathcal{O}(10^{-3})$ [41], if we allow up to 3σ deviations from the current best-fit value. In practice, this translates into restrictions on the mass splitting among the different Higgs bosons. Tight requirements ensue also from the radiative B -meson decay $\mathcal{B}(b \rightarrow s\gamma)$ and the $B_d^0 - \bar{B}_d^0$ mixing. Generically, the former process sets a lower bound on the charged Higgs mass of $M_{H^\pm} \gtrsim 300$ GeV for $\tan\beta \geq 1$ [65] in the case of type-II 2HDM, while the latter strongly disfavors the $\tan\beta \lesssim 1$ regions (for both type-I and type-II) and tends to enforce $\tan\beta$ to be roughly above 1.5–2 if the charged Higgs boson is kept relatively light (viz. $M_{H^\pm} \sim 100 - 150$ GeV, which is allowed for type-I models). Perturbative unitarity, as well as vacuum stability, impose as well very severe limitations. These translate into wide excluded areas across the $\tan\beta - \lambda_5$ plane. Unitarity places an upper limit of $|\lambda_5| \sim \mathcal{O}(10)$ for Higgs boson masses of few hundred GeV, and vacuum stability excludes the $\lambda_5 > 0$ region up to a very narrow band [67]. In short, in order to satisfy these restrictions we are confined to regions where $\tan\beta \simeq 1$ and $|\lambda_5| \simeq 5 - 10$ ($\lambda_5 < 0$) for maximum Higgs self-coupling enhancements. Additionally, any chosen Higgs mass spectrum ought to satisfy all the current limits from direct searches at LEP, Tevatron and LHC.

In practice, all these constraints are systematically included in our calculation by combining the latest version of the public codes 2HDMCALC-1.1 [76], SUPERISO-3.1 [73] and HIGGSBOUNDS-2.2 [77], hand in hand with several alternative and/or complementary in-house routines. Last but not least, we must deal with the phenomenological implications of the 5σ Higgs boson candidate recently unveiled at the LHC [1–4]. A most natural choice when embedding the current experimental picture into a concrete realization of the 2HDM is to identify the lightest neutral CP-even Higgs boson [h^0] with the ~ 125 GeV resonance. Under this assumption, the Higgs couplings to the gauge bosons become severely constrained, as the current data show no substantial departure with respect to the SM-like decay patterns. Consequently, we are left with very tight restrictions on the trigonometric factors $\tan\beta$ and $\sin\alpha$. It follows that we are essentially restrained to the so-called *decoupling* regime $\alpha = \beta - \pi/2$ (with $\alpha < 0$) or, equivalently, $\alpha = \beta + \pi/2$ (with $\alpha > 0$) – both cases featuring $g_{h^0VV}^2 \sim \sin^2(\beta - \alpha) \simeq 1$. If we instead identify the ~ 125 GeV resonance with the heavy neutral CP-even Higgs boson [H^0], the observed decay rates into gauge bosons enforce $\alpha \simeq \beta$ since then the corresponding coupling to gauge bosons yields $g_{H^0VV}^2 \sim \cos^2(\beta - \alpha) \simeq 1$. Independently, these conditions also disallow some specific choices of $\sin\alpha$. For instance, $\sin\alpha \simeq 0$ cannot be realized within a type-II 2HDM. In the decoupling limit, this choice would imply $\beta \simeq -\pi/2$, thus rendering an unduly enhanced $h^0 b\bar{b}$ interaction, $\sim |\sin\alpha/\cos\beta| \gg 1$, incompatible with the fermionic modes of the current Higgs candidate observations. Conversely, for $\alpha = \beta$ the choice

$\alpha \simeq 0$ would spoil the perturbativity of the Higgs/top Yukawa coupling. By similar arguments, one can prove that $\alpha \simeq \pi/2$ is not permitted within type-II realizations of the 2HDM. Notice, however, that $\alpha = 0$ (resp. $\alpha = \pi/2$), namely the fermiophobic limit for H^0 (resp. h^0) is still viable within type-I models owing to the different Higgs/quark interaction strengths $\sim \sin \alpha / \sin \beta$ (resp. $\sim \cos \alpha / \sin \beta$).

Further constraints can be imposed over $\tan \beta$. For example, we must comply with the aforementioned B-physics limits on both the low ($\tan \beta \lesssim 1$) and high ($\tan \beta \gtrsim 10$) $\tan \beta$ -ranges. Also the non-observation of enhanced $h \rightarrow b\bar{b}$ decays rules out the large $\tan \beta$ regimes of a type-II 2HDM. In addition, recent studies (cf. Ref. [75]) have concluded that the fermionic decay signatures of the ~ 125 GeV Higgs-like resonance, even if fully compatible with a SM-like Yukawa sector, exhibit a mild statistical tilt towards slightly enhanced (resp. suppressed) Higgs/top (resp. Higgs/bottom) couplings. These scenarios would be realized for $\tan \beta \lesssim 1$. Let us recall, finally, that moderate choices of $\tan \beta \sim \mathcal{O}(1)$ are particularly appealing and well motivated for the purposes of our analysis, as they enable to maximize the triple (3H) self-couplings through a relatively large value of the parameter $|\lambda_5|$ – therefore by resorting only to the intrinsic structures of the 2HDM Higgs potential.

A variety of processes can probe the potentially enhanced 2HDM Higgs boson self-interactions, and have indeed been intensively analysed over the past years – mostly in the context of linear colliders. Available studies include, on the one hand, the tree-level production of triple Higgs-boson final states [78]; the double Higgs-strahlung channels hhZ^0 [79]; and the inclusive Higgs-pair production via gauge-boson fusion [80]. In the same vein, also the $\gamma\gamma$ mode of a linac has been explored, in particular the loop-induced production of a single neutral Higgs boson [81] and of a Higgs boson pair [82]. In all the above mentioned cases, promising signatures were pinpointed, which could be revealing of an unconstrained multi-Higgs doublet pattern. Similar genuine 2HDM effects might also manifest as large radiative corrections to a number of Higgs production channels. One loop studies of pairwise Higgs boson final states were first addressed for charged Higgs bosons $e^+e^- \rightarrow H^+H^-$ [83] and later on carried to completion by a full-fledged study of the neutral Higgs sector $e^+e^- \rightarrow h^0A^0, H^0A^0$, including also the more traditional Higgs-strahlung events $e^+e^- \rightarrow h^0Z^0, H^0Z^0$ [67, 84]. All these studies reveal the possible existence of: i) sizable Higgs boson production rates, typically in the ballpark of $\mathcal{O}(10 - 100)$ fb for $\sqrt{s} = 500$ GeV at a future linear collider; ii) sizable quantum effects, up to $\delta \sim \pm 50\%$; and iii) a very characteristic complementarity of the dominant Higgs production modes at different center-of-mass energies – these properties being correlated, once more, to significant Higgs boson self-interactions, and so to a non-supersymmetric multi-Higgs doublet structure.

2.3 Electroweak Precision Quantities from muon decay

The relation between the EW gauge boson masses (M_W, M_Z) in terms of the Fermi constant (G_F) and the fine structure constant (α) is an essential tool for testing the quantum effects within the SM as well as to place bounds on its manifold conceivable extensions. Such relation can be derived in terms of the muon lifetime τ_μ , whose decay rate is precisely defined by the Fermi constant, G_F , via the expression [35–38]

$$\tau_\mu^{-1} = \frac{G_F^2 m_\mu^5}{192\pi^3} F\left(\frac{m_e^2}{m_\mu^2}\right) \left(1 + \frac{3}{5} \frac{m_\mu^2}{M_W^2}\right) (1 + \Delta_{\text{QED}}), \quad (2)$$

where $F(x) = 1 - 8x - 12x^2 \ln x + 8x^3 - x^4$. Following the standard conventions in the literature, the above defining equation for G_F includes the expression Δ_{QED} , i.e., the finite QED contribution obtained within the Fermi Model, which is known up to two-loop order. Calculating the muon lifetime within the SM at the quantum level and comparing with (2) yields the relation:

$$M_W^2 \left(1 - \frac{M_W^2}{M_Z^2}\right) = \frac{\pi\alpha}{\sqrt{2}G_F} (1 + \Delta r), \quad (3)$$

in which

$$\Delta r \equiv \frac{\hat{\Sigma}_W(0)}{M_W^2} + \Delta r^{[\text{vert,box}]}. \quad (4)$$

These expressions define the quantity Δr in a precise way. Let us notice that $\hat{\Sigma}_W(k^2)$ is the on-shell renormalized self-energy of the W-boson; it accounts for the universal (“oblique”) part of the electroweak radiative corrections to the muon decay. The non-universal (i.e. process-dependent) corrections – which stem from the vertex and box contributions to the muon decay – are encoded in the subleading term $\Delta r^{[\text{vert,box}]}$. The explicit expression for Δr consists of a combination of loop diagrams and counter terms. For the renormalization details, see e.g. [35–38]. Here we will only remind the reader of some basic facts which can be helpful to contextualize our 2HDM computation. To start with, let us write down the explicit structure of Δr after renormalization:

$$\begin{aligned} \Delta r = & \Pi_\gamma(0) - \frac{c_W^2}{s_W^2} \left(\frac{\delta M_Z^2}{M_Z^2} - \frac{\delta M_W^2}{M_W^2} \right) + \frac{\Sigma_W(0) - \delta M_W^2}{M_W^2} \\ & + 2 \frac{c_W}{s_W} \frac{\Sigma_{\gamma Z}(0)}{M_Z^2} + \Delta r^{[\text{vert,box}]}. \end{aligned} \quad (5)$$

We stress that this expression is finite because its original definition (4) depends only on the on-shell renormalized self-energy of the W-boson and the remainder $\Delta r^{[\text{vert,box}]}$ – which is also finite by virtue of the Ward-Takahashi identities of the EW theory. In the previous expression $\Pi_\gamma(k^2) \equiv \partial \Sigma_\gamma(k^2) / \partial k^2$ is the photon vacuum polarization, and we are using the notation $s_W^2 \equiv 1 - M_W^2 / M_Z^2$, and

$c_W^2 \equiv M_W^2/M_Z^2$. Furthermore, since the renormalization is in the on-shell scheme the weak gauge boson mass counter terms read: $\delta M_V^2 = \Re e \Sigma_V(M_V^2)$, with $V = W^\pm, Z^0$. By $\Sigma_V(q^2) \equiv \Sigma_V^T(q^2)$ we will hereafter denote the (transverse parts of the) unrenormalized gauge boson self-energies, which we conventionally extract from the corresponding vacuum polarization tensor:

$$\Pi_V^{\mu\nu}(q^2) = g^{\mu\nu} \Sigma_V^T(q^2) + q^\mu q^\nu \Sigma_V^L(q^2). \quad (6)$$

After introducing the renormalized photon vacuum polarization $\hat{\Pi}_\gamma(k^2) = \Pi_\gamma(k^2) - \Pi_\gamma(0)$ it is convenient to consider its fermionic part at $k^2 = M_Z^2$, i.e. $\hat{\Pi}_\gamma^{\text{ferm}}(M_Z^2)$. As it is well-known, for the light fermions (quarks and leptons, excluding the top quark) the quantity

$$\Delta\alpha = -\Re e \hat{\Pi}_\gamma^{\text{ferm}}(M_Z^2) \quad (7)$$

is independent of the EW part of the SM and goes into a finite renormalization of the QED fine structure constant: $\alpha \rightarrow \alpha(1 + \Delta\alpha)$. This can be resummed according to the renormalization group to provide the value of α at the scale of the Z -mass: $\alpha(M_Z^2) = \alpha/(1 - \Delta\alpha) \simeq 1/128$ which is $\sim 6\%$ larger than its low energy (Thomson limit) value $\alpha \simeq 1/137$. Such resummation takes into account all the leading logarithms of the type $\alpha^n \ln^n(M_Z/m_l)$ which enter the renormalization of α from the leptonic sector $l = e, \mu, \tau$. The light quark contribution, instead, is computed more precisely via a dispersion relation from the experimental hadronic data collected in low energy e^+e^- scattering. Finally, the top quark gives a negligible (decoupling-like, $\sim M_Z^2/m_t^2$) contribution to (7).

Let us now emphasize one more type of effect which will have special relevance for our analysis of the 2HDM contributions to Δr . We are referring to the so-called $\delta\rho$ parameter [45–48]. By inspecting (5), such contribution comes from the term

$$\frac{\delta M_Z^2}{M_Z^2} - \frac{\delta M_W^2}{M_W^2} \rightarrow \frac{\Sigma_Z(0)}{M_Z^2} - \frac{\Sigma_W(0)}{M_W^2} \equiv \delta\rho. \quad (8)$$

The $\delta\rho$ effect is finite for the matter fermions of the SM (for each doublet separately) and provides a very important (non-decoupling) contribution when large mass splitting are present within a given fermion family. Its main source comes of course from the top quark, or to be more precise from the top quark and bottom quark doublet. Even though the bottom quark contributes a negligible finite correction, it is essential to make the quark doublet contribution to $\delta\rho$ perfectly finite on its own. The corresponding impact on Δr is not just $-(c_W^2/s_W^2)\delta\rho^t$ as it actually contains additional terms (encapsulated in the so-called “remainder” Δr_{rem} , cf. Eq. (11) and the discussion further down) which are numerically significant:

$$\begin{aligned} \Delta r^{\text{top}} = & -\frac{\sqrt{2}G_F M_W^2}{16\pi^2} \left[3 \frac{c_W^2}{s_W^2} \frac{m_t^2}{M_W^2} + 2 \left(\frac{c_W^2}{s_W^2} - \frac{1}{3} \right) \ln \frac{m_t^2}{M_W^2} \right. \\ & \left. + \frac{4}{3} \ln c_W^2 + \frac{c_W^2}{s_W^2} - \frac{7}{9} \right]. \end{aligned} \quad (9)$$

For a more physical interpretation, let us remind the reader that $\delta\rho$ stands for the possible deviations of the value of the Fermi constant in neutral current processes (G_F^{NC}) – typically induced by neutrino interactions – from the corresponding Fermi constant in charged processes (G_F) such as muon decay. Both in the SM and in the 2HDM we have

$$\rho \equiv \frac{G_F^{NC}}{G_F} = \frac{M_W^2}{M_Z^2 c_W^2} = 1 + \delta\rho. \quad (10)$$

In the absence of weak hypercharge interaction $g' \rightarrow 0$ ($M_Z \rightarrow M_W$, $s_W^2 \rightarrow 0$) we would have $\delta\rho = 0$ and the Fermi constants in both kind of processes would have equal strength. In the SM, as well as in the 2HDM, the only sources of $\delta\rho$ come from quantum effects. These deviations are bound to satisfy $|\delta\rho| \lesssim \mathcal{O}(10^{-3})$ [41]. But this bound still gives a substantial margin for physics beyond the SM, as we shall see.

After clarifying the physical significance of the main terms in (5) we may now write down the general structure of Δr in the following traditional form [35–38]:

$$\Delta r = \Delta\alpha - \frac{c_W^2}{s_W^2} \delta\rho + \Delta r_{\text{rem}} = \Delta\alpha + \Delta r^{[\delta\rho]} + \Delta r_{\text{rem}}, \quad (11)$$

where the leading contributions $\Delta\alpha$ and $\delta\rho$ have been defined above, and we have introduced $\Delta r^{[\delta\rho]} \equiv -(c_W^2/s_W^2)\delta\rho$. The so-called “remainder” piece Δr_{rem} collects the remaining effects, which in the SM entail subleading (which should *not* be taken as synonymous of negligible) contributions⁵. For example, while $\Delta\alpha \simeq 0.06$, we have $\Delta r_{\text{rem}} \simeq 0.01$. For comparison, the top quark gives a contribution to (11) of around $\Delta r^{[\delta\rho](\text{top})} \simeq -0.03$, or -0.04 if using the more accurate expression (9). Although Δr_{rem} is smaller than the leading terms, all these contributions are in fact quite significant and produce an important numerical shift of the W -mass, lowering its zeroth order value ($M_W^{\text{tree}} \simeq 80.9$ GeV) by about 0.8%, i.e. more than 0.6 GeV. In particular, Δr_{rem} renders a non-negligible contribution of ~ 160 MeV to that total (see below). The additional effects that might come from physics beyond the SM are generally much smaller but the current high precision electroweak physics has improved sufficiently so as to make possible to detect shifts of Δr at the level of less than one per mil. At the end of the next subsection we shall further illustrate this point.

At present, the calculation of Δr in the SM is complete up to two loops [57, 86–89] and includes also the leading three and four-loop pieces [90]. As we have mentioned, the bulk of the contributions to Δr is linked to the renormalization of the fine structure constant. The next-to-leading source of contributions comes from $\delta\rho$, which in the SM is finite and dominated by the aforementioned $\mathcal{O}(m_t^2)$ terms from the top-quark loops. In the SM, however, the Higgs contribution to $\delta\rho$ is neither gauge invariant nor UV-finite, only the sum with the remaining bosonic part is finite and

⁵ Beyond the one-loop order, resummations of the leading one-loop contributions have been derived, see e.g. [85], and further contrasted to exact higher-order calculations [57, 86].

gauge independent. Numerically it is not very relevant as compared to the fermionic contribution to Δr and it increases only logarithmically with the Higgs boson mass. This feature reflects the so-called screening behavior of the SM Higgs boson [46], a property which does not generally hold in extended Higgs sectors, such as e.g. in the unconstrained 2HDM. As this issue is important for our considerations, let us quote explicitly the leading effect of the SM Higgs boson in the limit of large M_H . The contribution being not finite, it also depends on the choice of the dimensional regularization scale μ used in the 't Hooft-Veltman procedure (see the Appendix for more details). The splitting of terms in the full bosonic contribution is therefore somewhat arbitrary, but it is natural to set that scale at the EW value $\mu = M_W$. Finally, omitting the UV-divergent pieces that cancel with the remaining bosonic terms one arrives at

$$\delta\rho^H \simeq -\frac{3\sqrt{2}G_F M_W^2 s_W^2}{16\pi^2 c_W^2} \left\{ \ln \frac{M_H^2}{M_W^2} - \frac{5}{6} \right\} + \dots \quad (12)$$

and

$$\Delta r^H \simeq \frac{\sqrt{2}G_F M_W^2}{16\pi^2} \frac{11}{3} \left\{ \ln \frac{M_H^2}{M_W^2} - \frac{5}{6} \right\} + \dots \quad (13)$$

As we can see the dominant term $-(c_W^2/s_W^2)\delta\rho^H$ is corrected by non-negligible additional finite parts from Δr_{rem} having the same structure. The neat contribution of Eq. (13) is subsumed again in Δr_{rem} . Let us indeed note that numerically Δr^H is rather irrelevant as compared to, say, the top quark contribution and the overall Δr value ($\simeq 0.04$) within the SM; we find $\Delta r^H = \mathcal{O}(10^{-3})$ for $M_H = 200$ GeV and $\mathcal{O}(10^{-4})$ for $M_H = 125$ GeV. In spite of this meager yield, we wish to stress that the particular $\delta\rho^H$ piece in Eq. (12) is formally very important because it measures the departure from custodial symmetry, which is that global $SU(2)$ symmetry of the Higgs SM Lagrangian which is only broken by the weak hypercharge interaction $g' = g s_W/c_W$. The ‘‘custodial symmetry limit’’ thus corresponds to $g' \rightarrow 0$ ($M_Z \rightarrow M_W$, $s_W^2 \rightarrow 0$). In this limit the gauge bosons W^\pm and Z form a degenerate triplet of a global $SU(2)$ symmetry [48]. We may indeed confirm from the above expressions that the $\delta\rho^H$ effect takes on the form $\delta\rho^H \simeq (-3g'^2/16\pi^2) \ln M_H^2/M_W^2$ and hence it vanishes in the custodial symmetry limit $g'^2 \equiv g^2 s_W^2/c_W^2 \rightarrow 0$, as expected.

A natural question to ask is if there are significant (non-screening) custodial-breaking effects from Higgs physics beyond the SM, i.e. effects not just growing logarithmically with the Higgs boson masses but as powers of the masses themselves. Let us briefly mention the Higgs sector of the MSSM. Although it features a type II 2HDM, it is of a constrained nature owing to the underlying SUSY [9,71]. As a result there are no conspicuous non-screening effects and in this sense the situation does not differ significantly from the SM. There are notwithstanding alternative contributions to $\delta\rho$ in the MSSM which come from the stop/sbottom-mediated quantum effects and are potentially very relevant [11, 12, 49, 50, 52]. Finally, in the

general (unconstrained) 2HDM case the situation changes dramatically. The corresponding Δr contributions have been studied at one-loop [9, 59–64, 91] and have been employed in studies of combined 2HDM parameter space constraints [74]. However, to the best of our knowledge no systematic study that includes a complete account of Δr and M_W at a level comparable to the SM is available in the literature. We believe that in the light of the present experimental situation at the LHC it is highly desirable to cover this gap.

2.4 Δr , $\delta\rho$ and M_W in the 2HDM. Preliminary considerations

It is important to emphasize that Δr is sensitive (through quantum effects) to all the SM parameters (couplings and masses) as well as to the full list of parameters involved in any possible extension of the SM. In the relevant 2HDM case under consideration,

$$\Delta r = \Delta r(e, M_W, M_Z, m_f; M_i, \sin \alpha, \tan \beta, \lambda_5), \quad (14)$$

where m_f and $M_i = M_{h^0}, M_{H^0}, M_{A^0}, M_{H^\pm}$ are respectively the masses of the fermions and of the Higgs bosons. Finally, λ_5 is the parameter of the Higgs potential (1) which cannot be related to a physical mass of the 2HDM. That parameter enters Δr beyond one loop only, but we will see that it can still furnish significant quantum effects. In general these effects will enter Eq. (11) through $\delta\rho$ and Δr_{rem} . Let us clarify that the contributions to Δr from the charged Higgs bosons come only from $\delta\rho$ and Δr_{rem} in Eq. (2.11), as the charged Higgs boson loop effects on $\Delta\alpha$ leave no finite yield to the photon self-energy nor to the photon-Z mixing, as expected from gauge invariance.

In this work we revisit the calculation of $\delta\rho$ in the general 2HDM and shall consider also the full one-loop calculation of Δr , i.e. the complete quantity (5) or (11). As advertised, we will subsequently include higher order effects on $\delta\rho$ related with the self-couplings of the Higgs bosons, mainly governed by the λ_5 parameter. These effects are non-existent in the MSSM owing to the pure gauge nature of the self-couplings in the tree-level MSSM Higgs potential [9]. The dominant part of the 2HDM corrections comes from the one-loop contributions to $\delta\rho$ mediated by the various 2HDM Higgs bosons [59–64]. As in the case of the SM we perform the calculation in the Feynman gauge (cf. Fig. 1) and we call the result $\delta\rho_{2\text{HDM}}$. It amounts to a compact and finite expression whose full form is provided in the Appendix, see Eq. (52). Here we single out only the portion of $\delta\rho_{2\text{HDM}}$ that depends on the Higgs boson mass splittings, which may be called $\delta\rho_{2\text{HDM}}^*$.

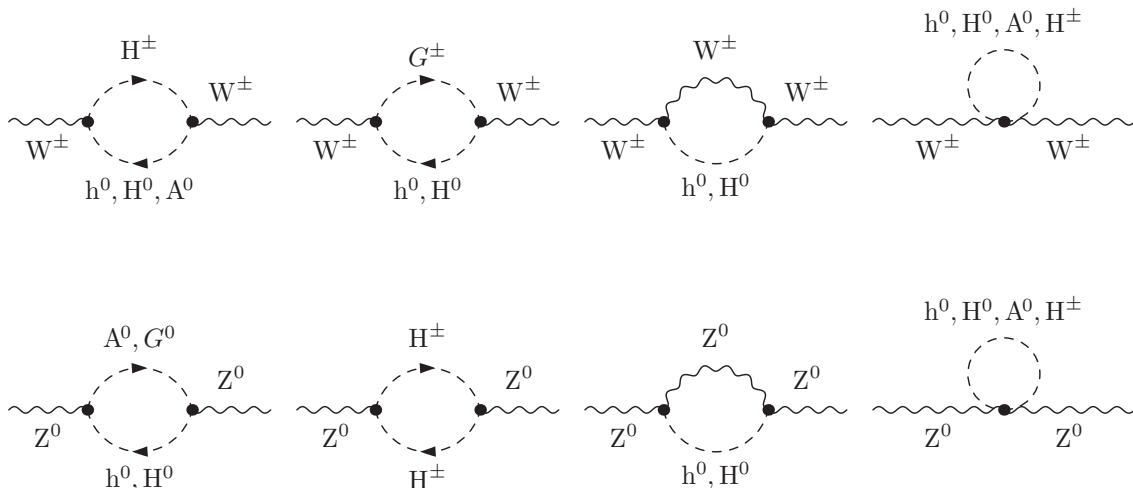


Fig. 1. Set of Feynman diagrams describing the pure 2HDM one-loop contributions to the W^\pm and Z^0 self-energies in the 't Hooft-Feynman gauge. All Feynman diagrams in this paper have been generated by means of FEYNARTS [92].

It can be cast as follows:

$$\begin{aligned} \delta\rho_{2\text{HDM}}^* &= \frac{-G_F}{8\sqrt{2}\pi^2} \left\{ M_{H^\pm}^2 \left[1 - \frac{M_{A^0}^2}{M_{H^\pm}^2 - M_{A^0}^2} \ln \frac{M_{H^\pm}^2}{M_{A^0}^2} \right] \right. \\ &+ \cos^2(\beta - \alpha) M_{h^0}^2 \left[\frac{M_{A^0}^2}{M_{A^0}^2 - M_{h^0}^2} \ln \frac{M_{A^0}^2}{M_{h^0}^2} \right. \\ &- \left. \frac{M_{H^\pm}^2}{M_{H^\pm}^2 - M_{h^0}^2} \ln \frac{M_{H^\pm}^2}{M_{h^0}^2} \right] \\ &+ \sin^2(\beta - \alpha) M_{H^0}^2 \left[\frac{M_{A^0}^2}{M_{A^0}^2 - M_{H^0}^2} \ln \frac{M_{A^0}^2}{M_{H^0}^2} \right. \\ &- \left. \frac{M_{H^\pm}^2}{M_{H^\pm}^2 - M_{H^0}^2} \ln \frac{M_{H^\pm}^2}{M_{H^0}^2} \right] \left. \right\}. \end{aligned} \quad (15)$$

From this expression, and by comparison with Eq. (12), it is clear that in the unconstrained 2HDM the contributions to $\delta\rho$ do not follow the screening theorem of the SM Higgs boson. Indeed, from the quadratic dependence on the various Higgs boson masses outside the logarithms and the fact that arbitrary mass splittings between these Higgs bosons are possible, one can expect that they could easily overshoot the limits on $\delta\rho$ within the 2HDM, namely the 3σ bound $|\delta\rho| \lesssim \mathcal{O}(10^{-3})$ obtained from the EW precision fits [41]. However, we note that if $M_{A^0} \rightarrow M_{H^\pm}$ then $\delta\rho_{2\text{HDM}}^* \rightarrow 0$. Hence if the mass splitting between M_{A^0} and M_{H^\pm} is not too large $\delta\rho_{2\text{HDM}}^*$ can be kept under control. This is also true for the full $\delta\rho_{2\text{HDM}}$, if at the same time we are not far away from the decoupling limit $\beta - \alpha = \pi/2$ – where the lightest CP-even state h^0 behaves SM-like (see the Appendix for more details).

Let us now provide some discussion on the general strategy we will follow to estimate Δr in the unconstrained 2HDM at one-loop and beyond. More detailed considerations will be made in sections 3 and 4, together with the full quantitative analysis of course. Let us assume that Δr in the defining equation (3) collects the expanded form of

the various contributions up to some order of perturbation theory where they are presumably computed. We can split $\Delta r_{2\text{HDM}}$ as follows:

$$\Delta r_{2\text{HDM}} = \Delta r_{2\text{HDM}}^{[1](\text{RG})} + \Delta r_{2\text{HDM}}^{(\text{boson})} + \Delta r_{2\text{HDM}}^{(\text{Ykw-QCD})}. \quad (16)$$

This structure assumes that all of the leading (and some next-to-leading) effects on Δr are involved within the 2HDM. There are various subclasses of contributions in it that will deserve some particular comment. At the moment we note that the first term on the *r.h.s.* of (16) is the improved one-loop correction, namely the total one-loop correction plus the renormalization group (RG) resummed effects of $\Delta\alpha$, which go into the important renormalization of the e.m. fine structure constant; the second term represents the complete 2-loop bosonic part, i.e. the pure EW contribution from gauge bosons, Goldstone bosons and Higgs bosons in all possible combinations; finally, the third term stands for the joint Yukawa-coupling and QCD effects to $\mathcal{O}(\alpha_{\text{ew}}\alpha_s)$, including some resummed contributions. Needless to say all these terms are rather complicated but many of them exhibit a structure very similar to that of the known SM case [93]. There is, however, a subset of higher order diagrams in the 2HDM which provide a qualitatively (and maybe also a quantitatively important) new contribution. The latter is buried in the $\Delta r_{2\text{HDM}}^{(\text{boson})}$ piece of (16) and for this reason it proves convenient to further split it as follows:

$$\Delta r_{2\text{HDM}}^{(\text{boson})} = \Delta r_{2\text{HDM}}^{(\text{boson}^*)} + \Delta r_{2\text{HDM}}^{(\lambda_5)}. \quad (17)$$

The special term here is the second one on the *r.h.s.* of the above expression, $\Delta r_{2\text{HDM}}^{(\lambda_5)}$, whose relevance will soon become apparent. We start by explaining the meaning of the first term, $\Delta r_{2\text{HDM}}^{(\text{boson}^*)}$, which stands in part for the ordinary gauge boson and Goldstone boson diagrams up to two loops. Among these diagrams we find the 2-loop pieces contributing to $\mathcal{O}(\alpha_{\text{ew}}^2)$, which are not particularly important from the numerical point of view, although

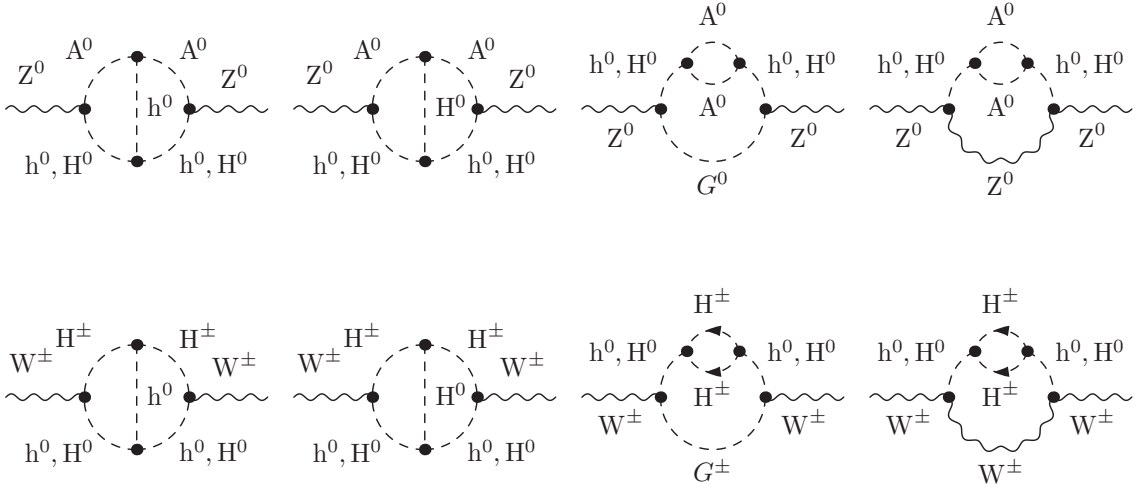


Fig. 2. Small representative sample of Feynman diagrams describing potentially significant 2-loop contributions to Δr within the 2HDM in the 't Hooft-Feynman gauge. The complete list of 2-loop diagrams of this class is much more extensive, and the full list of 2-loop graphs of all classes within the 2HDM (involving bosons and/or fermions) is huge. However, even with the displayed sample we can immediately appreciate the presence of trilinear Higgs boson couplings and their foreseeable significance. In the limit of large λ_5 , all these diagrams are of $\mathcal{O}(\alpha_{\text{ew}}\lambda_5^2)$ and constitute the (gauge invariant and finite) leading 2-loop contribution to Δr .

they are technically difficult to account for. Furthermore, $\Delta r_{\text{2HDM}}^{(\text{boson}^*)}$ involves as well the 2-loop diagrams containing Higgs bosons only, and also those graphs mixing gauge bosons and Higgs bosons; the corresponding amplitudes can be constructed from the one-loop diagrams of Fig. 1 after bridging them with another Higgs internal line (propagator). See Fig. 2 for a detailed sample of 2-loop diagrams constructed in this way. The graphs in that figure are proportional to the product of two trilinear Higgs boson self-couplings, λ_{hhh} , and two ordinary gauge couplings, i.e. the corresponding amplitudes are of $\mathcal{O}(\alpha_{\text{ew}}\lambda_{hhh}^2)$. There are other 2-loop graphs constructed from the aforementioned bridging procedure that involve three gauge couplings and one trilinear Higgs coupling, and hence are of $\mathcal{O}(g^3\lambda_{hhh})$. We can expect that some of these amplitudes, especially those involving two trilinear couplings, can be very important from the quantitative point of view because they can be enhanced even after preserving all known bounds on perturbative unitarity, custodial symmetry and vacuum stability. For a full display of the detailed structure of the trilinear λ_{hhh} self-couplings in the general 2HDM, see e.g. Ref. [67] and particularly its Table II. As an example we quote the coupling of three light \mathcal{CP} -even Higgs bosons:

$$\lambda_{h^0h^0h^0} = -\frac{3ie}{2M_W \sin 2\beta s_W} \left[M_{h^0}^2 (2 \cos(\alpha + \beta) + \sin 2\alpha \sin(\beta - \alpha)) - \cos(\alpha + \beta) \cos^2(\beta - \alpha) \frac{4\lambda_5 M_W^2 s_W^2}{e^2} \right]. \quad (18)$$

These structures can be enhanced, in principle, on three accounts: a) assuming large $\tan \beta \gg 1$ or small $\tan \beta \ll 1$, b) arranging for large mass splittings among the Higgs

bosons, and c) pushing the value of the characteristic λ_5 coupling (the free parameter which is unrelated to the Higgs masses) in the general 2HDM Higgs potential (1). Of these possibilities in practice only the last one can be used efficiently after enforcing all the known theoretical and phenomenological bounds described in Sec. 2.2.

Let us note in passing that the λ_{HHH}^2 contributions are not present in the SM at two loops (with H standing here for the SM Higgs boson) because the Z gauge boson cannot couple to HH in the SM and hence a double HHH vertex at two loops cannot be formed by the aforesaid bridging procedure. Only a single vertex HHH can appear at this order in the SM, thus giving rise to $\mathcal{O}(g^3\lambda_{\text{HHH}})$ effects from the Higgs self-interaction in combination with pure gauge boson couplings. But even in this case λ_{HHH} has no special enhancing property in the SM beyond the artificial raising of the Higgs boson mass, recall that $\lambda_{\text{HHH}} \sim g M_H^2/M_W$. For a relatively light Higgs boson, $M_H \gtrsim 125$ GeV the trilinear Higgs boson self-coupling in the SM is not very substantial. In particular, for a 125 GeV Higgs boson we get

$$\lambda_{\text{HHH}}(M_H = 125 \text{ GeV}) = \frac{3e M_H^2}{2 M_W s_W^2} \Big|_{M_H=125 \text{ GeV}} \simeq 188 \text{ GeV}. \quad (19)$$

To certify the meager impact of this numerical result notice that it yields roughly 2% of the Lee-Quick-Thacker bound only [94], which as we know represents the upper bound on the SM Higgs boson self-interaction ensuing from the perturbative unitarity requirement. In view of the fact that the presumed value of M_H is not much higher than M_W , the mentioned effects can be finally sub-

sumed into the fairly irrelevant pure bosonic $\mathcal{O}(\alpha_{\text{ew}}^2)$ part in the context of the SM [87, 88].

Let us now finally address the precise origin of the $\Delta r_{\text{2HDM}}^{(\lambda_5)}$ piece in Eq. (17). Such contribution appears when we select the λ_5^2 tag in the subclass of all the 2-loop diagrams containing two trilinear Higgs boson couplings. Recall that the λ_5 term is present in *all* the Higgs boson self-couplings λ_{hhh} . (At this important point we refer the reader once more to Table II of Ref. [67]). In particular, see the last term on the *r.h.s.* of Eq. (18). It was precisely in order to single out such peculiar and potentially relevant 2-loop λ_5^2 proportional effects in the 2HDM computation of Δr that we have introduced the last term of Eq. (17). In our approach we wish to explicitly detach this term from the 2-loop bosonic contribution. To do this in practice we split all the trilinear Higgs boson self couplings of the 2HDM as follows

$$\lambda_{hhh} = \lambda_{hhh}^* + c_h \lambda_5 \quad (20)$$

where λ_{hhh}^* is the part of the coupling not containing λ_5 , and c_h is a coefficient which can be easily identified from the list of trilinear couplings in Table II of [67]. Let us now emphasize that the part of the amplitudes which is proportional to λ_{hhh}^* is also incorporated into $\Delta r_{\text{2HDM}}^{(\text{boson}^*)}$ in Eq. (17) whereas the part which carries the λ_5^2 coefficient constitutes our precise definition of the piece $\Delta r_{\text{2HDM}}^{(\lambda_5)}$ in (17). In practice, we shall project the $\mathcal{O}(\lambda_5^2)$ component for all of the Higgs boson self-couplings from the generic structure (20), meaning that, at the end of the day, $\Delta r_{\text{2HDM}}^{(\lambda_5)}$ will be built upon $\mathcal{O}(\lambda_5^2)$ contributions; these are the leading (Higgs-mediated) effects beyond 1-loop in the limit of large Higgs boson self-interactions – for more details cf. our discussion in Section 4.

It is important to note that the formal separation of these two kind of contributions is well-defined, and it is worthwhile performing it because the λ_5 -part is potentially the most significant one from the phenomenological point of view. We note that even though both λ_{hhh}^* and c_h could also be enhanced at large or small $\tan\beta$, we do not contemplate this possibility in view of the perturbative unitarity constraints, alongside with the phenomenological preference for $\tan\beta \sim \mathcal{O}(1)$ values. As a result the entire enhancing power of the λ_{hhh} couplings resides exclusively in the λ_5 part, whereas the rest of the 2-loop bosonic yield is subsumed in $\Delta r_{\text{2HDM}}^{(\text{boson}^*)}$, altogether quite irrelevant in practice as in the SM case [87, 88].

The sum of all the 2-loop bosonic diagrams involved in the computation of $\Delta r_{\text{2HDM}}^{(\text{boson}^*)}$ in Eq. (17) is well defined, namely it is gauge invariant and finite. Most important for our purposes is that we have checked explicitly the gauge invariance and finiteness of the overall piece $\Delta r_{\text{2HDM}}^{(\lambda_5)}$ constructed from the above procedure (see section 4 for more details). This feature could be expected because the λ_5 coupling does not appear at one-loop in this calculation and hence that parameter is not needed for the renormalization of the gauge boson sector at 2-loops. As a result we can exploit this property and test the impact of the 2-loop diagrams involving one or two trilinear Higgs boson cou-

plings in the limit of large λ_5 . Of course “large” means, in this context, as large as allowed by the perturbative unitarity constraints, which are well-known in the literature [95] – see e.g. [67] for a discussion in our framework – and we certainly impose them as an important restriction in our calculation.

From the above considerations the following strategy is suggested to obtain an estimate of Δr in the general 2HDM, Eq. (16). First, the pure bosonic higher order effects independent of λ_5 are as tiny in the 2HDM as they are in the SM; and, second, in the regime $\tan\beta = \mathcal{O}(1)$ we should have in the 2HDM at most the same Yukawa couplings and QCD loop corrections as in the SM [57, 86–88]. We express these two statements in a nutshell as follows:

$$\Delta r_{\text{2HDM}}^{(\text{boson}^*)} \simeq \Delta r_{\text{SM}}^{(\text{boson})}; \quad \Delta r_{\text{2HDM}}^{(\text{Ykw-QCD})} \simeq \Delta r_{\text{SM}}^{(\text{Ykw-QCD})}, \quad (21)$$

where the bosonic part $\Delta r_{\text{2HDM}}^{(\text{boson}^*)}$ is of course the same quantity that we defined in (17) through the splitting (20), and $\Delta r_{\text{SM}}^{(\text{boson})}$ is the known 2-loop bosonic SM result. A practical recipe for a reasonable estimate of Δr in the general 2HDM should therefore be the following effective quantity:

$$\Delta r_{\text{2HDM}}^{\text{eff}} \simeq \Delta r_{\text{SM}} + \delta(\Delta r_{\text{2HDM}}^{[1]}) + \Delta r_{\text{2HDM}}^{(\lambda_5)}. \quad (22)$$

The first term, Δr_{SM} , stands for the full set of SM contributions known to date, hence with a structure completely similar to (16) but within the SM:

$$\Delta r_{\text{SM}} = \Delta r_{\text{SM}}^{[1](\text{RG})} + \Delta r_{\text{SM}}^{(\text{boson})} + \Delta r_{\text{SM}}^{(\text{Ykw-QCD})}. \quad (23)$$

It includes different sorts of one loop and higher order effects of various kinds [57, 86–88], as well as some resummed contributions – the most important one being of course the one affecting $\Delta\alpha$. The overall SM contribution (23) is usually accounted for quantitatively with the help of a detailed numerical parameterization (see section 3 for details). The second term on the *r.h.s.* of (22), i.e. $\delta(\Delta r_{\text{2HDM}}^{[1]})$, denotes the one-loop shift to Δr driven by the “genuine” (viz. non-standard) 2HDM contributions to the weak gauge boson self-energies. To determine this characteristic one-loop effect from the 2HDM we compute the set of (Higgs-mediated, $h = h^0, H^0, A^0, H^\pm$) Feynman diagrams displayed in Fig. 1, whose result we indicate by $\Delta r_{\text{2HDM}}^{h[1]}$, and then we subtract from it the one-loop contribution from the SM Higgs boson, H , denoted as $\Delta r_{\text{SM}}^{H[1]}$, namely

$$\delta(\Delta r_{\text{2HDM}}^{[1]}) = \Delta r_{\text{2HDM}}^{h[1]} - \Delta r_{\text{SM}}^{H[1]}, \quad (24)$$

see more details in the next section and in the Appendix.

Notice that the one-loop SM Higgs contribution is included as part of the first term on the *r.h.s.* of (22), as we have mentioned, and it would be counted twice if it was not subtracted. Therefore, upon subtracting (22) from (16) and using equations (17) and (21) and (23), we find

$$\begin{aligned} \Delta r_{\text{2HDM}} - \Delta r_{\text{2HDM}}^{\text{eff}} &\simeq \Delta r_{\text{2HDM}}^{[1](\text{RG})} \\ &\quad - \Delta r_{\text{SM}}^{[1](\text{RG})} - \delta(\Delta r_{\text{2HDM}}^{[1]}) = 0. \end{aligned} \quad (25)$$

From now on we will identify $\Delta r_{2\text{HDM}}$ with $\Delta r_{2\text{HDM}}^{\text{eff}}$ and will use Eq.(22) for the practical evaluation of the 2HDM contribution.

To summarize, Eq. (22) encodes a reasonable estimate of the basic contributions to Δr in the 2HDM under the presently known perturbative unitarity constraints. It actually provides an upper bound to the maximum value that this parameter can reach in the general 2HDM after taking into account the leading one loop and higher order effects. This is because on the one hand it includes the corresponding SM value, and on the other it collects the two distinctive sources of potentially relevant 2HDM effects: i) the genuine 1-loop Higgs boson effects beyond the SM, i.e. $\delta(\Delta r_{2\text{HDM}}^{[1]})$; ii) and the leading 2-loop $\mathcal{O}(\alpha_{\text{ew}}\lambda_5^2)$ effects triggered by the enhanced Higgs boson self-couplings in the limit of large λ_5 , i.e. $\Delta r_{2\text{HDM}}^{(\lambda_5)}$. The latter furnishes, at large λ_5 , the biggest source of enhancement at higher order within the known perturbative unitarity limits.

Let us finish this section with a simple estimate of the numerical impact on the W-mass which follows from a generic shift of the parameter Δr , which we denote $\delta(\Delta r)$. In the case under consideration that shift may essentially receive the following two genuine 2HDM contributions at one loop and beyond, which we have discussed above:

$$\delta(\Delta r) = \delta(\Delta r_{2\text{HDM}}^{[1]}) + \Delta r_{2\text{HDM}}^{(\lambda_5)}. \quad (26)$$

From Eq. (3) and taking the values for M_Z and G_F as experimental inputs our evaluation of Δr can be translated into a theoretical prediction for the W-boson mass, $[M_W^{\text{th}}]$, and further confronted to $[M_W^{\text{exp}}]$. For this we need to solve the equation

$$M_W^2 = \frac{1}{2} M_Z^2 \left[1 + \sqrt{1 - \frac{4\pi\alpha}{\sqrt{2}G_F M_Z^2} [1 + \Delta r(M_W^2)]} \right]. \quad (27)$$

For $\Delta r = 0$ one obtains the tree-level value $M_W^{\text{tree}} \simeq 80.94$ GeV. But as mentioned above the full theoretical result is smaller because quantum effects imply $\Delta r > 0$. Mind that since Δr itself depends on M_W , Eq. (27) must be worked out iteratively if one aims at a precise prediction. To within first order, Eq. (27) implies that a shift $\delta(\Delta r)$ in Δr translates into a small shift in the W mass given by

$$\delta M_W \simeq -\frac{1}{2} M_W \frac{s_W^2}{c_W^2 - s_W^2} \delta(\Delta r), \quad (28)$$

with $s_W^2 \simeq 0.22$. In the SM, as well as in all known promising extensions of it, the quantum effects yield Δr of order few percent and positive, hence improving the agreement of the theoretical prediction with experiment. For example, in the SM $\Delta r \simeq 0.04 > 0$. The physically measured value of M_W ($M_W^{\text{exp}} \simeq 80.38$ GeV) is in fact smaller than the tree-level value by about 0.8%, i.e. some ~ 600 MeV smaller. This is consistent with (28) since Δr itself is small and so that equation applies reasonably well to the entire Δr value.

Furthermore, Eq. (28) tells us that even a tiny departure $|\delta(\Delta r)| \simeq 10^{-3}$ from physics beyond the SM induces a shift of $|\delta M_W| \simeq 16$ MeV in the W mass. This shift is significant since it is very close to the present experimental error in the W mass ($M_W^{\text{exp}} = 80.385 \pm 0.015$ GeV). It follows that further improvement (lessening) of that error will enable us to discriminate very subtle quantum effects, perhaps digging already into physics beyond the SM. Interestingly enough we have indicated above that the 2HDM can induce genuine shifts of this order from the two sources indicated on the *r.h.s.* of (26). In the next sections we shall confirm by explicit numerical analysis that the maximum size of the total shift $\delta(\Delta r)$ can be of order of a few times 10^{-3} and displace the value of M_W a few tens of MeV – it can reach as high as $\delta M_W \simeq 35 - 40$ MeV in the optimal cases presented here. This potentially significant thrust from the genuine quantum effects in the 2HDM sector can bring the theoretical prediction on M_W larger and hence offers a better agreement with the experiment than the SM prediction, which persistently tends to stay too low as compared to the experimental value.

3 2HDM prediction for Δr and M_W at full one loop. Detailed analysis

Hereafter we carry out a dedicated numerical analysis of the different EW precision quantities under scope. To start with, we focus on the pure one-loop evaluation of Δr , and thereby of M_W^{th} , in the framework of the general 2HDM. Let us emphasize from the beginning the meaning of our denomination “full one loop” in the title of this section. It refers to the order of perturbation theory at which we compute the genuine 2HDM effects on the complete Δr quantity, and not just to $\delta\rho$. However, we incorporate in our calculation of Δr (following the procedure explained in Sec. 2.4) the known higher order effects within the SM because otherwise it would be meaningless to compare with the experiment in view of the current high precision of the measurements. It is only in a second stage (cf. Sec. 4), where we perform a closer look to the genuine higher order effects emerging from the 2HDM. Specifically we will focus there on the parameter $\delta\rho$ within the 2HDM and examine the Higgs boson self-interactions and their enhancement capabilities therein. In doing this we will find appropriate to resort to a Born-improved Lagrangian approach for a first reliable approximation to these higher order genuine 2HDM contributions.

The unrenormalized gauge boson self-energies $\Sigma_V^{2\text{HDM}}$, as defined in Eq. (6), reunite all the information we need to compute the 2HDM contributions to Δr at one-loop: in our notational setup (cf. Eqs. (22) and (24)) the full one-loop payoff is denoted

$$\Delta r_{2\text{HDM}}^{[1]} = \Delta r_{\text{SM}}^{[1]} + \delta(\Delta r_{2\text{HDM}}^{[1]}), \quad (29)$$

where the second term on the *r.h.s.* of this equation was defined in (24).

| | M_{h^0} [GeV] | M_{H^0} [GeV] | M_{A^0} [GeV] | M_{H^\pm} [GeV] |
|-------------------------------------|-----------------|-----------------|-----------------|-------------------|
| Set I | 125 | 135 | 200 | 220 |
| Set II | 115 | 125 | 200 | 220 |
| Set III | 125 | 200 | 200 | 215 |
| Set IV | 125 | 300 | 300 | 310 |
| Set V | 125 | 126 | 260 | 300 |
| Set VI | 125 | 126 | 210 | 250 |
| Set VII | 125 | 126 | 160 | 200 |
| Set VIII | 125 | 126 | 110 | 150 |
| Set V' ($M_{H^\pm} < M_{A^0}$) | 125 | 126 | 300 | 260 |
| Set VI' ($M_{H^\pm} < M_{A^0}$) | 125 | 126 | 250 | 210 |
| Set VII' ($M_{H^\pm} < M_{A^0}$) | 125 | 126 | 200 | 160 |
| Set VIII' ($M_{H^\pm} < M_{A^0}$) | 125 | 126 | 150 | 110 |

Table 1. Higgs boson mass sets employed throughout our computation. Owing to the phenomenological restrictions from B -physics observables (cf. Sec. 2.2), Sets IV and V can be realized both for type I and type II 2HDM's, while the other scenarios would mostly be suitable for a type-I 2HDM setup only. Sets III and IV have been specially devised to reproduce the characteristic mass splittings of the MSSM Higgs bosons (see the text for details). Sets V-VIII feature two neutral, \mathcal{CP} -even states with masses around 125 GeV, and a constant splitting $[|M_{A^0} - M_{H^\pm}| = 40 \text{ GeV}]$ between their \mathcal{CP} -odd [A^0] and charged [H^\pm] companions. The two possible mass hierarchies, which we refer to as *direct* [$M_{H^\pm} > M_{A^0}$] and *inverted* [$M_{H^\pm} < M_{A^0}$] (sets marked with a prime) are analysed separately.

The various contributions are described by the collection of Feynman diagrams we display in Fig. 1. For a consistent calculation of $\Delta r_{\text{2HDM}}^{[1]}$ we must remove the existing overlap between the one-loop 2HDM effects carried by the light, neutral \mathcal{CP} -even Higgs boson (h^0), and those driven by the SM Higgs boson (H_{SM}) – which are contained in Δr_{SM} itself. This is achieved, in practice, by subtracting from $\Sigma_{W,Z}$ the h^0 -mediated one-loop diagrams in the SM-like limit $\beta = \alpha - \pi/2$. What remains is the genuine 2HDM effect encoded in $\delta(\Delta r_{\text{2HDM}}^{[1]})$. Explicit details are given in the Appendix. We perform our calculation in the 't Hooft-Feynman gauge and regularize the UV divergences using standard dimensional regularization [96], which is both Lorentz and gauge invariant. Analytical manipulations at this stage are carried out with the help of the packages FEYNARTS and FORMCALC [92, 97].

Let us now describe our numerical setup. As for the Higgs boson spectra, we define several mass choices (cf. Table 1) that span over representative parameter space regions, featuring in particular the ~ 125 GeV Higgs-like resonance spotlighted by ATLAS and CMS and in agreement with all the phenomenological limits discussed in Sec. 2.2. Set I describes a light, neutral \mathcal{CP} -even Higgs state [h^0] taking on the role of the 5σ Higgs-candidate. It is thus preferably studied in the decoupling regime $\alpha = \beta - \pi/2$. Notice that this scenario can in principle accommodate a fermiophobic heavy Higgs [H^0] ($\alpha = 0$) for type-I 2HDM's. Further on we shall entertain this possibility, even though a more accurate determination of the fermionic decay modes of the putative Higgs boson candidate might soon rule out this region of the parameter space. In Set II we still assume a type-I 2HDM, but in contrast to the previous set we identify the ~ 125 GeV resonance with the heavier neutral \mathcal{CP} -even Higgs field [H^0], whereas the lighter h^0 is assumed to have escaped detection so far. In this latter case we are of course setting

$\alpha \simeq \beta$, since this choice insures SM-like couplings of H^0 to gauge bosons, and suppressed couplings for h^0 . Sets I and II, thus, represent alternative choices of Higgs bosons, featuring a non-constrained mass spectrum and in full compliance with the current experimental picture. Sets III and IV, on the other hand, consider (as in the case of Set I) $\alpha = \beta - \pi/2$ and are devised to mimic typical MSSM-like spectra – say a relatively light h^0 state playing the role of the ~ 125 GeV resonance along with heavier (almost mass-degenerate) companions [H^0, A^0, H^\pm]. The mass spectrum in both sets has been numerically derived from selected MSSM parameter configurations with the help of FEYNHIGGS [98]. In particular, Set III corresponds to the so-called *decoupling regime* of the MSSM for *maximal mixing* (cf. the recent analysis of Ref. [99]). Similarly, we define Set IV, now with heavier masses for the scalar companions of the light Higgs boson, as a realization of the *decoupling regime* for *typical mixing* [99] of the MSSM. Let us note that owing to the phenomenological restrictions described in Sec. 2.2, Set III must correspond to type-I while Set IV can be either type-I or type-II 2HDM.

Finally, we construct the two groups V-VIII and V'-VIII' of mass sets. In both groups we have two neutral, \mathcal{CP} -even, almost mass-degenerate Higgs bosons with $M_h \sim 125$ GeV while the charged Higgs and the neutral \mathcal{CP} -odd states are typically heavier and with a constant mass splitting $|M_{A^0} - M_{H^\pm}| = 40$ GeV. The distinction of the two groups lies in the two possible mass hierarchies: $M_{H^\pm} > M_{A^0}$ (which we conventionally dub *direct* hierarchy); and $M_{H^\pm} < M_{A^0}$ (*inverted* hierarchy – corresponding to the sets V'-VIII' marked with a prime). The fact that the two \mathcal{CP} -even states lie around ~ 125 GeV is particularly interesting, as they enable the two complementary regions $\alpha \simeq \beta - \pi/2$ and $\alpha \simeq \beta$ to be phenomenologically viable – alongside with part of the intermediate regimes. This is so because, regardless of whether the trigonometric couplings are arranged as in the decoupling (SM-like) limit

$[\sin(\beta - \alpha) \simeq 1]$; or, conversely, if they are anchored such that $[\cos(\beta - \alpha) \simeq 1]$, in either case we find a neutral, \mathcal{CP} -even state with SM-like couplings to the gauge bosons. The latter can thus take on the role of the ~ 125 resonance unveiled at the LHC – while its mass-degenerate companion will remain virtually decoupled.

As reflected in Eq. (22), the 2HDM prediction for Δr is generated in our approach from the combination of the SM result Δr_{SM} and the genuinely new pieces sourced by the 2HDM degrees of freedom. Since we are interested here to evaluate the full one-loop 2HDM correction beyond the conventional SM effects [$\Delta r_{\text{2HDM}}^{[1]}$], we will include in this section the $\delta(\Delta r_{\text{2HDM}}^{[1]})$ piece from (22) only. Recall that the other piece in (22), $\Delta r_{\text{2HDM}}^{(\lambda_5)}$, first enters at two loops. Its quantitative impact will be assessed in the next section, as it requires a careful theoretical digression before we can tackle it.

In practice we shall evaluate Δr_{SM} from Eq. (3) upon extracting the SM theoretical value [M_{W}^{SM}] from the compact numerical parametrization of Ref. [57, 86, 88],

$$\begin{aligned} M_{\text{W}}^{\text{SM}} = & M_{\text{W}}^0 - d_1 \text{dH} - d_2 \text{dH}^2 + d_3 \text{dH}^4 + d_4 (dh - 1) \\ & - d_5 \text{d}\alpha + d_6 \text{d}t - d_7 \text{d}t^2 - d_8 \text{dH} \text{d}t \\ & + d_9 \text{d}h \text{d}t - d_{10} \text{d}\alpha_s + d_{11} \text{d}Z, \end{aligned} \quad (30)$$

The coefficients introduced thereof read

$$\begin{aligned} M_{\text{W}}^0 &= 80.3800 \text{ GeV}; & d_6 &= 0.5270 \text{ GeV}; \\ d_1 &= 0.05253 \text{ GeV}; & d_7 &= 0.0698 \text{ GeV}; \\ d_2 &= 0.010345 \text{ GeV}; & d_8 &= 0.004055 \text{ GeV}, \\ d_3 &= 0.001021 \text{ GeV}, & d_9 &= 0.000110 \text{ GeV}, \\ d_4 &= -0.0000070 \text{ GeV}, & d_{10} &= 0.0716 \text{ GeV}, \\ d_5 &= 1.077 \text{ GeV}, & d_{11} &= 115.0 \text{ GeV}; \\ \text{dH} &= \ln\left(\frac{M_{\text{H}}}{100 \text{ GeV}}\right); & \text{d}t &= \left(\frac{m_t}{174.3 \text{ GeV}}\right)^2 - 1; \\ \text{d}\alpha &= \frac{\Delta\alpha}{0.05907} - 1; & \text{d}\alpha_s &= \frac{\alpha_s(M_Z)}{0.119} - 1; \\ \text{d}Z &= M_Z / (91.1875 \text{ GeV}) - 1; & \text{d}h &= \left(\frac{M_{\text{H}}}{100 \text{ GeV}}\right)^2; \end{aligned} \quad (31)$$

with the top-quark mass [$m_t = 173.5 \text{ GeV}$] and the Z-boson mass [$M_Z = 91.1875 \text{ GeV}$] evaluated at their current best averaged values [41]; while $\alpha_s(M_Z) = 0.118$ and $\Delta\alpha = 0.05911$. Notice that $M_{\text{W}}^0 = 80.3800 \text{ GeV}$ in the above parameterization is *not* meant to be the zeroth order value of M_{W} (which we already indicated previously as $M_{\text{W}}^{\text{tree}}$), but a fiducial mass value which is chosen very close to the central value of the experimentally measured M_{W} – cf. Eq. (33) below. Therefore all the correcting terms on the *r.h.s.* of (30) are expected to be small for any reasonable model, and some of them are very much close to zero because the involved physical quantity is known with high accuracy (e.g. $\text{d}Z \simeq 0$).

The parametrization (30)-(31) reproduces the full set of available quantum corrections within the SM. It relies on the following decomposition of Δr in all the one-loop and

higher order effects computed to date [57, 86]:

$$\begin{aligned} \Delta r_{\text{SM}} = & \Delta r^{(\alpha)} + \left[\Delta r_{\text{bos}}^{(\alpha^2)} + \Delta r_{\text{ferm}}^{(\alpha^2)} + \Delta r^{(\alpha\alpha_s)} + \Delta r^{(\alpha\alpha_s^2)} \right. \\ & \left. + \Delta r^{(G_F^2 \alpha_s m_t^4)} + \Delta r^{(G_F^3 m_t^6)} \right]. \end{aligned} \quad (32)$$

For more clarity we keep in (32) the notation of the afore-said references, and hence the first term $\Delta r^{(\alpha)}$ denotes the complete one-loop contribution; in our notation, it corresponds to $\Delta r_{\text{SM}}^{[1]}$ in (29). The remaining terms are higher order contributions which have been explicitly computed in the literature over the years⁶; thus $\Delta r_{\text{bos}}^{(\alpha^2)}$ [89, 101] and $\Delta r_{\text{ferm}}^{(\alpha^2)}$ [86, 101, 102] stand for the respective bosonic and fermionic electroweak two-loop corrections; $\Delta r^{(\alpha\alpha_s)}$ and $\Delta r^{(\alpha\alpha_s^2)}$ for the corresponding two-loop and three-loop QCD corrections [93]; and finally we have the pure electroweak $\mathcal{O}(G_F^3 m_t^6)$ and mixed electroweak-QCD $\mathcal{O}(G_F^2 \alpha_s m_t^4)$ terms, which track the leading 3-loop contributions [103]. The remaining theoretical uncertainty from the unknown higher order corrections is estimated to lie around $\Delta M_{\text{W}}^{\text{SM}} \simeq 4 \text{ MeV}$ [40].

In accordance with the prescription (22), we then add up to the previous result the genuine 2HDM piece $\delta(\Delta r_{\text{2HDM}}^{[1]})$ from the 2HDM Higgs boson-mediated self energies [$\Sigma_{\text{W,Z}}$], as displayed in Fig. 1 (see the Appendix for explicit analytical details). Finally, we rephrase the overall Δr yield obtained in this way in terms of M_{W}^{th} by iteratively solving Eq. (27). This is our estimate of Δr_{2HDM} at this point. As explained in the beginning of this section, we call it the “full one-loop 2HDM result”, in the sense that all of the genuine one-loop effects from the 2HDM degrees of freedom have been taken into account on the Δr quantity within the 2HDM, but at the same time we have incorporated to this result the complete current knowledge of the leading SM quantum effects at various orders of perturbation theory following the above method.

The upshot of our numerical analysis is summarized in Figs. 3-5. Figures 3 and 4 display the full one-loop 2HDM predictions for Δr and M_{W}^{th} , respectively, as a function of the neutral, CP-odd Higgs boson mass [M_{A^0}]. To start with, we fix all the Higgs masses as in Sets I-IV from Table 1; then we sweep over a range $190 < M_{\text{A}^0} < 350 \text{ [GeV]}$ while varying the masses of the remaining Higgs fields accordingly, so that the mass splittings among the heavier 2HDM Higgs fields are maintained as in each of the considered mass sets. At the same time we keep fixed the mass of h^0 at the value $M_{h^0} = 125 \text{ GeV}$. For Set II we actually anchor both M_{h^0} and M_{H^0} at the constant values indicated in the figure – recall that, in this scenario, the heavy \mathcal{CP} -even neutral field [H^0] is meant to describe the putative

⁶ Recall that Δr in the defining equation (3) collects the expanded form of the various contributions up to the order of perturbation theory where the calculation has been carried out. In contrast to the form sketched in (23), no resummation is assumed here of the $\Delta\alpha$ and $\delta\rho$ effects since the terms obtained e.g. at two loop order from the resummation of leading one-loop effects are already contained in the explicit two-loop contribution.

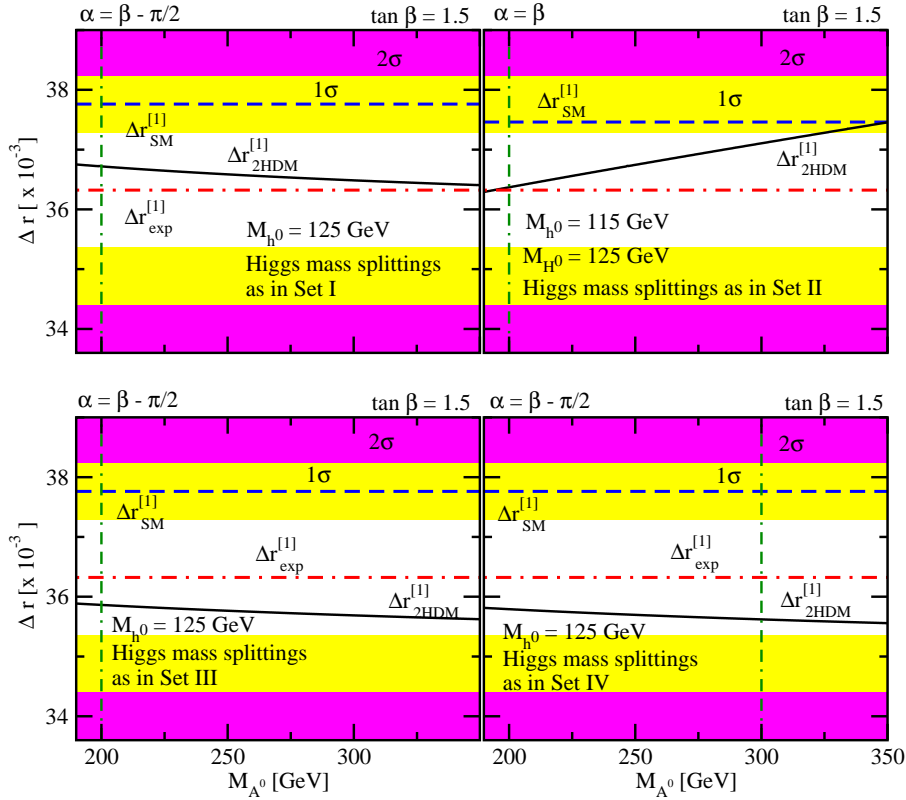


Fig. 3. Full one-loop evaluation of the parameter Δr in the 2HDM, cf. Eq. (29) (solid line, in black), as a function of the neutral, \mathcal{CP} -odd Higgs boson mass [M_{A^0}]. The masses of the remaining heavy Higgs bosons (M_{H^0}, M_{H^\pm}) are also varied alongside, with the mass splittings fixed according to the mass sets from Table 1 as indicated in each panel. The vertical line signals the point in the Higgs boson mass range that corresponds to the exact mass values quoted in Table 1. In the particular case of Set II, in which the SM-like Higgs boson is identified with the heavy \mathcal{CP} -even Higgs boson [H^0], its mass M_{H^0} is also kept constant, so that in practice we scan over M_{A^0} and M_{H^\pm} only. The calculation is performed at fixed $\tan\beta = 1.5$, with $\alpha = \beta - \pi/2$ (resp. $\alpha = \beta$) for Sets I,III and IV (resp. Set II), in agreement with the SM-like decay patterns of the 125 GeV Higgs boson candidate. As a reference, we also display the SM prediction Δr_{SM} (dashed line, in blue) and the experimental value Δr^{exp} (dotted-dashed line, in red). The associated 1σ and 2σ C.L. bands are explicitly indicated.

~ 125 GeV Higgs boson. We carry out the calculation at a fixed value of $\tan\beta = 1.5$, in compliance with the stringent conditions dictated by $B_d^0 - \bar{B}_d^0$ and $\mathcal{B}(b \rightarrow s\gamma)$ physics, including the perturbative unitarity and vacuum stability bounds (see Sec. 2.2). On the same grounds we enforce SM-like Higgs/gauge boson couplings for the corresponding ~ 125 GeV Higgs boson in our numerical analysis – which amounts to work in the *decoupling limit* $\alpha = \beta - \pi/2$ for Sets I, III and IV, and $\alpha = \beta$ for Set II. Finally, Sets V – VIII and V' – VIII', with two neutral, \mathcal{CP} -even, ~ 125 GeV states, interpolate between both scenarios, and are examined in Figure 5. We shall comment on them later on.

The different panels of Fig. 3 present the $\Delta r_{\text{2HDM}}^{[1]}$ results for Sets I - IV of Higgs bosons masses. Therewith we also display the SM value Δr_{SM} , computed as described above, together with the experimental value $\Delta r_{\text{exp}}^{[1]}$ obtained from Eq. (3) using the experimental inputs

$$\begin{aligned} M_W^{\text{exp}} &= 80.385 \pm 0.015 \text{ GeV} & M_Z &= 91.1876 \pm 0.0021 \text{ GeV} \\ \alpha(0) &= 1/137.03599 & G_F &= 1.16637 \cdot 10^{-5} \text{ GeV}^{-2}. \end{aligned} \quad (33)$$

Plugging the above values into Eq. (3) we get

$$\Delta r_{\text{exp}} = \frac{\sqrt{2} G_F}{\pi \alpha} M_W^2 \left(1 - \frac{M_W^2}{M_Z^2} \right) - 1 = 36.322 \times 10^{-3}. \quad (34)$$

In Fig. 4 the corresponding 2HDM and SM theory predictions for M_W^{th} are represented as a function of M_{A^0} under the same conditions as in Fig. 3. One can also appreciate the deviations of the theoretical W-boson mass with respect to the latest experimental value $M_W^{\text{exp}} = 80.385 \pm 0.015$ GeV. Confidence levels for M_W^{exp} and Δr_{exp} are also included in our plots as colored areas corresponding to the 1σ (yellow) and 2σ (magenta) regions. In the case of Δr , we compute these uncertainties from those of M_W^{exp} by standard error propagation methods. The re-

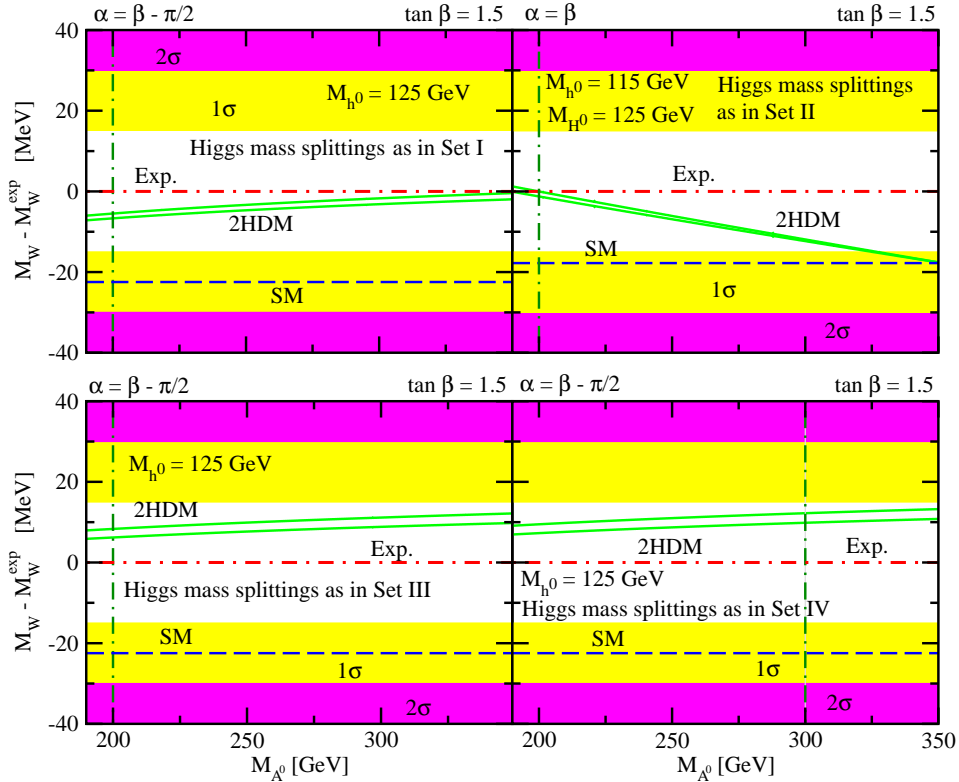


Fig. 4. Full one-loop prediction for the W-boson mass [$M_W^{\text{th}} \equiv M_W^{\text{SM}} + \delta M_W^{\text{2HDM}}$] in the general 2HDM as a function of the neutral, \mathcal{CP} -odd Higgs boson mass [M_{A^0}]. The results are presented as a deviation [δM_W] = $M_W^{\text{th}} - M_W^{\text{exp}}$ with respect to the experimental value $M_W^{\text{exp}} = 80.385 \pm 0.015$ GeV. The masses of the remaining heavy Higgs bosons (M_{H^0}, M_{H^\pm}) are also varied alongside, preserving the mass splitting of the mass sets from Table 1 as indicated in each panel. The vertical line signals the point in the Higgs boson mass range that corresponds to the precise mass values quoted in Table 1. In the particular case of Set II, in which the SM-like Higgs boson is identified with the heavy \mathcal{CP} -even Higgs boson [H^0], its mass M_{H^0} is also kept constant, so that in practice we scan over M_{A^0} and M_{H^\pm} only. The calculation is performed at fixed $\tan \beta = 1.5$, with $\alpha = \beta - \pi/2$ (resp. $\alpha = \beta$) for Sets I, III and IV (resp. Set II), in agreement with the SM-like decay patterns of the 125 GeV Higgs boson candidate. The green band provides an estimate on the theoretical uncertainty. As a reference, we also display the SM prediction M_W^{SM} (dashed line, in blue). The associated 1σ and 2σ C.L. bands for the measured value M_W^{exp} are explicitly indicated.

gion comprised between the two parallel thin strips (in green) in Fig. 4 supplies an estimate of the 2HDM theoretical uncertainty [ΔM_W^{th}]. The latter we quantify by means of Eq. (27) upon substituting $1 + \delta(\Delta r_{\text{2HDM}}^{[1]}) \rightarrow 1/(1 - \delta(\Delta r_{\text{2HDM}}^{[1]}))$, which leads to a slightly modified prediction [\tilde{M}_W^{th}]. Such a shift operates an approximate resummation of the 2HDM contributions, in such a way that the difference relative to the central value, [$\Delta \tilde{M}_W^{\text{th}}/M_W^{\text{th}} \equiv |\tilde{M}_W^{\text{th}} - M_W^{\text{th}}|/M_W^{\text{th}}$], should be indicative of the size of the pure 2HDM higher-order effects neglected when truncating our perturbative expansion at $\mathcal{O}(\alpha_{\text{ew}})$ – and that fall typically within the range of $\sim 1 - 5$ MeV. As we will see later on, this estimate is well in agreement with the leading 2HDM higher-order corrections computed in Section 4. Such 2HDM uncertainty is yet to be combined with its SM counterpart $\Delta M_W^{\text{SM}} \simeq 4$ MeV, as well as with the parametric uncertainties – dominated by the top mass measurement $\Delta m_t = \pm 0.9$ GeV [100] and entailing ap-

proximately $\Delta M_W^{\text{param}} \simeq 10$ MeV. Therefore, the errors added in quadrature lead to a total uncertainty of roughly 12 MeV.

Complementary vistas on the Δr behavior across the 2HDM parameter space are displayed in Fig. 5. We compute once again the full-fledged one-loop 2HDM prediction [$\Delta r_{\text{2HDM}}^{[1]}$] and compare it to the SM result [Δr_{SM}] and the experimental value [Δr_{exp}]. We keep a fixed $\tan \beta = 1.5$ but we now sweep all over the $\sin(\beta - \alpha)$ range. In doing so, we effectively interpolate between the two corners with SM-like Higgs/gauge boson couplings. In the light of the LHC findings, regions away from $\sin(\beta - \alpha) \simeq 1$ – or conversely $\sin(\beta - \alpha) \simeq 0$ – would be disfavored, if not simply excluded, at a certain confidence level. We will refrain from considering a more accurate treatment of this issue, as it is still subdued by large statistical uncertainties and surely not relevant for our present discussion. Fig. 5 displays a featureless Δr_{2HDM} profile as a function of $\sin(\beta - \alpha)$, which follows from the approximate mass-degeneracy of the neutral \mathcal{CP} -even Higgs bo-

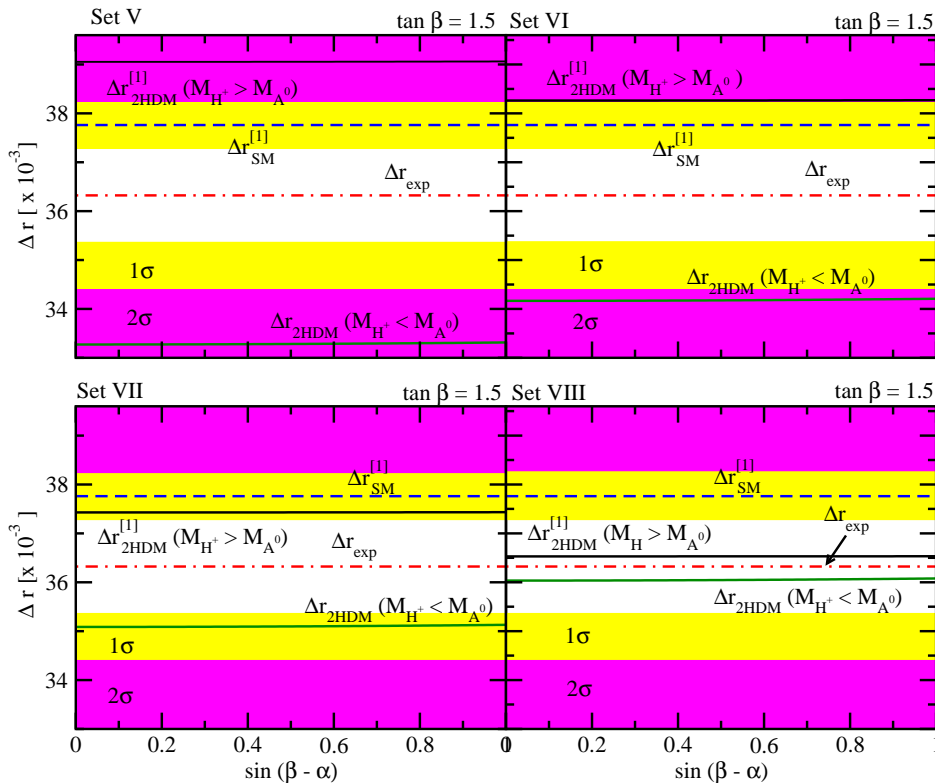


Fig. 5. Full one-loop evaluation of the parameter Δr in the general 2HDM, cf. Eq. (29) (solid line, in black) as a function of $\sin(\beta - \alpha)$. The calculation is performed at fixed $\tan\beta = 1.5$, for sets V to VIII and V' to VIII' of Higgs boson masses, and for the two different M_{A^0}/M_{H^\pm} mass hierarchies. As a reference, we also display the SM prediction Δr_{SM} (dashed line, in blue) and the experimental value Δr^{exp} (dotted-dashed line, in red). The associated 1σ and 2σ C.L. bands are explicitly indicated.

son states. Worth noticing is also the influence of $\delta\rho$ (what is tantamount to say, the size of $\Delta r^{[\delta\rho]}$ in the notation of Eq. (11)): the lighter the Higgs boson masses – and the narrower their splittings – the smaller becomes $\Delta r^{[\delta\rho]}$. One can easily understand this behavior from equations (15) and (52). One visible signature that stands out in these plots is that the tension between the theoretical prediction $[\Delta r_{2\text{HDM}}]$ and the experimental value $[\Delta r_{\text{exp}}]$ shrinks significantly when comparing the outcomes for the different mass choices from Sets V to VIII. For Set V, for instance, we have $|\delta\rho| \sim \mathcal{O}(10^{-3})$ – at the very border of the permitted custodial symmetry bounds. The predicted $\Delta r_{2\text{HDM}}$ is then pushed more than 2σ away from the experimental result – with an even larger tension than the SM prediction. In contrast, for Set VIII the theoretical prediction $[\Delta r_{2\text{HDM}}]$ moves closer to $[\Delta r_{\text{exp}}]$, departing from it roughly $\sim 0.6\%$ – the SM prediction staying circa $\sim 4\%$ away. All these effects are qualitatively similar, although opposite in sign, when we swap the mass hierarchy. Remarkably, we find that $[M_{A^0} > M_{H^\pm}]$ pulls our prediction for M_W^{th} slightly further away from M_W^{exp} , as compared to $[M_{A^0} < M_{H^\pm}]$. For the EW observables under scope, therefore, the scenarios we have considered here tend to favor 2HDM realizations with the charged Higgs being heavier than the neutral, \mathcal{CP} -odd one.

The predicted M_W^{th} values within the 2HDM are seen to follow a smooth and monotonous variation, with changes of $\mathcal{O}(10)$ MeV – equivalently, $\delta(\Delta r) \sim \mathcal{O}(10^{-3})$ as retrieved by the previous Fig. 3 – when sweeping the Higgs boson mass range $190 < M_{A^0} < 350$ [GeV]. The largest possible theoretical W-boson mass shift from genuine 2HDM effects is substantial: $|\delta M_W^{\text{2HDM}}| \simeq 35$ MeV (more than twice the current experimental error on M_W). Larger variations ensue from a trade-off between two different – and somewhat opposite – conditions, which are the following: i) heavier Higgs bosons, in correspondence with the mass suppression of the one-loop Higgs-mediated contributions to $\Sigma_{W,Z}$, yield relatively tamed quantum effects; and ii) broader splittings among the different Higgs boson masses lead to a stronger breaking of the approximate $SU(2)$ custodial symmetry, and hence to an augmented contribution $\Delta r^{[\delta\rho]}$. We will also identify a similar balance between both tendencies when examining the leading higher order quantum corrections, as discussed further down.

The SM theoretical prediction following from the full parametrization (30)-(31) with $M_H = 125$ GeV reads

$$M_W^{\text{SM}} = 80.363 \text{ GeV}. \quad (35)$$

The difference $M_W^{\text{SM}} - M_W^{\text{exp}}$ corresponds to the horizontal line marked as SM in all the plots of Fig. 4 – except

for Set II, for which the identification $h^0 \equiv H$ implies that M_W is to be evaluated at $M_H = 115$ GeV, yielding $M_W = 80.367$ GeV. We see in these plots that the SM value is systematically too low, it typically fails to match the central value M_W^{exp} by more than 20 MeV below it. This deviation is not worrisome right now because it lies within the 1σ region, but this could change in the future when the error in M_W^{exp} may dramatically decrease at the ~ 5 MeV level. At this point the SM prediction, whose intrinsic theoretical error is estimated to be ~ 4 MeV [40], could be in good shape or on the contrary it might already clash with experiment. In contrast, the 2HDM numerical prediction is seen to have the ability to easily cure the differences with respect to the experimental value, should the conflict with the SM prediction become confirmed. From Fig. 4 it is evident that the 2HDM prediction can stay very close to the central experimental value M_W^{exp} and moreover it can accommodate deviations of up to 20 – 35 MeV with respect to it, depending on the Higgs mass sets used from Table 1.

It is well-known that the MSSM has also the potential to shrink the gap between M_W^{exp} and M_W^{SM} . To illustrate it in our framework, let us e.g. consider the SUSY-inspired Set III from Table 1, which features the *maximal mixing* MSSM scenario [99]. The latter contains relatively light $\mathcal{O}(100)$ GeV gaugino masses, along with heavy $\mathcal{O}(1)$ TeV squarks and sleptons and moderately massive stops in the $\mathcal{O}(700)$ GeV ballpark. Using FEYNHIGGS [98] we evaluate M_W^{MSSM} including all the presently known contributions (up to leading two-loop order) and get:

$$\begin{aligned} M_W^{\text{MSSM}} = 80.373 \text{ GeV} &\Rightarrow M_W^{\text{MSSM}} - M_W^{\text{SM}} = 10 \text{ MeV}; \\ M_W^{\text{MSSM}} - M_W^{\text{exp}} &= -12 \text{ MeV}. \end{aligned} \quad (36)$$

For the same masses, the corresponding 2HDM prediction (taking e.g. the decoupling limit $\alpha = \beta - \pi/2$, cf. also Table 2) yields

$$\begin{aligned} M_W^{2\text{HDM}} = 80.394 \text{ GeV} &\Rightarrow M_W^{2\text{HDM}} - M_W^{\text{SM}} = 31 \text{ MeV}; \\ M_W^{2\text{HDM}} - M_W^{\text{exp}} &= 9 \text{ MeV}. \end{aligned} \quad (37)$$

Let us recall from Fig. 4 that the SM prediction lies roughly -22 MeV below M_W^{exp} . In this example, both the 2HDM and the MSSM are comparably competitive in softening the $M_W^{\text{th}} - M_W^{\text{exp}}$ tension. Interestingly, this picture does not hold any longer if we decouple the genuine SUSY degrees of freedom, i.e. all sparticle masses apart from the MSSM Higgs bosons. Raising all SUSY particle masses up to $\sim \mathcal{O}(1.5)$ TeV in this example – it has essentially no impact here on the resulting two-loop SUSY Higgs masses –, the MSSM prediction converges to the SM,

$$\begin{aligned} M_W^{\text{MSSM}} = 80.361 \text{ GeV} &\Rightarrow M_W^{\text{MSSM}} - M_W^{\text{SM}} = -2 \text{ MeV}; \\ M_W^{\text{MSSM}} - M_W^{\text{exp}} &= -24 \text{ MeV}, \end{aligned} \quad (38)$$

and therefore the $M_W^{\text{th}} - M_W^{\text{exp}}$ tension at the level of ~ 20 MeV is back once more between the MSSM and the experimental measurement of the W^\pm mass, as expected from decoupling arguments. This example illustrates that in the MSSM, in contrast to the general 2HDM, the bulk capability to reconcile M_W^{exp} and M_W^{th} relies on the genuine SUSY contributions, while the SUSY Higgs-mediated effects play a subdominant role. This is after all a reflect of SUSY invariance, which links the Higgs boson masses and the mixing angle α to the gauge couplings, enforcing a very constrained Higgs boson sector – with a naturally mild custodial symmetry violation. Comprehensive surveys of the MSSM parameter space, including a detailed discussion on the SUSY-decoupling scenarios, can be found e.g. in Refs. [56]. Further discussion on the 2HDM versus MSSM comparison is presented later on in Section 4.

Let us remind the reader at this point that, within the approach employed in this section, we are not yet sensitive to the potential effects from the λ_5 parameter. Neither the results show any direct sensitivity to whether they are obtained within a type-I or a type-II 2HDM setup, as this depends on the specific Yukawa couplings of each model. Still, we should bear in mind that both features, namely the strength of the Higgs self couplings and the pattern of Higgs/fermion Yukawa interactions are indirectly present through their interplay with the theoretical and phenomenological constraints – which are duly taken into account in our analysis (cf. Sec. 2.2). Let us recall in particular the lower bound of ~ 300 GeV for the charged Higgs boson mass for type II models.

We conclude this section by emphasizing what we believe is our most important observation, hitherto unnoticed (to the best of our knowledge) in the literature, to wit: the bulk presence of the term $\delta(\Delta r_{2\text{HDM}}^{[1]})$ – defined in Eq. (24) – provides a significant shift on the W -mass genuinely caused by the 2HDM heavy Higgs companions. This shift softens the influence of the SM(-like) Higgs boson [h^0] on the W -boson mass prediction and therefore relaxes the current M_W^{th} -versus- M_W^{exp} tension, which is well known to grow with M_{h^0} and constitutes one of the main reasons why global fits to Electroweak precision data tend to favor light Higgs bosons – rendering the minimum χ^2 -values for masses even below the LEP bounds (cf. e.g. [105]). What our results reflect is that such trend no longer holds in the context of the general 2HDM. Here, and essentially for all the surveyed scenarios, the neat effect of adding new scalar $SU_L(2)$ doublets leads to a systematic downward shift of Δr , and so upward on M_W^{th} , which tends to improve the agreement with the corresponding experimental measurement. Said differently, when compared to the SM expectations for a ~ 125 GeV SM-like Higgs boson mass, the genuine 2HDM contribution [$\delta(\Delta r_{2\text{HDM}}^{[1]})$] tends to pull down the overall $\Delta r_{2\text{HDM}}^{[1]}$ prediction. Accordingly, M_W^{th} becomes larger, and hence closer to the corresponding experimental measurement M_W^{exp} . This is the most relevant message to be conveyed at this point of our analysis. In the next section we focus on the additional influence of the 2HDM quantum effects through the λ_5 parameter.

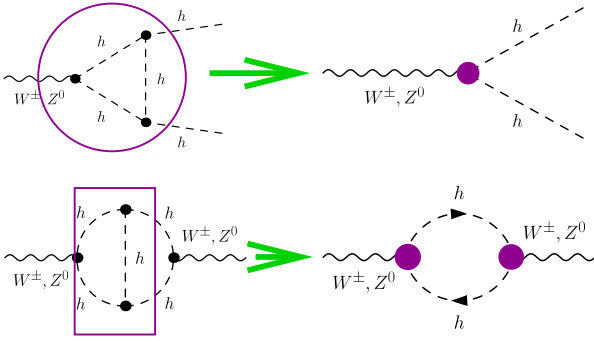


Fig. 6. Pictorial sketch of the form factors devised to capture the leading 2HDM higher order corrections to $\delta\rho$. In the limit of large Higgs boson self-interactions, these are dominantly driven by the Higgs-mediated contributions to the weak gauge boson self energies, as displayed in the lower part of the figure (cf. Fig. 2 for a specific sample). As a first stage we compute the one-loop Higgs-mediated corrections to the different Higgs/gauge (and Goldstone) boson interactions to order $\mathcal{O}(\lambda_5^2)$; these correspond to a UV finite, gauge invariant subset of contributions which encapsulates the (dominant) effects triggered by the enhanced Higgs boson self-interactions (upper-left corner). We then rewrite such corrections as one-loop form factors and use them to effectively *dress* the leading-order Higgs/gauge boson couplings (upper-right corner). The resulting set of Born-improved effective vertices (depicted as colored blobs) can be finally plugged back in the calculation of the one-loop gauge boson self energies (lower-right and lower-left corners).

4 Higher order 2HDM effects from enhanced Higgs boson self-interactions

A number of recent studies [67, 84] have pointed out and exploited the possibility that the Higgs/gauge boson couplings eventually undergo a drastic modification at the quantum level in the limit of large Higgs boson self-interactions. These modifications are in practice restrained by certain theoretical and phenomenological bounds, but their net effect can still be quite sizeable in different contexts. In the present case the potential enhancements can actually be traded through the aforementioned $\mathcal{O}(\lambda_5^2)$ terms in the Higgs boson self-coupling structure. Such scenarios are not only phenomenologically viable, but also very well supported on theoretical grounds. As a matter of fact, the rise of scalar resonances constitutes a prominent manifestation of models with strong dynamics in the EWSB sector [15, 106]. Interestingly, strong self-interactions among Higgs, or Higgs-like states, are most often identified with rather heavy mass spectra – reflecting the relations among masses and self-couplings settled through the Higgs potential. Nevertheless, the 2HDM comprises a wider range of possibilities – as not all of the Higgs self-couplings are tied to the corresponding physical Higgs masses. The fact that we can freely dial the parameter λ_5 enables to recreate genuine 2HDM regimes with relatively light, and yet strongly coupled Higgs bosons.

As we have preliminarily discussed in Sec. 2.4, EW precision quantities – most significantly Δr and $\delta\rho$ – become sensitive to the Higgs boson self-couplings via 2-loop effects on the gauge boson self-energies. This is illustrated in Fig. 6. Here we do not target at an explicit 2-loop calculation. Instead, we aim at getting insight into the foreseeable quantitative impact that such Higgs boson self-couplings may exert on the theoretical prediction for the W-boson mass [M_W^{th}]. In fact, since a fully-fledged 2-loop calculation is too cumbersome and probably unnecessary at this point, we resort to a Born-improved Lagrangian approach leading to a set of effective couplings or form factors. The advantage of it is that we can focus more easily on the main potential sources of enhancement and moreover we can even have access to their influence beyond the 2-loop level.

In practice we devise our set of effective couplings as follows:⁷

1. To start with, let us recall that after SSB of the EW gauge symmetry we can always trade the original Higgs self-couplings λ_i (except λ_5) for the physical masses, mixing angles and gauge couplings. This is explicitly done e.g. in Sec. III of Ref. [67] – cf. Eq. (12) there. From here we can easily implement the limit of large Higgs self-couplings by projecting out the λ_5 -dependent part of each of the Higgs self-interactions in the model and neglecting the other terms. According to this procedure we can redefine $\lambda_i \rightarrow \tilde{\lambda}_i$ for all the original self-couplings λ_i in the Higgs potential – cf. Eq. (1) – as follows:

$$\begin{aligned} \tilde{\lambda}_1 &= \frac{1}{4} \lambda_5 (1 - \tan^2 \beta); & \tilde{\lambda}_2 &= \frac{1}{4} \lambda_5 (1 - \cot^2 \beta); \\ \tilde{\lambda}_3 &= -\frac{1}{4} \lambda_5; & \tilde{\lambda}_4 &= \lambda_6 = 0. \end{aligned} \tag{39}$$

The above approximation has its counterpart in the physical basis. Following the splitting procedure (20), we collect the λ_5 terms associated to the Higgs self-couplings in that basis. They render structures of the sort:

$$\begin{aligned} \lambda_{h^0 h^0 h^0} &\rightarrow c_h \lambda_5 = \\ &\left(i \frac{6 M_W s_W}{e} \frac{\cos(\alpha + \beta) \cos^2(\beta - \alpha)}{\sin 2\beta} \right) \times \lambda_5, \end{aligned} \tag{40}$$

and analogously for all the self-interactions λ_{hhh} relating the different Higgs boson fields to each other (we refer once more e.g. to Table II of Ref. [67]). Notice that the strength of all the λ_{hhh} couplings, and so also their related potential enhancements, are now fully determined as functions of λ_5 and $\tan\beta$ – with

⁷ Approaches along these lines are certainly not foreign in the literature, see for example Ref. [27]. In our opinion, however, scarce attention has been devoted to the underlying assumptions and corresponding limitations.

no remaining dependence on the Higgs nor the gauge boson masses. As it will become clear soon, this is a necessary step in order to preserve gauge invariance within our framework. In Fig. 7 we illustrate how this approximation performs when compared to the complete analytical form of the triple (3h) self-interactions (see e.g. Table III of Ref. [67]). All couplings in this figure are normalized to the value of the 3H self-coupling in the SM, for a Higgs boson mass of $M_H = 125$ GeV, see Eq.(19). Noteworthy is that the 3h enhancements within the 2HDM, as indicated in Fig. 7 for values of $|\lambda_5| \sim \mathcal{O}(10)$, are perfectly consistent with the Lee-Quick-Thacker unitarity bound for the SM 3H coupling [94]:

$$\lambda_{\text{HHH}} \simeq \left. \frac{3eM_H^2}{2s_W M_W} \right]_{M_H=1 \text{ TeV}} \simeq 1.3 \times 10^4 \text{ GeV}. \quad (41)$$

The main virtue of Fig. 7 is that it makes apparent how both descriptions of the λ_{hhh} couplings — viz. the full one versus the truncated approach $\lambda_{hhh} \rightarrow c_h \lambda_5$ defined by (20) — nicely agree in the purported limit of large Higgs boson self-interactions. At the end of the day, the goodness of this approximation will depend on the extent to which this limit is effectively realized by a given choice of λ_5 and $\tan \beta$.

2. Second, we examine the leading quantum effects on the different Higgs/gauge boson couplings in order to absorb them into effective vertices. These we can generically sort out into three categories:

- i) Higgs/Higgs/gauge boson couplings: g_{hhV}
- ii) Higgs/gauge/gauge boson couplings: g_{hVV}
- iii) Higgs/gauge/Goldstone boson couplings: g_{hGV}

with $[h = h^0, H^0, A^0, H^\pm]$ standing for a generic 2HDM Higgs field; $V = [W^\pm, Z^0]$ for a weak gauge boson; and $G = [G^\pm, G^0]$ for the associated charged and neutral Goldstone modes, namely the longitudinal components of the gauge bosons in the 't Hooft-Feynman gauge. In practice, structures of type iii) are formally equivalent to those of type i), as they involve two scalar and one vector fields. In the regimes of interest here, namely in the large Higgs self-interaction limit, the leading corrections to the above couplings are thus driven by the interchange of virtual Higgs bosons. A sample of the corresponding Feynman diagrams is provided in Fig. 8, in which we single out the case of the $g_{h^0 A^0 Z^0}$ and $g_{h^0 W^\pm H^\pm}$ effective couplings. The one-loop corrections to each of these couplings involve both triangle diagrams and self-energy insertions; the former account for the genuine $\mathcal{O}(\lambda_5^2)$ one-loop vertex corrections, whereas the latter involve also $\mathcal{O}(\lambda_5^2)$ pieces from the finite wave function renormalization of the external Higgs boson legs. Starting from the 1-loop vertices of Fig. 8 we can easily recognize them as being part of some of the vertices in the 2-loop diagrams of Fig. 2. When the vertices in the former collapse to a point we obtain the kind of solid (colored) blobs indicated in Fig. 6. These blobs represent static form factors attached to the corresponding vertices, i.e. evaluated at zero momentum, and are therefore appropriate to es-

timate the higher order effects on the $\delta\rho$ -parameter (even if they are actually not suitable for addressing the corresponding effects on the full Δr parameter, see later on).

The practical recipe in our approach is now clear. Based solely on power counting and dynamical considerations, the one-loop effects from Fig. 8 can be conveniently cast as form factors of the guise:

$$\begin{aligned} a_{hhV} &\sim \frac{1}{16\pi^2} \left(\frac{\lambda_{hhh}}{M_h} \right)^2 f_{hhV}(p^2/M_h^2)(p \cdot \epsilon) \sim \mathcal{O}(\alpha_{\text{ew}} \lambda_5^2); \\ b_{hVV} &\sim \frac{1}{16\pi^2} \left(\frac{\lambda_{hhh}}{M_h} \right)^2 f_{hVV}(p^2/M_h^2)(\epsilon \cdot \epsilon) \sim \mathcal{O}(\alpha_{\text{ew}} \lambda_5^2); \\ c_{hGV} &\sim \frac{1}{16\pi^2} \left(\frac{\lambda_{hhh}}{M_h} \right)^2 f_{hGV}(p^2/M_h^2)(p \cdot \epsilon) \sim \mathcal{O}(\alpha_{\text{ew}} \lambda_5^2). \end{aligned} \quad (42)$$

These form factors carry the sought-for fingerprint of the Higgs boson self-interactions, which we generically flag here as $[\lambda_{hhh}]$. The typical Higgs boson mass scale M_h in Eq. (42) restores the corresponding dimensions and accounts for the correct decoupling properties. At the same time, it partially balances the enhancement effect of the Higgs self-interactions in the numerator. By $f(p^2/m_h^2)$ we denote a generic rational function, depending on the (ratios of the) relevant scales involved in the Higgs boson-mediated one-loop diagrams, namely the masses of the virtual particles and the transferred momentum. These form factors we evaluate at zero momentum. Put another way, we reduce the loop structure to a point-like interaction in which $\lambda_{hhh}^2 \rightarrow \lambda_5^2$ appears as the only effective coupling in the large λ_5 limit. Finally, $1/16\pi^2$ stands for the usual numerical factor from the one-loop integrals. We carry out this calculation with the help of FORMCALC [97]. Explicit analytical details we provide in the Appendix, cf. Eqs. (61)-(65). Equivalent form factors could of course be entertained for the MSSM case. However, in stark contrast to the general 2HDM, they would show a pure $\mathcal{O}(g^3)$ gauge structure and would therefore be inconspicuous from a phenomenological viewpoint, in the sense that no characteristic MSSM signature could easily emerge from them.

Noteworthy is also the following. The one-loop form factors (42) computed this way are UV finite and gauge invariant. The finiteness follows by simple power counting. The gauge invariance ensues from the fact that we consistently retain all $\mathcal{O}(\alpha_{\text{ew}} \lambda_5^2)$ contributions – but not more. It should be clear that it is because of our exclusive selection of the characteristic λ_5^2 tag in these diagrams that we are granted to successfully isolate a meaningful (gauge invariant) and finite contribution. By the same token the sum of all the original 2-loop diagrams as such carrying the λ_5^2 tag (cf. Fig. 2 for a representative sample) is gauge invariant and finite. Had we kept also the full dependence of the trilinear couplings on the Higgs and gauge boson masses, we

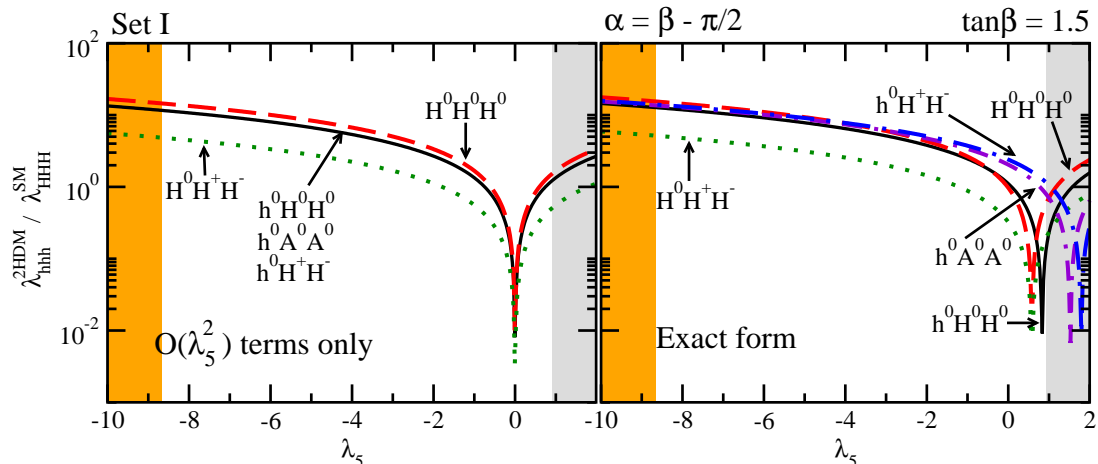


Fig. 7. Coupling strength $[\lambda_{\text{hhh}}]$ for a sample of triple Higgs self-interactions, as a function of the parameter λ_5 . The couplings are normalized to the strength of the 3H self-coupling in the SM, assuming that the SM Higgs boson mass yields $M_H = 125$ GeV. As a result we get $\lambda_{\text{HHH}}^{\text{SM}}(M_H = 125 \text{ GeV}) = 188.24 \text{ GeV}$. We can check that the obtained λ_{hhh} values lie systematically below the Lee-Quick-Thacker bound $\lambda_{\text{HHH}}^{\text{SM}}(M_H \simeq 1 \text{ TeV}) \simeq 1.3 \times 10^4 \text{ GeV}$ [94]. The figure compares the size of these 3h self-couplings when considering i) the projection of the $\mathcal{O}(\lambda_5)$ components only (left panel) and ii) its exact analytical form (right panel) – see the text for details. Without loss of generality, we dwell here on set I of Higgs boson masses and we fix $\tan\beta = 1.5$. The shaded regions on the left (resp. right) side are excluded by unitarity (resp. vacuum stability).

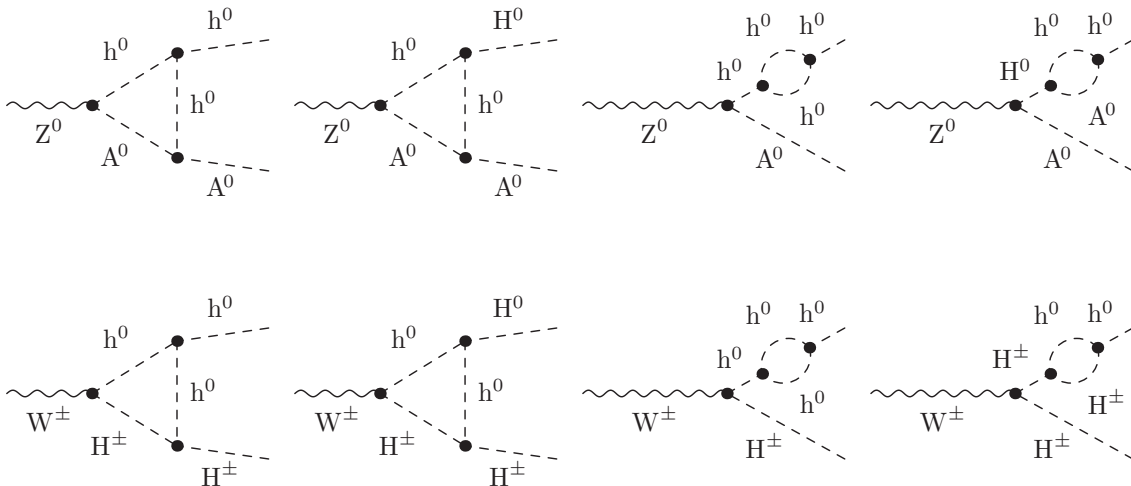


Fig. 8. Sample of Feynman diagrams that account for the $\mathcal{O}(\lambda_5^2)$ one-loop corrections to the $h^0 A^0 Z^0$ and $h^0 W^\pm H^\pm$ gauge couplings in the 2HDM.

would have been forced to take into account the remaining set of contributions not only from the Higgs bosons, but also from the gauge sector (viz. the gauge and Goldstone boson-mediated diagrams) in order to insure the overall gauge invariance of the Higgs/gauge form factors (42). The fact that we single out these $\mathcal{O}(\lambda_5^2)$ pieces from the 3h self-interactions could be viewed as if we were effectively decoupling the dynamics of the Higgs and the gauge sectors of the 2HDM. Of course this is not a *decoupling* in the usual sense, namely it is not due to the presence of a hierarchy of masses – notice, indeed, that the mass spectra under examination typically feature $M_V \lesssim M_H$. Rather than “decoupling” we are “detaching” the λ_5 -effects from

the rest of the quantum contributions in a consistent way. There is actually some independence at the level of QFT renormalizability between, say, the gauge and Yukawa sectors on the one side, and the λ_5 -structure of the Higgs boson self-interactions on the other side. These sectors contain independent parameters (gauge and Yukawa couplings in the former versus trilinear couplings in the latter). They all carry some characteristic renormalizability “flagpoles”, which can nevertheless be mixed. For example, in the case of the Higgs self-interactions there is one part that still carries the gauge flagpole, but there is another which does not (the λ_5 -part). It is precisely this part that has no crosstalk with the others since it is gauge invariant

and finite *per se*. As a result there can be, in principle, an arbitrary hierarchy of strengths between the Higgs self-couplings and the (merely gauge) Higgs/gauge and Higgs/fermion interactions. This is what allows to detach one sector from the other without jeopardizing in any possible way the QFT renormalizability of the theory. In turn, this is what authorizes the 2HDM Higgs bosons to couple to each other much stronger than they do to the gauge bosons. Such property is impossible in the MSSM, where the gauge flagpole is inherent (owing to the underlying supersymmetry) to the entire structure of the Higgs self-interactions.

To summarize: in our calculation the λ_5 parameter plays the role of a flagpole which marks an independent sector of the theory. By selecting it we can factorize a gauge invariant and UV-finite piece from the entire calculation. In the limit of large λ_5 such well-defined piece encapsulates the dominant quantum effects on the tree-level Higgs/gauge interactions.

3. Finally, we can fold these tree-level Higgs/gauge interaction Lagrangians with the form factors $[a_{\text{hhV}}, b_{\text{hVV}}, b_{\text{hVG}}]$ derived above and build up a corresponding set of Born-improved Lagrangians:

$$\begin{aligned}\mathcal{L}_{\text{hhV}}^{\text{eff}} &= g_{\text{hhV}} (1 + a_{\text{hhV}}) [(\partial_\mu h) V^\mu h - h V^\mu \partial_\mu h]; \\ \mathcal{L}_{\text{hVV}}^{\text{eff}} &= g_{\text{hVV}} (1 + b_{\text{hVV}}) h V_\mu V^\mu; \\ \mathcal{L}_{\text{hVG}}^{\text{eff}} &= g_{\text{hVG}} (1 + c_{\text{hVG}}) [(\partial_\mu h) V^\mu G - h V^\mu \partial_\mu G].\end{aligned}\quad (43)$$

The general structure of the associated form factors can be illustrated e.g. in the case of the effective $h^0 A^0 Z^0$ coupling,

$$\begin{aligned}a_{h^0 A^0 Z^0} \Big|_{p^2=0} &= \Re e V_{h^0 A^0 Z^0} - \frac{1}{2} \Re e \Sigma'_{h^0} \\ &\quad - \frac{1}{2} \Re e \Sigma'_{A^0} - \frac{\tan(\beta - \alpha)}{M_{H^0}^2} \Re e \hat{\Sigma}_{h^0 H^0} \Big|_{p^2=0},\end{aligned}\quad (44)$$

where the explicit form of the two and three point functions is given in the Appendix.

Additional momentum-dependent tensor structures $\sim p_\mu p_\nu V^\mu V^\nu$ within the hVV form factor do not include $\mathcal{O}(\lambda_5^2)$ contributions and are henceforth disregarded in our treatment of $\delta\rho$ at higher orders. The idea of absorbing the bulk of the quantum effects into *improved* leading-order effective interactions (43) is of course not new. A well known example is the enhanced bottom/sbottom Yukawa coupling in the large $\tan\beta$ limit of the MSSM [108] – see also [107]. The approximation will be meaningful as long as we probe these effective couplings at momentum scales significantly smaller than the typical Higgs boson masses. For quantities which are momentum-dependent, though, such effective coupling treatment may no longer be suitable. But in our case the approach is fully justified, as we are using this approximation only to estimate

some higher order effects on the $\delta\rho$ parameter, a static prominent piece of Δr , namely $\Delta r^{[\delta\rho]} \equiv -(c_{\text{W}}^2/s_{\text{W}}^2)\delta\rho$, for which the gauge boson self energies are to be evaluated at zero momentum – cf. Eq. (8). This is the reason why the effective coupling treatment elaborated here is not directly exportable to e.g. a full-fledged calculation of Δr . As we will discuss in more detail, the $\Delta r^{[\delta\rho]}$ component proves insufficient to completely describe the quantum effects from the Higgs bosons, which means that the momentum-dependent part of the gauge boson self energies (evaluated on-shell $p^2 = M_V^2$) cannot be neglected, and in fact may be quantitatively relevant.

Following the above method, an estimate of $\delta\rho$ beyond one-loop – viz. including the dominant $\mathcal{O}(\alpha_{\text{ew}} \lambda_5^2)$ terms – is now at reach with a moderate, albeit still non-trivial, amount of work as compared to the full 2-loop calculation. The obtained numerical results are presented in the upper panels of Fig. 9. Here we plot the evolution of $\delta\rho$ versus the Higgs self-coupling λ_5 and for the Sets I-IV of Higgs boson masses quoted in Table 1. For each set, we fix $\tan\beta$ so that the quantum effects governed by the enhanced 3h self-interactions maximize for the largest attainable $|\lambda_5|$ values within bounds. Alongside the pure 2HDM one-loop effects $[\delta\rho^{[1]} \equiv \delta\rho_{2\text{HDM}}^{[1]}]$ – which correspond to the flat, dashed line – we superimpose the improved, λ_5 -dependent, curves $[\delta\rho^{[1-\text{eff}]}]$ derived via Eqs. (43). By dialing the parameter λ_5 we portray the dependence of $\delta\rho^{[1-\text{eff}]}$ on the Higgs boson self-interaction enhancements. With decreasing λ_5 values, the difference $\Delta(\delta\rho^{\text{eff}}) \equiv (\delta\rho^{[1-\text{eff}]} - \delta\rho^{[1]})$ obviously goes to zero – and in this case the curves $\delta\rho^{[1]}$ and $\delta\rho^{[1-\text{eff}]}(\lambda_5)$ tend to merge.

A complementary numerical account is provided in Table 2. Here we consider Sets I-IV of Higgs boson masses from Table 1, with corresponding SM-like couplings for the ~ 125 GeV \mathcal{CP} -even Higgs boson (h^0 or H^0) state in all the cases. Moreover, we also investigate the particular instances $\alpha = 0$ (for Set I) and $\alpha = \pi/2$ (for Set II), these are the so-called *fermiophobic* Higgs limits of type-I 2HDM. Most significantly, in this table we quantify the maximum attainable departures $|\Delta(\delta\rho^{\text{eff}})|$ from the plain one-loop predictions. These optimal scenarios are realized for particular choices of $\tan\beta$ and λ_5 (as quoted in the last rows of the table), saturating the 2HDM unitarity bounds [95]. Such configurations are preferably achieved for small $\tan\beta \sim 1 - 2$ and moderate (negative) $\lambda_5 \sim -5/ -10$.

These results clearly spell out the physical meaning of $\delta\rho$ as a measure of the $SU(2)$ custodial symmetry violation. The plain one-loop prediction for $\delta\rho$ ranges from $\mathcal{O}(10^{-4})$ (for Sets I and II, viz. for relatively light Higgs bosons with unconstrained mass splittings) to $\mathcal{O}(10^{-5})$ (for Sets III and IV, wherein the heavier Higgs bosons are tailored to mimic the mass splittings of SUSY-like spectra). We may track down this same feature too from the right panels of Fig. 10, in which we again superimpose the mere one-loop prediction $[\delta\rho^{[1]}]$ and the improved one $[\delta\rho^{[1-\text{eff}]}]$, as a function of λ_5 , for the complementary mass Sets V-VIII. The sizable value of $\delta\rho$, at the $\mathcal{O}(10^{-3})$ level for Set V (this means nearly overshooting the custodial

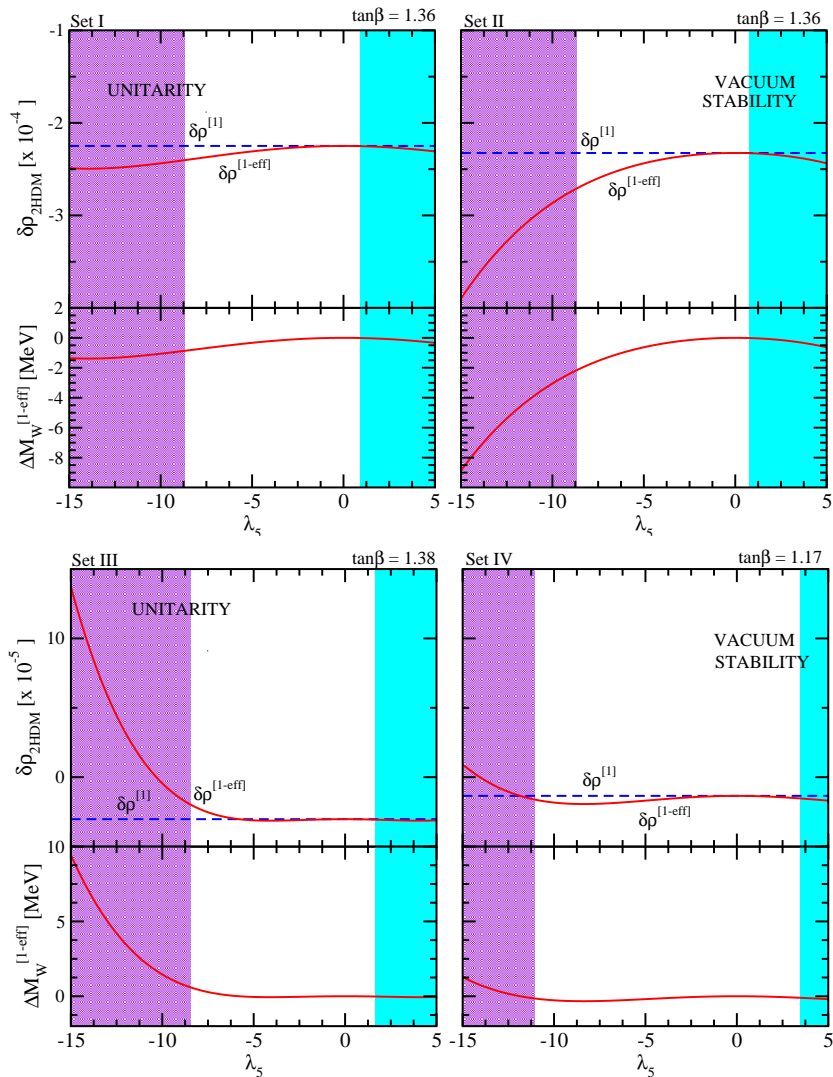


Fig. 9. 2HDM contribution to the parameter $\delta\rho$, as a function of the self-coupling λ_5 , for different sets of Higgs boson masses. We superimpose the pure one-loop $[\delta\rho^{[1]}]$ and the improved one-loop $[\delta\rho^{[1-\text{eff}]}]$ results. The latter trades the dominant higher order effects from the enhanced Higgs boson self-interactions. The quantitative impact of these higher order corrections on the prediction of the W-boson mass is displayed in the lower panels. The latter we compute via the contribution from $\delta\rho^{[1-\text{eff}]}$ to Δr , see Eq. (46). For each set of Higgs boson masses, the value of $\tan\beta$ is chosen such that the 3h self-couplings maximize for the largest allowed $|\lambda_5|$ values. The shaded areas account for the unitarity (left) and vacuum stability bounds (right).

symmetry limit $|\delta\rho| \lesssim 10^{-3}$) depletes very remarkably when the heavier Higgs boson masses – and so the different mass splittings – are pulled down all the way from Set V to Set VIII (cf. Table 1).

By the same token, the relative importance of the leading higher order corrections to $\delta\rho$ becomes drastically promoted in some cases (at the highest available values of λ_5), as we quantify explicitly on the left panels of Fig. 10. This is in part because these higher order quantum effects are added to a decreasing one-loop piece $[\delta\rho^{[1]}]$ – which falls down by roughly one order of magnitude if we compare again Sets V and VIII. At the same time, the boost in the relative departure $\Delta(\delta\rho^{\text{eff}})/\delta\rho^{[1]}$ is also partly explained due to the smaller mass suppression of the one-loop Higgs-

| | Set V | Set VIII |
|-----------------|-----------------------|-----------------------|
| a_{H^0H+W-} | 8.06×10^{-2} | 1.56×10^{-1} |
| $a_{H^0A^0Z^0}$ | 6.21×10^{-2} | 1.70×10^{-1} |
| a_{A^0H+W-} | 1.47×10^{-3} | 1.16×10^{-2} |
| $b_{h^0Z^0Z^0}$ | 2.60×10^{-2} | 3.70×10^{-2} |
| b_{h^0W+W-} | 2.60×10^{-2} | 3.70×10^{-2} |

Table 3. Coupling strengths a_{hhV} and b_{hVV} – cf. Eq. (42) – for a representative set of hhV and hVV effective interactions. We compare them numerically for Sets V and VIII (cf. Table 1), assuming $\alpha = \beta - \pi/2$ and fixing $\tan\beta$ and λ_5 such that the triple Higgs boson self-coupling enhancements maximize – in a way compatible with all the bounds.

| | Set I $\alpha = \beta - \pi/2$ | Set I $\alpha = 0$ | Set II $\alpha = \beta$ | Set II $\alpha = \pi/2$ | Set III $\alpha = \beta - \pi/2$ | Set IV $\alpha = \beta - \pi/2$ |
|--|-----------------------------------|-----------------------|----------------------------|----------------------------|-------------------------------------|------------------------------------|
| $\Delta r_{\text{SM}} [\times 10^{-3}]$ | 37.744 | 37.744 | 37.443 | 37.443 | 37.744 | 37.744 |
| $\Delta r_{2\text{HDM}}^{[1]} [\times 10^{-3}]$ | 36.701 | 36.650 | 36.352 | 36.409 | 35.845 | 35.603 |
| $\delta(\Delta r_{2\text{HDM}}^{[1]}) [\times 10^{-3}]$ | -1.043 | -1.094 | -1.091 | -1.034 | -1.899 | -2.141 |
| $ \delta(\Delta r_{2\text{HDM}}^{[1]})/\Delta r_{2\text{HDM}}^{[1]} [\%]$ | 2.8 | 3.0 | 3.0 | 2.8 | 5.3 | 6.0 |
| $\delta\rho^{[1]} [\times 10^{-4}]$ | -2.249 | -2.192 | -2.325 | -2.387 | -0.302 | -0.134 |
| $\delta\rho^{[1-\text{eff}]} [\times 10^{-4}]$ | -2.403 | -2.348 | -2.709 | -3.014 | -0.197 | -0.160 |
| $ \Delta(\delta\rho^{\text{eff}})/\delta\rho^{[1]} [\%]$ | 6.8 | 7.1 | 16.5 | 26.3 | 35.0 | 19.0 |
| $\delta M_W^{[1]} [\text{MeV}]$ | 17.257 | 18.078 | 18.021 | 17.102 | 31.071 | 34.967 |
| $\Delta M_W^{[1-\text{eff}]} [\text{MeV}]$ | -0.865 | -0.880 | -2.166 | -3.537 | 0.596 | -0.144 |
| $\tan\beta$ | 1.36 | 1.36 | 1.36 | 1.36 | 1.38 | 1.17 |
| λ_5 | -8.68 | -8.68 | -8.68 | -8.68 | -8.46 | -11.08 |

Table 2. Detailed numerical analysis of the different electroweak quantities under survey, these are: Δr , $\delta\rho$ and M_W . We examine different choices of Higgs boson masses (cf. Table 1) and trigonometric couplings. The values of $\tan\beta$ and λ_5 (see the bottom rows of the table) maximize the enhanced higher order effects induced by the Higgs boson self-interactions. The notation $\delta(\Delta r_{2\text{HDM}}^{[1]})$ spells out the “genuine” one-loop 2HDM effects (i.e. after consistent subtraction of the SM part) – cf. Eqs. (22) – (24). In turn, $\delta\rho^{[1]}$ and $\delta M_W^{[1]}$ denote the one-loop shifts on these parameters from those genuine 2HDM one-loop effects, while $\Delta(\delta\rho^{\text{eff}})$ and $\Delta M_W^{[1-\text{eff}]}$ represent the corresponding higher order effects on $\delta\rho$ and M_W beyond one-loop, computed in our approach – cf. Eqs. (43) and (46).

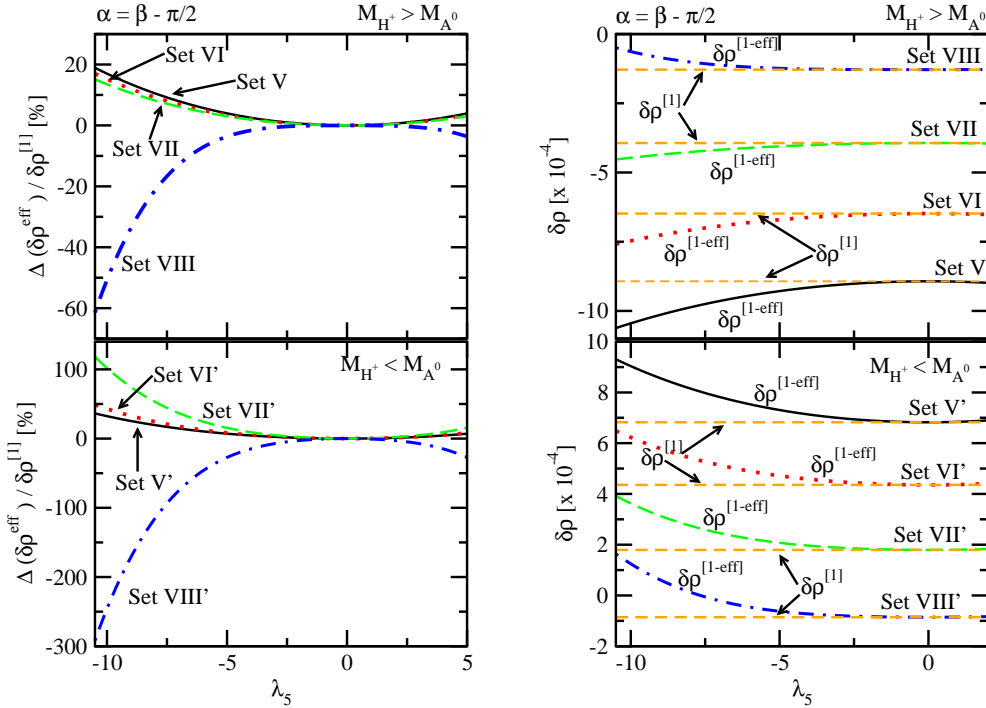


Fig. 10. Impact of the leading higher order corrections to $\delta\rho$. On the left panels we evaluate their influence through the relative departure $[\Delta(\delta\rho^{\text{eff}})/\delta\rho^{[1]} \equiv (\delta\rho^{[1-\text{eff}]} - \delta\rho^{[1]})/\delta\rho^{[1]} [\%]]$ as a function of the self-coupling λ_5 . We consider the Higgs boson mass sets from Table 1 with both direct (Sets V–VIII, top panel) and inverted (Sets V’–VIII’, bottom panel) mass hierarchies between the A^0 and the H^{\pm} fields. We set $\alpha = \beta - \pi/2$ and fix $\tan\beta$ as quoted in Table 1, so that the 3h self-coupling enhancements maximize for a given λ_5 – saturating the unitarity bounds for each of the mass sets, cf. Table 4. Complementarily, on the right panels we present the absolute value of $\delta\rho$, again as a function of λ_5 and for the different sets of masses. In each case we superimpose the mere one-loop results $[\delta\rho^{[1]}]$ and those including the dominant higher-order corrections $[\delta\rho^{[1-\text{eff}]}(\lambda_5)]$. Let us notice that unitarity and vacuum stability constraints are not explicitly included in the figure; the phenomenologically viable λ_5 range for each of masses is explicitly quoted in Table 4.

mediated effects. In Table 3 we settle this statement quantitatively, by comparing the actual coupling strength of a number of effective interactions for Sets V and VIII – this is to say, when we assume heavier (resp. lighter) Higgs bosons (cf. Table 1).

We can also rephrase these results as a relative contribution to Δr (cf. Eq. (11)), namely via the term $\Delta r^{[\delta\rho]}$, of the order of $\sim 5\%$ to $\sim 50\%$ to the overall 2HDM prediction $[\Delta r_{2\text{HDM}}]$. This quantity grows along with the mass splittings between the different Higgs bosons. That explains e.g. why, for Sets I and II, these $\delta\rho$ -driven contributions are more sizable than those for the SUSY-like Sets III and IV (that stagnate at the $\mathcal{O}(10^{-5})$ level). In contrast, for the last two sets the total Δr values are larger. This simply means that the *on-shell* gauge boson self-energies or, in other words, the non-static contributions to Δr , are more relevant here, as compared to the self-energies evaluated at *zero momentum*. The induced shift (from strict one-loop 2HDM effects) on the W-boson mass prediction $[\Delta M_W^{[1]}]$ is correspondingly larger for the SUSY-inspired mass sets. Specifically, $\Delta M_W^{[1]} \sim 15$ MeV for Sets I and II, versus $\Delta M_W^{[1]} \sim 30$ MeV for Sets III and IV – cf. Table 2 and Fig. 4. This is not surprising, after all. As we have already analyzed in Section 3, the MSSM tends to relax –sometimes very substantially – the existing tension between the SM theory predictions and the experimental measurements of electroweak precision quantities [56]. We may turn around this observation and say –emphasizing once more the claim made in Sec. 3 – that our study shows that the general 2HDM can perform equally well than the MSSM in the task of fostering the agreement between the theoretical prediction of the W-mass versus its experimentally measured value.

In this respect, it is interesting to emphasize again that in the MSSM case the Higgs bosons alone induce a rather moderate contribution to the EW quantities Δr and $\delta\rho$, as compared to the situation when the squark, slepton and chargino-neutralino sectors are not very heavy. Having already dwelled on Δr and M_W in Section 3, let us now quantify the typical size of the MSSM contributions to $\delta\rho$. Again, we start by considering Set III of Higgs boson masses (cf. Table 1), based on the (*maximal mixing*) MSSM benchmark – which comprises $\mathcal{O}(100)$ GeV charginos and neutralinos, ~ 700 GeV stops, large Higgs-stop trilinear couplings, and the remaining sfermions above 1 TeV. Employing FEYNHIGGS [98] to extract the full MSSM contribution to $\delta\rho$ within this scenario, we find $\delta\rho_{\text{MSSM}} = 2.186 \times 10^{-4}$. In addition we can separately evaluate the contribution driven by the MSSM Higgs sector alone by means of our 2HDM calculation, namely by plugging the mixing angle value $\alpha_{\text{MSSM}} = -0.188$ which corresponds to that specific MSSM benchmark. Once more we can use FEYNHIGGS for its numerical evaluation, and we obtain $\delta\rho_{\text{MSSM}}^{\text{Higgs}} = -2.910 \times 10^{-5}$. This result clearly illustrates how the pure SUSY Higgs-induced contribution to $\delta\rho$ falls roughly one order of magnitude below the total MSSM budget. The SUSY embedding for Set IV, in turn, features much heavier [viz. $\mathcal{O}(500)$ GeV] weak gauginos,

with $\sim 1 - 2$ TeV sfermion masses and weaker Higgs-stop couplings. In this case we find $\delta\rho_{\text{MSSM}} = 5.211 \times 10^{-6}$ for the total payoff of the MSSM, whilst $\delta\rho_{\text{MSSM}}^{\text{Higgs}} = -1.338 \times 10^{-5}$ for the specific SUSY Higgs part. As expected, the effects from the more massive SUSY degrees of freedom are relatively suppressed and the total contribution from sfermions and chargino-neutralinos is, in this particular case, comparable (albeit opposite in sign) to that of the Higgs bosons, so the overall MSSM yield is significantly smaller than in the previously discussed case.

Let us now come back to the role of the leading higher-order corrections governed by enhanced Higgs boson self-couplings of the 2HDM. We spotlight significant effects which, in some particular corners of the parameter space, may well trigger relative deviations with respect to the one-loop prediction as large as $\Delta(\delta\rho^{\text{eff}})/\delta\rho^{[1]} \sim \mathcal{O}(30)\%$ or above. Quite remarkably, these numerical results could be foreseen from the rough analytical estimate

$$\delta\rho_{2\text{HDM}}^{[1-\text{eff}]} \simeq \delta\rho_{2\text{HDM}}^{[1]} \left(1 + \frac{1}{16\pi^2} \frac{|\lambda_{\text{hhh}}|^2}{M_h^2} \right)^2, \quad (45)$$

which follows from the approximate form factors quoted in Eq. (42). On the one hand, the triple Higgs boson self-couplings may reach maximum values of $\lambda_{\text{hhh}} \sim \mathcal{O}(10^3)$ GeV, as we can read off Fig. 7 and Eq. (18); and, on the other, the typical Higgs boson masses considered in our analysis are of $\mathcal{O}(100)$ GeV. Plugging these numbers into Eq. (45) we indeed retrieve $\Delta(\delta\rho^{\text{eff}})/\delta\rho^{[1]} \sim 50 - 100\%$, which agrees with the outcomes of our full numerical calculation to a remarkable extent.

The parametric dependence on λ_5 , as displayed in Figs. 9-12, exhibits the expected behavior $\delta\rho \sim (A\lambda_5^4 + B\lambda_5^2 + C)$, which results from the structure of the (Born-improved) Higgs/gauge boson couplings $g_{hhV}^{\text{eff}} \sim g(1 + \mathcal{O}(\lambda_5^2))$ – entering of course square in the gauge boson self-energies. It is for this reason that the leading correction to $\delta\rho$ is of $\mathcal{O}(\lambda_5^4)$. Evidently this correction goes beyond the 2-loop level and therefore it tests in an effective way the largest possible effects that can be expected from the λ_5 parameter at all orders. This kind of effective approach is not new, let us note that it is fully within the line of reasoning presented in the work of Ref. [67], which was devoted to compute not only the full one-loop effects but also to test the largest possible quantum corrections that the trilinear Higgs boson self-couplings could produce at all orders in the pairwise production of neutral 2HDM Higgs bosons in a linear collider. We remark that the one-loop diagrams used in that calculation are essentially identical to those we are using here to construct the improved couplings (43) for the present calculation, i.e. we are proceeding along the same philosophy as in Ref. [67].

The leading large λ_5 corrections, if effectively realized in nature, would also manifest as a shift $\Delta M_W^{[1-\text{eff}]}$ on the W-boson mass prediction. This shift we can roughly

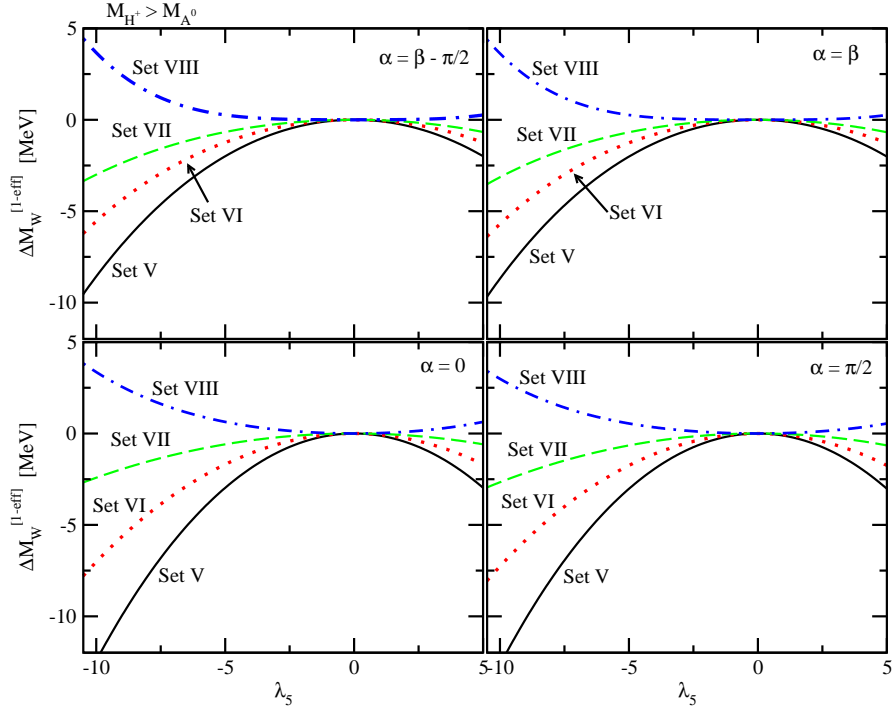


Fig. 11. Overall shift in the theoretical prediction for the W-boson mass (cf. Eq. (46)), driven by the leading Higgs-mediated higher-order corrections, as a function of the self-coupling λ_5 . The results are displayed separately for Sets V-VIII (cf. Table 1) with a *direct* mass hierarchy [$M_{H^\pm} - M_{A^0} > 0$], and for different choices of the mixing angle α . We fix $\tan \beta$ as quoted in Table 4, so that the 3H self-coupling enhancements maximize at the largest allowed $|\lambda_5|$ values – also given in the table.

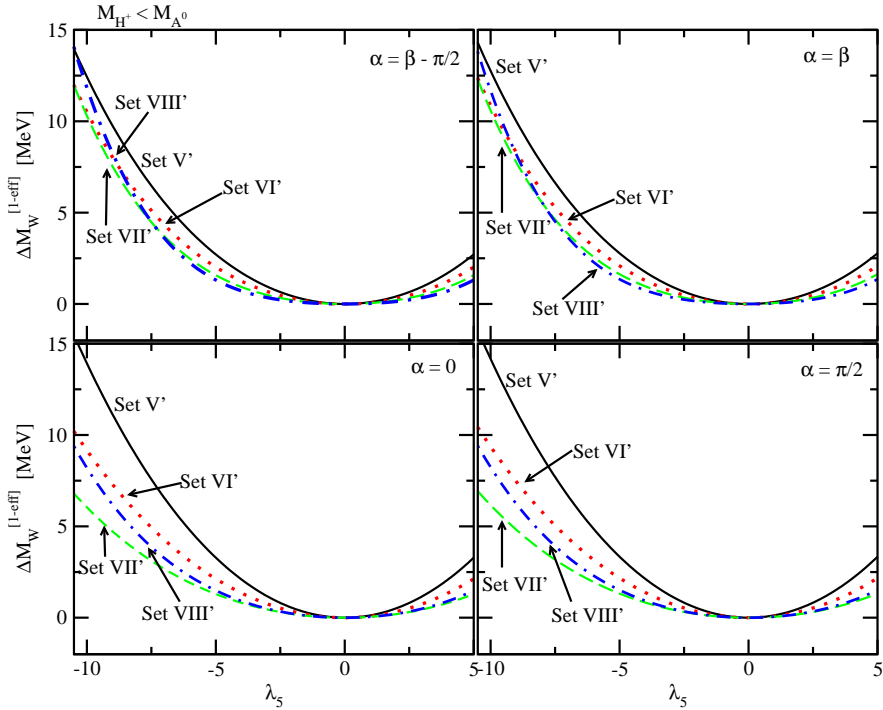


Fig. 12. Analogous setup and results as in Fig. 11, for Sets V'-VIII' of Higgs boson masses with an *inverted* mass hierarchy [$M_{H^\pm} - M_{A^0} < 0$].

estimate by means of $\Delta r^{[\delta\rho]}$, whereby

$$\begin{aligned} |\Delta M_W^{[1-\text{eff}]}| &\equiv |\delta M_W^{[1-\text{eff}]} - \delta M_W^{[1]}| \\ &\simeq \frac{M_W}{2} \frac{c_W^2}{c_W^2 - s_W^2} \times \left| \delta\rho^{[1-\text{eff}]} - \delta\rho^{[1]} \right| \\ &\simeq 5.67 \times 10^4 \text{ [MeV]} \Delta(\delta\rho^{\text{eff}}). \end{aligned} \quad (46)$$

Obviously this formula follows the same pattern as (28) up to the factor c_W^2/s_W^2 inherent to the definition of $\Delta r^{[\delta\rho]}$. The results for this estimate of $\Delta M_W^{[1-\text{eff}]}$ are displayed in the lower panels of Fig. 9. Notice that departures from the mere one-loop order by an amount of $\Delta(\delta\rho^{\text{eff}})/\delta\rho^{[1]} \sim \mathcal{O}(30)\%$ translate, for the mass sets under consideration, into a mass shift of up to $\Delta(\delta M_W) \sim \mathcal{O}(3)$ MeV – as we can confirm from Table 2 and from the lower panels of Fig. 9. The largest absolute higher-order corrections to $\delta\rho$ – attained of course for the maximum allowed (negative) values of λ_5 – are possible within non-SUSY-like Higgs boson mass spectra (Sets I and II). For the SUSY-like Sets III and IV, however, these effects are much more tamed, and amount to barely $\mathcal{O}(1)$ MeV. Recall that despite the inconspicuous λ_5 -yield in this case, the full one-loop 2HDM correction on Δr is larger for those sets and therefore the overall impact is more sizeable (cf. third row of Table 2 and Figs. 3-4).

We also study the complementary Sets V-VIII and V'-VIII' (i.e. considering both the direct and the inverted mass hierarchies) in Figs. 11 and 12 respectively, and also in Table 4. For each of the mass sets we have different lower – and upper constraints on λ_5 , that we explicitly account in the left-most columns of the table. The parameter $\tan\beta$ we fix accordingly, so that the Higgs self-coupling enhancements maximize for the largest allowed $|\lambda_5|$. The maximum attainable relative deviations on the $\delta\rho$ -parameter [$\Delta(\delta\rho^{\text{eff}})/\delta\rho^{[1]}$], alongside with the associated shift on the predicted W-boson mass [$\Delta M_W^{[1-\text{eff}]}$], are documented in the right columns. The results fall in the very same ballpark as for sets I-IV that we have examined previously. Again, the relative impact of the higher order effects can reach $\Delta(\delta\rho^{\text{eff}})/\delta\rho^{[1]} \sim \mathcal{O}(30\%)$, but in this case dragging the W-boson mass predictions up to $\Delta M_W^{[1-\text{eff}]} \simeq 10 - 15$ MeV in those regimes (viz. Sets V and V') which saturate the custodial symmetry bounds $|\delta\rho| \lesssim 10^{-3}$. For this reason, within these complementary mass sets we identify corrections to M_W that can be up to three times bigger than in the original Sets I-IV. We should nonetheless point out that such remarkable effects beyond one-loop critically rely on a very large departure from the custodial symmetry limit, and hence are not favored by the EW precision data. Barring these borderline situations, a milder custodial symmetry breaking – e.g. at the level $|\delta\rho| \sim \mathcal{O}(10^{-4})$ – typically renders one loop corrections of up to $\delta M_W^{[1]} \simeq 40$ MeV combined with higher order mass shifts [$\Delta M_W^{[1-\text{eff}]}$] in the ballpark of $\mathcal{O}(1 - 5)$ MeV. This result is nevertheless quite significant, as it implies that the characteristic higher order 2HDM corrections can be

a few times larger than the pure bosonic $\mathcal{O}(\alpha_{ew}^2)$ two-loop corrections (which perform at the $\lesssim 1$ MeV level), and even comparable to most higher order corrections within the SM. Finally, they can be as large as the estimated theoretical uncertainty ($\delta M_W^{\text{th}} \simeq 4$ MeV) of the SM effects beyond the 2-loop order [40]. In all cases the results are seen to be very much responsive to λ_5 , while they barely depend on the precise choice of the mixing angle α .

The results illustrate once more the compromise between the two different trends that govern the overall impact of the higher order effects, and that somehow counterbalance each other: i) heavier – versus lighter masses: the heavier the Higgs bosons, the weaker will be the loop-induced effects they generate – these shall be typically suppressed by inverse powers of such masses; ii) wider – versus narrower mass splittings; as we have discussed, these will determine the size of the pure one-loop piece [$\delta\rho^{[1]}$], and hence of the consequent mass shift [$\delta M_W^{[1]}$] and the corresponding higher-order contributions. This explains e.g. why Set V is the most responsive one, as it combines a sizable mass splitting between the \mathcal{CP} -even, the \mathcal{CP} -odd and the charged Higgs fields; and yet relatively light (viz. $M_h \sim 125$ GeV) neutral, \mathcal{CP} -even states.

5 Discussion and Conclusions

In this work we have revisited the traditional electroweak (EW) parameter Δr from the viewpoint of the general (unconstrained) Two-Higgs-Doublet Model (2HDM) [59–63]. That quantity, whose definition – cf. Eq. (3) – was introduced more than thirty years ago [43,44]– spells out the quantum link between the EW gauge boson masses (M_W, M_Z) and the Fermi constant (G_F), and thereby enables an accurate theoretical prediction for the mass of the W-boson [M_W^{th}], based on the precise knowledge of the Z-boson mass [M_Z], the fine structure constant [α] and Fermi's constant [G_F] as experimental inputs. Analyses of Δr have been instrumental in the past, both as precision tests of the SM and as a strategy to seek for hints of new physics, as well as to derive constraints on the parameter space of theories beyond the SM. After carefully reexamining the one-loop 2HDM contributions ($\Delta r_{2\text{HDM}}$) to the parameter Δr at one loop, namely at $\mathcal{O}(\alpha_{ew})$, we have folded these effects with all the known higher order SM corrections to that quantity in a consistent way within the allowed region of the 2HDM parameter space. Of course the overlap of the SM Higgs boson contribution and the lightest neutral \mathcal{CP} -even state of the 2HDM has also been consistently removed. With this procedure we have been able to bring to date the numerical analysis of Δr and the corresponding prediction of the W-mass within the 2HDM in a way comparable to the SM case.

In the numerical analysis we have scrutinized a variety of regimes with phenomenological relevance and in full compliance with a brought-to-date set of restrictions that severely constrain the parameter space of the model – most significantly the unitarity and vacuum stability conditions, together with the low energy flavor physics

| $M_{\mathbf{H}^\pm} > M_{\mathbf{A}^0}$ | | | | $\alpha = \beta - \pi/2$ | | $\alpha = \beta$ | | $\alpha = \frac{\pi}{2}$ | | $\alpha = 0$ | |
|---|--------------------|--------------------|--------------|---|---|---|---|---|---|---|---|
| | λ_5^{\min} | λ_5^{\max} | $\tan \beta$ | $\frac{\Delta(\delta\rho^{\text{eff}})}{\delta\rho^{[1]}}$ [%] | $\Delta M_{\mathbf{W}}^{1\text{-eff}}$ [MeV] | $\frac{\Delta(\delta\rho^{\text{eff}})}{\delta\rho^{[1]}}$ [%] | $\Delta M_{\mathbf{W}}^{1\text{-eff}}$ [MeV] | $\frac{\Delta(\delta\rho^{\text{eff}})}{\delta\rho^{[1]}}$ [%] | $\Delta M_{\mathbf{W}}^{1\text{-eff}}$ [MeV] | $\frac{\Delta(\delta\rho^{\text{eff}})}{\delta\rho^{[1]}}$ [%] | $\Delta M_{\mathbf{W}}^{1\text{-eff}}$ [MeV] |
| Set V | -10.82 | 0.93 | 1.19 | 20.22 | -10.19 | 20.51 | -10.34 | 29.76 | -15.00 | 29.15 | -14.70 |
| Set VI | -9.55 | 0.87 | 1.29 | 13.77 | -5.04 | 14.10 | -5.16 | 18.21 | -6.66 | 17.53 | -6.41 |
| Set VII | -8.04 | 0.81 | 1.42 | 8.30 | -1.84 | 8.57 | -1.91 | 7.76 | -1.72 | 6.97 | -1.55 |
| Set VIII | -6.55 | 0.76 | 1.58 | -9.96 | 0.72 | -3.37 | 0.71 | -14.00 | 1.02 | -16.26 | 1.18 |
| $M_{\mathbf{H}^\pm} < M_{\mathbf{A}^0}$ | | | | | | | | | | | |
| Set V' | -9.83 | 0.88 | 1.27 | 31.46 | 12.07 | 31.86 | 12.38 | 35.64 | 13.78 | 35.08 | 13.52 |
| Set VI' | -8.37 | 0.83 | 1.39 | 27.36 | 6.71 | 27.68 | 6.93 | 25.75 | 6.40 | 25.32 | 6.25 |
| Set VII' | -6.85 | 0.77 | 1.55 | 34.93 | 3.53 | 24.65 | 6.17 | 23.39 | 5.82 | 25.00 | 2.57 |
| Set VIII' | -5.40 | 0.72 | 1.75 | -34.04 | 1.64 | -39.28 | 1.68 | -40.62 | 1.79 | -37.78 | 1.77 |

Table 4. Parameter space survey for Sets V-VIII and V'-VIII' in Table 1. The left-most columns quote the allowed λ_5 range, in agreement with the constraints from perturbative unitarity and vacuum stability. Alongside we indicate the corresponding value of $\tan \beta$ that maximizes the Higgs boson self-interaction enhancements for the largest allowed $|\lambda_5|$. Within these optimal scenarios, and for different choices of α , in the right part of the table we quantify i) the relative size of the higher order effects on the $\delta\rho$ -parameter, $\Delta(\delta\rho^{\text{eff}})/\delta\rho^{[1]}$; and ii) the induced shift on the W-boson mass prediction [$\Delta M_{\mathbf{W}}^{1\text{-eff}}$], as defined by Eq. (46).

observables $\mathcal{B}(b \rightarrow s\gamma)$ and $B_d^0 - \bar{B}_d^0$. Needless to say, we have included as well the important phenomenological implications associated to the recent ~ 125 GeV Higgs-like state observed at the ATLAS and CMS detectors. We have examined various sets of Higgs boson masses, and used them to test the different response to considering: i) relatively light versus relatively heavy spectra; ii) relatively broad versus relatively narrow spectra; iii) a fully unconstrained choice versus a supersymmetric MSSM-like one. In all cases the genuine 2HDM effects on Δr exhibit a characteristic dependence on the Higgs boson masses, which manifests as a sort of antagonism between the following two tendencies: 1) the boosting of the 2HDM contributions to Δr from a significant mass splitting among the 2HDM Higgs states (caused by a stronger violation of the underlying $SU(2)$ custodial symmetry); 2) the weakening of the 2HDM contributions to Δr when employing heavier sets of Higgs boson masses – obviously related to the suppression of the corresponding loop corrections.

Let us also note that while our final results do of course depend on the details of the Higgs mass spectra, they are essentially unresponsive to the precise setup of Yukawa-coupling structures, i.e. they are insensitive to type-I or type-II 2HDM. This is not surprising at first sight, as no Higgs/fermion couplings enter the leading (one-loop) evaluation of the gauge boson self-energies. What is less obvious is that at higher orders, where the 2HDM Yukawa couplings could, in principle, play a non-negligible role, they are finally impotent, too, owing to the stringent theoretical and phenomenological constraints currently in force, in particular the condition that the regime of $\tan \beta = \mathcal{O}(1)$ is highly preferred. As a result the strength of the 2HDM Yukawa couplings is essentially the same as in the SM case within the physically allowed region. The different impact of type-I or type-II 2HDM on the evaluation of Δr enters our calculation in a completely indirect way, namely only through the specific (and significantly unequal) parameter space restrictions affecting each one of these models.

Doubtlessly an expected but most salient feature of our analysis of Δr within the general 2HDM is the following: the sole addition of a second $SU_L(2)$ Higgs boson doublet significantly relaxes the persistent $M_{\mathbf{W}}^{\text{th}} - M_{\mathbf{W}}^{\text{exp}}$ tension existing between theory and experiment. With only one Higgs doublet the global fits to EW precision data favor a Higgs boson lighter than expected (even below the LEP bounds) – precisely due to the dependence of Δr , and so of $M_{\mathbf{W}}^{\text{th}}$, on the Higgs boson mass(es). With an additional doublet the SM-like Higgs boson can stay comfortably at a mass value closer to the present experimental measurements since the rest of the (heavier) Higgs bosons provide the mechanism to compensate for the difference. All the explored scenarios feature very similar trends concerning both the obtained results and parameter space dependence for the quantities under scrutiny. We identify a variety of regions within the 2HDM parameter space leading to typical variations of Δr in the ballpark of $\delta(\Delta r) \sim \mathcal{O}(10^{-3})$, which translate into W-mass shifts of $\delta M_{\mathbf{W}}^{2\text{HDM}} \sim 20 - 40$ MeV. Being the current experimental error on the W-mass of $\delta M_{\mathbf{W}}^{\text{exp}} = \pm 15$ MeV (and the current discrepancy with the SM value of the same order of magnitude: $M_{\mathbf{W}}^{\text{SM}} - M_{\mathbf{W}}^{\text{exp}} \simeq -20$ MeV), it is pretty obvious that the 2HDM effects are potentially very important to help the SM theoretical prediction (which is in deficit) to better match the experimental value. This is the more true if we recall that the future measurements may reduce the mass uncertainty further (hopefully at the ~ 5 MeV level), which means that we might be able to eventually confirm or exclude the SM value at a rather significant confidence level.

While the above feature has been previously emphasized in the literature within the MSSM case, we confirm here for the first time that the general 2HDM shares this virtue. This may perhaps be viewed as not too surprising a posteriori since this fact basically depends (at one-loop) on the bulk contribution of the interactions of the gauge bosons with the new 2HDM Higgs states as compared to the single Higgs state in the SM. Let us

note that in the context of the MSSM the Higgs sector is highly constrained and in general it provides a rather modest contribution to Δr . However, there we still have the additional one-loop contributions from the genuine supersymmetric particles (e.g. from squarks, sleptons, and chargino-neutralinos). At one loop all these genuine SUSY effects are gauge-like interactions (since no Yukawa-like enhancement is possible at all at this order), and therefore they may amply compensate for the meager output from the MSSM Higgs sector, especially if the masses of some of the sfermions and/or chargino-neutralinos remain relatively light, i.e. at the few hundred GeV level. It is thanks to this feature that the overall theoretical predictions on Δr (and M_W) can be more in accordance with experiment within the MSSM than in the SM.

What we have shown in this work is that this is also the case for the general non-supersymmetric 2HDM, albeit for a completely different reason. Here the Higgs sector is less constrained and we have found that upon enforcing all the known restrictions from perturbative unitarity, vacuum stability, flavor and custodial symmetry, and direct search limits, the Higgs sector alone is indeed able to render corresponding Δr and M_W predictions perfectly comparable to the total payoff of the MSSM. We believe it is useful and remarkable to have verified this fact explicitly, as it was not obvious a priori that the stringent current constraints on the 2HDM parameter space would still permit such possibility.

No less remarkable in our study is the possible (and distinctive) quantum effects that the general 2HDM can provide beyond one-loop. This has been explored in the second part of our study, where we have dwelled upon the role of the higher order effects induced by the Higgs boson self-interactions on these EW precision quantities, specifically on the bearing they may have on the parameter $\delta\rho$ and hence on the characteristic Δr part carrying its influence (viz. $-c_W^2 \delta\rho/s_W^2$). Owing to the various constraints, the Higgs boson self-interactions are most efficiently enhanced in the limit of large values of the λ_5 -parameter in the general 2HDM Higgs potential. In turn the weak gauge boson self energies are responsive to them via Higgs boson-mediated corrections only at the two-loop level and beyond, which obviously makes the full task of computing them rather cumbersome. We have worked out a numerical estimate of such higher order effects by means of a Born-improved Lagrangian approach which tracks the leading λ_5 self-coupling effects in the limit of large values of this parameter (within the allowed bounds). First, we have computed the dominant radiative corrections to all Higgs/gauge boson interactions in this limit. These corrections can be accounted for via a gauge invariant, UV-finite subset of (Higgs-mediated) one-loop diagrams from which we retain the $\mathcal{O}(\alpha_{\text{ew}} \lambda_5^2)$ contributions. Second, we have rewritten these one-loop amplitudes as static form factors and used them to effectively *dress* the bare Higgs/gauge boson interactions.

Quantitatively speaking, these higher order quantum effects on the $\delta\rho$ parameter may entail characteristic corrections to the 2HDM one-loop result as large as $\sim 30\%$

– for Higgs boson self-interactions already bordering the unitarity limit. The corresponding impact on the theoretical prediction of the W-boson mass is typically of a few MeV. This is already a noteworthy result, since these typical effects are of the order of the present theoretical uncertainty within the SM prediction. Let us however mention that in limiting regions of the parameter space the higher-order 2HDM corrections could shift the W -mass predictions up to $\sim 10 - 15$ MeV. Overall we find that the estimated higher-order effects within the 2HDM are small enough to remain beneath the limited precision of the current EW data, but at the same time they could be at reach of the expected experimental precision attainable at the LHC and future TeV-range linear colliders. Finally, to better appreciate the potential significance of these effects, it is instructive to note that they can be not only substantially larger than the pure bosonic $\mathcal{O}(\alpha_{\text{ew}}^2)$ two-loop contribution within the SM (which is long known to be of order of 1 MeV, at most) but they could even be of the same order than the remaining set of higher order pure QCD, EW and mixed QCD-EW effects.

The upshot of our study is that the general 2HDM possesses, under the full set of currently known theoretical and phenomenological constraints, both the capability to improve the bulk theoretical prediction of the W-mass as compared to the SM, and also the possibility to provide distinctive quantum effects that could reveal its underlying dynamics through the role played by the 2HDM Higgs boson self-interactions. We have demonstrated that their characteristic impact on Δr might not be inconspicuous at all, and could in fact be quite relevant for an accurate theoretical determination of the EW precision quantities. Ultimately, they could emerge above the experimental precision and signal a smoking gun of physics beyond the SM and the MSSM⁸. In this respect it is interesting to remark the apparently detected excess at the LHC in the $H \rightarrow \gamma\gamma$ decay mode with respect to the SM prediction. Very recently, some studies have suggested that such excess could be explained from the general 2HDM, specifically owing to the additional one-loop contribution from the charged Higgs bosons coupling to the photon, see e.g. [33, 34] and references therein. In point of fact, this kind of possible enhancement was previously noticed in the first detailed studies of single Higgs boson photoproduction and decay in the context of the 2HDM [81]. If so, relatively light charged Higgs bosons could be around the corner, maybe even within the LHC reach. If confirmed, the excess in the diphoton decay at the LHC combined with the detailed measurement of Δr and the W^\pm mass could strengthen the case for the general 2HDM as a powerful source of new Higgs boson physics beyond the SM. Of course an eventual direct detection of the charged Higgs bosons would round off the job. Bearing in mind the remarkable improvement in the experimental accuracy which is expected for the forthcoming W-mass measurements at the LHC

⁸ The potential importance of these distinctive quantum effects on Δr , as a trademark structure of (non-supersymmetric) extended Higgs sectors, was first suggested to the best of our knowledge in Ref. [67].

[viz. $\delta M_W^{\text{exp}} \sim 10 \text{ MeV}$], the analysis of the quantum effects on Δr combined with the valuable information from the direct searches may become instrumental in the near future. Now that the LHC seems to be finally closing in on the Higgs issue, efforts on the theory side are of foremost importance to broaden the assortment of strategies that will be necessary to bring this research program to a most successful completion.

The authors are very grateful to Wolfgang Hollik for enlightening conversations on this topic and also for providing useful references. The work of JS has been supported in part by the research Grant PA-2010-20807; by the Consolider CPAN project; and also by DIUE/CUR Generalitat de Catalunya under project 2009SGR502.

Appendix For the sake of completeness, we provide here-with a more detailed analytical account on selected aspects of our calculation. All UV divergences we handle by means of conventional dimensional regularization in the 't Hooft-Veltman scheme, setting the number of dimensions to $d = 4 - \epsilon$. As usual, we introduce an (arbitrary) mass scale μ in front of the loop integrals in order not to alter the dimension of the result in d dimensions with respect to $d = 4$. After renormalization (in the on-shell scheme, in our case) the results for the physical quantities are finite in the limit $d \rightarrow 4$. Furthermore, in the practical aspect of the calculation all one-loop structures are reduced in terms of standard Passarino-Veltman coefficients in the conventions of Ref. [97].

• **One loop functions at zero momentum:** the one-loop vacuum integrals that enter the evaluation of the parameter $\delta\rho$, which is built upon the weak gauge boson self energies at vanishing momenta, cf. Eq. (8), read as follows:

$$\begin{aligned} & \mu^{4-d} \int \frac{d^d q}{(2\pi)^d} \frac{g^{\mu\nu}}{q^2 - A + i\epsilon} = \frac{i g^{\mu\nu}}{16 \pi^2} A (\Delta_\epsilon - \log(A)) \\ & = \frac{i g^{\mu\nu}}{16 \pi^2} A_0(A); \end{aligned} \quad (47)$$

$$\begin{aligned} & \mu^{4-d} \int \frac{d^d q}{(2\pi)^d} \int_0^1 dx \frac{4 k^\mu k^\nu}{[q^2 - Ax - B(1-x) + i\epsilon]^2} \\ & = \frac{i g^{\mu\nu}}{16 \pi^2} [A (\Delta_\epsilon - \log A) + B (\Delta_\epsilon - \log B) + F(A, B)] \\ & = \frac{i g^{\mu\nu}}{4 \pi^2} \tilde{B}_{00}(A, B); \end{aligned}$$

$$\begin{aligned} & \mu^{4-d} \int \frac{d^d q}{(2\pi)^d} \int_0^1 dx \frac{g^{\mu\nu}}{[q^2 - Ax - B(1-x) + i\epsilon]^2} \\ & = \frac{i g^{\mu\nu}}{16 \pi^2} A \left[A (\Delta_\epsilon - \log A) - \frac{A+B}{2} + F(A, B) \right] \\ & = \frac{i g^{\mu\nu}}{16 \pi^2} \tilde{B}_0(A, B); \end{aligned} \quad (49)$$

where $\Delta_\epsilon = 2/\epsilon + 1 - \gamma_E + \log(4\pi\mu^2)$ and the function $F(x, y)$ is defined as follows:

$$F(x, y) = F(y, x) = \begin{cases} \frac{x+y}{2} - \frac{xy}{x-y} \log\left(\frac{x}{y}\right) & x \neq y \\ 0 & x = y \end{cases}. \quad (50)$$

The tilded notation for the Passarino-Veltman functions, e.g.

$$\tilde{B}(m_1^2, m_2^2) \equiv B(0, m_1^2, m_2^2), \quad (51)$$

indicates that these integrals are evaluated at zero momentum. The parameters A, B can be identified with the (squared of the) masses of the virtual particles propagating in the loop, $A \equiv m_1^2$, $B \equiv m_2^2$.

With these expressions at hand, it is straightforward to write down a compact analytical form for $\delta\rho_{2\text{HDM}}$ at one-loop in the 't Hooft-Feynman gauge, starting from the definition of Eq. (8):

$$\begin{aligned} \delta\rho_{2\text{HDM}} = & \frac{-\alpha}{16 \pi s_W^2 M_W^2} \left\{ \cos^2(\beta - \alpha) \left[F(M_{h^0}^2, M_{H^\pm}^2) \right. \right. \\ & \left. \left. - F(M_{h^0}^2, M_{A^0}^2) \right] \right. \\ & + \sin^2(\beta - \alpha) \left[F(M_{H^0}^2, M_{H^\pm}^2) - F(M_{H^0}^2, M_{A^0}^2) \right] \\ & + F(M_{A^0}^2, M_{H^\pm}^2) \\ & - 3 \cos^2(\beta - \alpha) \left[F(M_{H^0}^2, M_W^2) + F(M_{h^0}^2, M_Z^2) \right. \\ & \left. \left. - F(M_{H^0}^2, M_Z^2) - F(M_{h^0}^2, M_W^2) \right] \right\}. \end{aligned} \quad (52)$$

From the above equation we can explicitly read off how the size of $\delta\rho$ depends on the mass splitting between the different Higgs bosons, as well as on the strength of the Higgs/gauge boson couplings – which is modulated by $\tan\beta$ and the mixing angle α . The first two lines of the full expression (52) is the part that we have denoted $\delta\rho_{2\text{HDM}}^*$ in Sec. 2.4, see Eq. (15). We remark that for $M_{A^0} \rightarrow M_{H^\pm}$ and $|\beta - \alpha| \rightarrow \pi/2$ (in which the h^0 field behaves SM-like) the full $\delta\rho_{2\text{HDM}} \rightarrow 0$. This is the precise formulation of the decoupling regime for the unconstrained 2HDM.

In the case of the SM the Higgs contribution to the (48) $\delta\rho$ -parameter (8) is not finite if taken in an isolated form.

The complete bosonic contribution to Δr is of course finite and gauge invariant, and therefore unambiguous. To define a Higgs part of it is then a bit a matter of convention. What is important is that the complete M_H -dependence is exhibited correctly and coincides in all conventions. After removing the UV-parts which cancel against other bosonic contributions one arrives at

$$\delta\rho_{\text{SM}}^H = -\frac{3\sqrt{2}G_F}{16\pi^2} \left[M_Z^2 \ln \frac{M_Z^2}{\mu^2} - M_W^2 \ln \frac{M_W^2}{\mu^2} - \frac{4}{3} (M_Z^2 - M_W^2) + F(M_H, M_Z) - F(M_H, M_W) \right]. \quad (53)$$

The explicit dependence on the scale μ is unavoidable in quantities which are not UV-finite by themselves. It is however natural to set e.g. the EW scale choice $\mu = M_W$. In the limit $M_H^2 \gg M_W^2$ we can see Veltman's screening theorem at work in the SM, as there remain no M_H^2 terms but a logarithmic Higgs mass dependence. Indeed, in that limit the expression (53) reduces to

$$\delta\rho_{\text{SM}}^H \simeq -\frac{3\sqrt{2}G_F M_W^2 s_W^2}{16\pi^2 c_W^2} \left\{ \ln \frac{M_H^2}{M_W^2} - \frac{5}{6} \right\}, \quad (54)$$

which coincides with the result quoted in Eq.(12) of Sec. 2.3.

The SM Higgs boson contribution to $\delta\rho$ can also be retrieved from the 2HDM result (52) by selecting the h^0 parts of the contributions involving the h^0 and the gauge bosons, namely in the last line of that equation. By performing the identification $H \equiv h^0$ and removing the trigonometric factors we are led to

$$\begin{aligned} \delta\rho_{\text{SM}}^H &= \frac{3\alpha}{16\pi s_W^2 M_W^2} \left[F(M_H^2, M_Z^2) - F(M_H^2, M_W^2) \right] \\ &= -\frac{3\sqrt{2}G_F M_W^2 s_W^2}{16\pi^2 c_W^2} \ln \frac{M_H^2}{M_W^2} + \dots \end{aligned} \quad (55)$$

We see that the last expression coincides with Eq.(53) up to finite additive parts, which of course reflects the arbitrariness of the scale setting μ . As we said, this is not important because the full bosonic contribution to Δr is finite and unambiguous. The fact that we can recover the SM result from (52) in such a way suggests that the expression in the first line of (55) should be subtracted from (52) in order to compute the genuine 2HDM effects on $\delta\rho$, i.e. the Higgs boson quantum effects beyond those associated to the Higgs sector of the SM. This is in fact the practical recipe that we follow in this paper. Finally, let us notice that the $\delta\rho_{2\text{HDM}}^*$ part of (52), i.e. the one which is completely unrelated to the SM Higgs contribution, is precisely the part of the full $\delta\rho_{2\text{HDM}}$ that violates the screening theorem in the 2HDM, as it is manifest from Eq. (15) of Sec. 2.4.

• **2HDM contributions to the gauge boson self-energies:** We quote herewith their complete analytical form, in terms

of the standard Passarino-Veltman coefficients and following the conventions of Ref. [97]. The self-energies are evaluated for on-shell gauge bosons, e.g. $p^2 = M_V^2$ [$V = W^\pm, Z^0$], in the way they enter the calculation of Δr .

– Two Higgs-boson contributions:

$$\begin{aligned} \Sigma_W]_{2\text{HDM}}^{\text{Higgs}} &= \frac{\alpha}{16\pi s_W^2} \left[-A_0(M_{h^0}^2) - A_0(M_{H^0}^2) \right. \\ &\quad - A_0(M_{A^0}^2) - 2A_0(M_{H^\pm}^2) \\ &\quad + 4\cos^2(\beta - \alpha) B_{00}(M_W^2, M_{h^0}^2, M_{H^\pm}^2) \\ &\quad + 4\sin^2(\beta - \alpha) B_{00}(M_W^2, M_{H^0}^2, M_{H^\pm}^2) \\ &\quad \left. + 4B_{00}(M_W^2, M_{A^0}^2, M_{H^\pm}^2) \right]. \end{aligned} \quad (56)$$

$$\begin{aligned} \Sigma_Z]_{2\text{HDM}}^{\text{Higgs}} &= \frac{\alpha}{16\pi s_W^2 c_W^2} \left[-A_0(M_{h^0}^2) - A_0(M_{H^0}^2) \right. \\ &\quad - A_0(M_{A^0}^2) - 2(c_W^2 - s_W^2)^2 A_0(M_{H^\pm}^2) \\ &\quad + 4\cos^2(\beta - \alpha) B_{00}(M_Z^2, M_{h^0}^2, M_{A^0}^2) \\ &\quad + 4\sin^2(\beta - \alpha) B_{00}(M_Z^2, M_{H^0}^2, M_{A^0}^2) \\ &\quad \left. + 4(c_W^2 - s_W^2)^2 B_{00}(M_Z^2, M_{H^\pm}^2, M_{H^\pm}^2) \right]. \end{aligned} \quad (57)$$

– Higgs/gauge boson and Higgs/Goldstone boson contributions:

$$\begin{aligned} \Sigma_W]_{2\text{HDM}}^{\text{Higgs/gauge}} &= \\ &= \frac{\alpha}{4\pi s_W^2} \left\{ \cos^2(\beta - \alpha) \left[B_{00}(M_W^2, M_{H^0}^2, M_W^2) \right. \right. \\ &\quad - B_{00}(M_W^2, M_{h^0}^2, M_W^2) \\ &\quad - \cos^2(\beta - \alpha) M_W^2 \left[B_0(M_W^2, M_{H^0}^2, M_W^2) \right. \\ &\quad \left. \left. - B_0(M_W^2, M_{h^0}^2, M_W^2) \right] \right\}. \end{aligned} \quad (58)$$

$$\begin{aligned} \Sigma_Z]_{2\text{HDM}}^{\text{Higgs/gauge}} &= \\ &= \frac{\alpha}{4\pi s_W^2 c_W^2} \left\{ \cos^2(\beta - \alpha) \left[B_{00}(M_Z^2, M_{H^0}^2, M_Z^2) \right. \right. \\ &\quad - B_{00}(M_Z^2, M_{h^0}^2, M_Z^2) \\ &\quad - \cos^2(\beta - \alpha) M_Z^2 \left[B_0(M_Z^2, M_{H^0}^2, M_Z^2) \right. \\ &\quad \left. \left. - B_0(M_Z^2, M_{h^0}^2, M_Z^2) \right] \right\}. \end{aligned} \quad (59)$$

Let us notice that, in the last two expressions, we have explicitly removed the overlap with the SM Higgs boson contribution, to wit:

$$\begin{aligned}
\Sigma_V]_{2\text{HDM}} &\equiv \Sigma_V - \Sigma_V]_{\text{SM}} \propto \\
&\left[\cos^2(\beta - \alpha) B_{00}(M_V^2, M_{H^0}^2, M_V^2) \right. \\
&+ \sin^2(\beta - \alpha) B_{00}(M_V^2, M_{H^0}^2, M_V^2) \\
&- M_V^2 \cos^2(\beta - \alpha) B_0(M_V^2, M_{H^0}^2, M_V^2) \\
&- M_V^2 \sin^2(\beta - \alpha) B_0(M_V^2, M_{H^0}^2, M_V^2) \\
&- B_{00}(M_V^2, M_H^2, M_V^2)|_{H \equiv h^0} \\
&\left. + M_V^2 B_0(M_V^2, M_H^2, M_V^2)|_{H \equiv h^0} \right].
\end{aligned} \tag{60}$$

• **Effective Higgs/gauge boson interactions** To better illustrate how we build up in practice the effective Higgs/gauge boson couplings employed in this study, herewith we provide explicit analytical details for the construction of one of such Born-improved interactions. We carry out the calculation with the help of the standard algebraic packages FEYNARTS and FORMCALC [92, 97]. Without loss of generality, let us take the concrete case of the Z boson coupling to the \mathcal{CP} -odd and the light \mathcal{CP} -even neutral Higgs bosons $[g_{h^0 A^0 Z^0}]$. A sample of the Feynman diagrams describing the $\mathcal{O}(\lambda_5^2)$ corrections to this coupling is displayed in the upper row of Fig. 8. The general structure of the associated form factor $a_{h^0 A^0 Z^0}$ may be cast as:

$$\begin{aligned}
a_{h^0 A^0 Z^0} \Big]_{p^2=0} &= \underbrace{\Re e V_{h^0 A^0 Z^0}}_{\text{vertex}} - \underbrace{\frac{1}{2} \Re e \Sigma'_{h^0} - \frac{1}{2} \Re e \Sigma'_{A^0}}_{\text{wave-function}} \\
&\quad - \underbrace{\frac{\tan(\beta - \alpha)}{M_{H^0}^2} \Re e \hat{\Sigma}_{h^0 H^0}}_{\text{mixing}} \Big]_{p^2=0}. \tag{61}
\end{aligned}$$

Notice that we define our form factors to be real, in order to preserve the hermiticity of the Born-improved Lagrangians derived from them. The different building blocks of Eq. (61) correspond to:

a) $V_{h^0 A^0 Z^0}$, the genuine vertex corrections (cf. e.g. the first two diagrams in the upper row of Fig. 8). For illustration purposes, we provide its complete analytical form:

$$\begin{aligned}
V_{h^0 A^0 Z^0}(0) &= \frac{1}{16 \pi^2} \left\{ \lambda_{H^0 A^0 A^0} \lambda_{h^0 h^0 H^0} \tilde{C}_2(M_{A^0}^2, M_{h^0}^2, M_{H^0}^2) \right. \\
&+ \lambda_{h^0 A^0 A^0} \lambda_{h^0 A^0 A^0} \tilde{C}_1(M_{A^0}^2, M_{A^0}^2, M_{h^0}^2) \\
&- \lambda_{h^0 A^0 A^0} \lambda_{h^0 h^0 h^0} \tilde{C}_2(M_{A^0}^2, M_{h^0}^2, M_{h^0}^2) \\
&+ \tan(\beta - \alpha) \left[\lambda_{h^0 A^0 A^0} \lambda_{h^0 h^0 H^0} \tilde{C}_1(M_{A^0}^2, M_{h^0}^2, M_{H^0}^2) \right. \\
&- \lambda_{H^0 A^0 A^0} \lambda_{h^0 A^0 A^0} \tilde{C}_1(M_{A^0}^2, M_{A^0}^2, M_{H^0}^2) \\
&\left. \left. + \lambda_{H^0 A^0 A^0} \lambda_{h^0 H^0 H^0} \tilde{C}_2(M_{A^0}^2, M_{H^0}^2, M_{H^0}^2) \right] \right\}. \tag{62}
\end{aligned}$$

b) the wave-function corrections associated to each of the external Higgs boson legs (including, as we single out in the last term of Eq. (61), the $h^0 - H^0$ mixing one-loop diagrams):

$$\begin{aligned}
\Sigma'_{h^0}(0) &= \frac{1}{16 \pi^2} \left\{ \lambda_{h^0 h^0 H^0}^2 \tilde{B}'_0(M_{h^0}^2, M_{H^0}^2) \right. \\
&+ \lambda_{h^0 H^\pm H^\pm}^2 \tilde{B}'_0(M_{H^\pm}^2, M_{H^\pm}^2) + \\
&+ \frac{1}{2} \left[\lambda_{h^0 H^0 H^0}^2 \tilde{B}'_0(M_{H^0}^2, M_{H^0}^2) + \lambda_{h^0 A^0 A^0}^2 \tilde{B}'_0(M_{A^0}^2, M_{A^0}^2) \right. \\
&\left. \left. + \lambda_{h^0 h^0 h^0}^2 \tilde{B}'_0(M_{h^0}^2, M_{h^0}^2) \right] \right\}. \tag{63}
\end{aligned}$$

$$\begin{aligned}
\Sigma'_{A^0}(0) &= -\frac{1}{16 \pi^2} \left[\lambda_{h^0 A^0 A^0}^2 \tilde{B}'_0(M_{A^0}^2, M_{h^0}^2) \right. \\
&\left. + \lambda_{H^0 A^0 A^0}^2 \tilde{B}'_0(M_{H^0}^2, M_{A^0}^2) \right]. \tag{64}
\end{aligned}$$

$$\begin{aligned}
\hat{\Sigma}_{h^0 H^0}(0) &= \frac{1}{32 \pi^2} \left\{ \lambda_{H^0 A^0 A^0} \lambda_{h^0 A^0 A^0} [\tilde{B}_0(M_{A^0}^2, M_{A^0}^2) \right. \\
&- \Re e B_0(q^2, M_{A^0}^2, M_{A^0}^2)] \\
&+ \lambda_{h^0 h^0 h^0} \lambda_{h^0 h^0 H^0} [\tilde{B}_0(M_{h^0}^2, M_{h^0}^2) \\
&- \Re e B_0(q^2, M_{A^0}^2, M_{A^0}^2)] \\
&+ \lambda_{H^0 H^0 H^0} \lambda_{h^0 H^0 H^0} [B_0(0, M_{H^0}^2, M_{H^0}^2) \\
&- \Re e B_0(q^2, M_{A^0}^2, M_{A^0}^2)] \\
&+ 2 \left(\lambda_{h^0 H^0 H^0} \lambda_{h^0 h^0 H^0} [\tilde{B}_0(M_{h^0}^2, M_{H^0}^2) \right. \\
&- \Re e B_0(q^2, M_{h^0}^2, M_{H^0}^2)] \\
&+ \lambda_{h^0 H^+ H^-} \lambda_{H^0 H^+ H^-} [\tilde{B}_0(M_{H^\pm}^2, M_{H^\pm}^2) \\
&- \Re e B_0(q^2, M_{H^\pm}^2, M_{H^\pm}^2)] \left. \right\}. \tag{65}
\end{aligned}$$

In the last equation, the $h^0 - H^0$ mixing self-energy $\hat{\Sigma}_{h^0 H^0}(q^2) = \Sigma_{h^0 H^0}(q^2) + \delta Z_{h^0 H^0}(q^2 - M_{H^0}^2)/2 + \delta Z_{h^0 H^0}(q^2 - M_{h^0}^2)/2 - \delta M_{h^0 H^0}^2$ involves the renormalization of the mixing angle α , that we anchor via the relation $\Re e \hat{\Sigma}_{h^0 H^0}(q^2) = 0$ according to [67], with the renormalization scale chosen at the average mass $q^2 \equiv (M_{h^0}^2 + M_{H^0}^2)/2$. As mentioned above, the tilded Passarino-Veltman functions are evaluated at vanishing external momentum.

Let us note in passing that, for the case of the g_{hVV} -type couplings, and due to the fact that just one single scalar leg is present there, only pieces of type b) shall give rise to $\mathcal{O}(\lambda_5^2)$ contributions. The same holds as well for the Higgs/gauge/Goldstone boson couplings $[g_{hVG}]$.

References

1. J. Incandela, CERN Seminar, Update on the Standard Model Higgs searches in CMS, July, 4 2012. CMS-PAS-HIG-12-020.

2. F. Gianotti, CERN Seminar, Update on the Standard Model Higgs searches in ATLAS, July, 4 2012. ATLAS-CONF-2012-093.
3. S. Chatrchyan et al. (CMS Collaboration), Phys.Lett.B (2012), arXiv:1207.7235 [hep-ex].
4. G. Aad et al. (ATLAS Collaboration), Phys.Lett.B (2012), arXiv:1207.7214 [hep-ex].
5. P. W. Higgs, Phys. Lett. **12**, 132–133 (1964).
6. P. W. Higgs, Phys. Rev. Lett. **13**, 508–509 (1964).
7. F. Englert and R. Brout, Phys. Rev. Lett. **13**, 321–322 (1964).
8. G. S. Guralnik, C. R. Hagen and T. W. B. Kibble, Phys. Rev. Lett. **13**, 585–587 (1964).
9. J. F. Gunion, H. E. Haber, G. L. Kane and S. Dawson, *The Higgs hunter's guide*, Addison-Wesley, Menlo-Park, 1990.
10. A. Djouadi, Phys. Rept. **457**, 1–216 (2008), arXiv:hep-ph/0503172 [hep-ph].
11. P. H. Chankowski et al., Nucl. Phys. Proc. Suppl. **37B**, 232–239 (1994).
12. R. Barbieri and L. Maiani, Nucl. Phys. **B224**, 32 (1983).
13. G. C. Branco, P. M. Ferreira, L. Lavoura, M. N. Rebelo, M. Sher and J. P. Silva, Phys. Rept. **516**, 1 (2012), arXiv:1106.0034 [hep-ph].
14. S. Ferrara, editor, *Supersymmetry*, volume 1-2, North Holland/World Scientific, Singapore, 1987.
15. D. B. Kaplan, H. Georgi and S. Dimopoulos, Phys. Lett. **B136**, 187 (1984); K. Agashe, R. Contino and A. Pomarol, Nucl. Phys. **B719**, 165–187 (2005), arXiv:hep-ph/0412089; J. Mrazek et al., Nucl. Phys. **B853**, 1–48 (2011), arXiv:1105.5403 [hep-ph]; G. Burdman and C. E. F. Haluch, JHEP **12**, 038 (2011), arXiv:1109.3914 [hep-ph]; M. Geller, S. Bar-Shalom and A. Soni, arXiv:1302.2915 [hep-ph];
16. M. Schmaltz and D. Tucker-Smith, Ann. Rev. Nucl. Part. Sci. **55**, 229–270 (2005), arXiv:hep-ph/0502182; M. Perelstein, Prog. Part. Nucl. Phys. **58**, 247–291 (2007), arXiv:hep-ph/0512128.
17. J. F. Gunion and H. E. Haber, Phys. Rev. **D72**, 095002 (2005), arXiv:hep-ph/0506227; P. M. Ferreira, H. E. Haber, M. Maniatis, O. Nachtmann and J. P. Silva, Int. J. Mod. Phys. **A26**, 769–808 (2011), arXiv:1010.0935 [hep-ph].
18. E. Ma, Phys. Rev. **D73**, 077301 (2006), arXiv:hep-ph/0601225.
19. S. Kanemura, Y. Okada and E. Senaha, Phys. Lett. **B606**, 361–366 (2005), arXiv:hep-ph/0411354; J. M. Cline, K. Kainulainen and M. Trott, JHEP **1111**, 089 (2011), arXiv:1107.3559 [hep-ph]; A. Tranberg and B. Wu, JHEP **1207**, 087 (2012), arXiv:1203.5012 [hep-ph].
20. B. Stech, Phys. Rev. D **86**, 055003 (2012), arXiv:1206.4233 [hep-ph].
21. N. G. Deshpande and E. Ma, Phys. Rev. **D18**, 2574 (1978).
22. R. Barbieri, L. J. Hall and V. S. Rychkov, Phys. Rev. **D74**, 015007 (2006), arXiv:hep-ph/0603188; E. L undstrom, M. Gustafsson and J. Edsj o, Phys. Rev. **D79**, 035013 (2009), arXiv:0810.3924 [hep-ph]; A. Arhrib, R. Benbrik and N. Gaur, Phys. Rev. D85 095021 (2012), arXiv:1201.2644 [hep-ph].
23. L. L opez-Honorez, E. Nezri, J. F. Oliver and M. H. G. Tytgat, JCAP **0702**, 028 (2007), arXiv:hep-ph/0612275; T. Hambye and M. H. G. Tytgat, Phys. Lett. **B659**, 651–655 (2008), arXiv:0707.0633 [hep-ph]; L. L opez-Honorez and C. E. Yaguna, JCAP **1101**, 002 (2011), arXiv:1011.1411 [hep-ph]; M. Gustafsson, PoS **CHARGED2010**, 030 (2010); B. Gorczyca and M. Krawczyk, Acta Phys. Polon. **B42**, 2229–2236 (2011), arXiv:1112.4356 [hep-ph]; M. Krawczyk and D. Sokolowska, Fortsch. Phys. **59**, 1098–1102 (2011), arXiv:1105.5529 [hep-ph].
24. R. Schabinger and J. D. Wells, Phys. Rev. **D72**, 093007 (2005), arXiv:hep-ph/0509209; B. Patt and F. Wilczek, arXiv:hep-ph/0605188.
25. C. Englert, T. Plehn, M. Rauch, D. Zerwas and P. M. Zerwas, Phys.Lett. **B707**, 512–516 (2012), (2011), arXiv:1112.3007 [hep-ph]; C. Englert, T. Plehn, D. Zerwas and P. M. Zerwas, Phys. Lett. **B703**, 298–305 (2011), arXiv:1106.3097 [hep-ph]; B. Batell, S. Gori and L.-T. Wang, JHEP **1206**, 172 (2012), arXiv:1112.5180 [hep-ph].
26. E. Cerver o and J.-M. G erard, Phys. Lett. **B712**, 255–260 (2012), arXiv:1202.1973 [hep-ph].
27. J. S. Lee and A. Pilaftsis, Phys. Rev. D86 035004 (2012), arXiv:1201.4891 [hep-ph].
28. G. Panotopoulos and P. Tuz on, JHEP **07**, 039 (2011), arXiv:1102.5726 [hep-ph].
29. S. Bar-Shalom, S. Nandi and A. Soni, Phys. Rev. **D84**, 053009 (2011), arXiv:1105.6095 [hep-ph].
30. A. Arhrib et al., Phys. Rev. **D84**, 095005 (2011), arXiv:1105.1925 [hep-ph].
31. M. Aoki et al., Phys. Rev. **D84**, 055028 (2011), arXiv:1104.3178 [hep-ph]; S. Chang, J. A. Evans and M. A. Luty, Phys. Rev. **D84**, 095030 (2011), arXiv:1107.2398 [hep-ph]; A. Arhrib, C.-W. Chiang, D. K. Ghosh and R. Santos, (2011), arXiv:1112.5527 [hep-ph]; S. Kanemura, K. Tsumura and H. Yokoya, Phys. Rev. D85 095001 (2012), arXiv:1111.6089 [hep-ph]; K. Blum and R. T. D’Agnolo, Phys.Lett. B714 66–69 (2012), arXiv:1202.2364 [hep-ph]; W. Mader, J. -h. Park, G. M. Pruna, D. St ockinger and A. Straessner, JHEP **1209**, 125 (2012), arXiv:1205.2692 [hep-ph]; N. Craig, J. A. Evans, R. Gray, C. Kilic, M. Park, S. Somalwar and S. Thomas, arXiv:1210.0559 [hep-ph].
32. P. M. Ferreira, R. Santos, M. Sher and J. P. Silva, Phys. Rev. D **85**, 077703 (2012), arXiv:1112.3277 [hep-ph]; Phys. Rev. **D85**, 035020 (2012), arXiv:1201.0019 [hep-ph]; G. Burdman, C. E. F. Haluch and R. D. Matheus, Phys. Rev. D **85**, 095016 (2012), arXiv:1112.3961 [hep-ph]; D. Carmi, A. Falkowski, E. Kuflik and T. Volansky, JHEP **1207**, 136 (2012), arXiv:1202.3144 [hep-ph]; H. S. Cheon and S. K. Kang, arXiv:1207.1083 [hep-ph]; N. Craig and S. Thomas, arXiv:1207.4835 [hep-ph]; D. S. M. Alves, P. J. Fox and N. J. Weiner, arXiv:1207.5499 [hep-ph]; Y. Bai, V. Barger, L. L. Everett and G. Shaughnessy, arXiv:1210.4922 [hep-ph]; S. Chang, S. K. Kang, J. -P. Lee, K. Y. Lee, S. C. Park and J. Song, arXiv:1210.3439 [hep-ph]; C. -Y. Chen and S. Dawson, arXiv:1301.0309 [hep-ph].
33. W. Altmannshofer, S. Gori and G. D. Kribs, arXiv:1210.2465 [hep-ph].
34. A. Celis, V. Ilisie, and A. Pich, arXiv:1302.4022 [hep-ph].
35. W. Hollik, Fortsch. Phys. **38**, 165 (1990).
36. W. Hollik, J.Phys.G **G29**, 131–140 (2003).
37. W. Hollik, J. Phys. Conf. Ser. **53**, 7–43 (2006).

38. W. Hollik, *Renormalization of the Standard Model*, in: Precision tests of the Standard Electroweak Model, Ed. P. Langacker, Advanced Series on Directions in High Energy Physics, Vol. 14 (World Scientific, 1995).
39. J. D. Wells, [arXiv:hep-ph/0512342](#); A. Sirlin and A. Ferroglia, [arXiv:1210.5296 \[hep-ph\]](#).
40. The LEP Collaborations, the LEP Electroweak Working Group, the Tevatron Electroweak Working Group, the SLD Electroweak and Heavy Flavour Working Groups, Precision electroweak measurements and constraints on the Standard Model, CERN-PH-EP/2009-023; <http://www.cern.ch/LEPEWWG>.
41. J. Beringer et al. (Particle Data Group Collaboration), *Phys. Rev.* **D86**, 010001 (2012).
42. G. Bozzi, J. Rojo and A. Vicini, *Phys. Rev.* **D83**, 113008 (2011), [arXiv:1104.2056 \[hep-ph\]](#); C. Berniacki and D. Wackerroth, *Phys. Rev. D* **85**, 093003 (2012), [arXiv:1201.4804 \[hep-ph\]](#).
43. A. Sirlin, *Phys. Rev.* **D22**, 971–981 (1980).
44. W. J. Marciano and A. Sirlin, *Phys. Rev.* **D22**, 2695 (1980).
45. D. A. Ross and M. J. G. Veltman, *Nucl. Phys.* **B95**, 135 (1975);
46. M. J. G. Veltman, *Acta Phys. Polon.* **B8**, 475 (1977).
47. M. J. G. Veltman, *Nucl. Phys.* **B123**, 89 (1977).
48. M. B. Einhorn, D. R. T. Jones and M. J. G. Veltman, *Nucl. Phys.* **B191**, 146 (1981).
49. R. Barbieri, M. Frigeni, F. Giuliani and H. Haber, *Nucl. Phys.* **B341**, 309–321 (1990).
50. D. Garcia and J. Solà, *Mod. Phys. Lett.* **A9**, 211–224 (1994), preprint UAB-FT-313 (April 1993).
51. P. H. Chankowski et al., *Nucl. Phys.* **B417**, 101–129 (1994), preprint MPI-Ph/93-79 (November 1993).
52. P. Gosdzinsky and J. Solà, *Phys. Lett.* **B254**, 139–147 (1991).
53. P. Gosdzinsky and J. Solà, *Mod. Phys. Lett.* **A6**, 1943–1952 (1991).
54. J. Grifols and J. Solà, *Phys. Lett.* **B137**, 257 (1984).
55. J. Grifols and J. Solà, *Nucl. Phys.* **B253**, 47 (1985).
56. A. Dabelstein, W. Hollik and W. Mosle, (1995), [arXiv:hep-ph/9506251](#); S. Heinemeyer, W. Hollik, D. Stöckinger, A. M. Weber and G. Weiglein, *JHEP* **08**, 052 (2006), [arXiv:hep-ph/0604147](#); J. R. Ellis, S. Heinemeyer, K. A. Olive and G. Weiglein, (2006), [arXiv:hep-ph/0604180](#); R. Benbrik, M. G. Bock, S. Heinemeyer, O. Stål, G. Weiglein et al., (2012), [arXiv:1207.1096 \[hep-ph\]](#).
57. A. Freitas, S. Heinemeyer and G. Weiglein, *Nucl. Phys. Proc. Suppl.* **116**, 331–335 (2003), [arXiv:hep-ph/0212068](#); G. Weiglein, *Nucl. Phys. Proc. Suppl.* **160**, 185–189 (2006); J. Haestier, D. Stockinger, G. Weiglein and S. Heinemeyer, (2005), [arXiv:hep-ph/0506259](#); S. Heinemeyer and G. Weiglein, *JHEP* **10**, 072 (2002), [arXiv:hep-ph/0209305](#); S. Heinemeyer and G. Weiglein, (2001), [arXiv:hep-ph/0102317](#); J. van der Bij and M. Veltman, *Nucl. Phys.* **B231**, 205 (1984).
58. S. Heinemeyer, W. Hollik, F. Merz and S. Peñaranda, *Eur. Phys. J.* **C37**, 481–493 (2004), [arXiv:hep-ph/0403228](#); S. Peñaranda, S. Heinemeyer and W. Hollik, (2005), [arXiv:hep-ph/0506104](#).
59. J. M. Frere and J. A. M. Vermaseren, *Z. Phys. C* **19**, 63 (1983).
60. S. Bertolini, *Nucl. Phys.* **B272**, 77 (1986).
61. W. Hollik, *Z. Phys. C* **32**, 291 (1986).
62. W. Hollik, *Z. Phys. C* **37**, 569 (1988).
63. C. D. Froggatt, R. G. Moorhouse and I. G. Knowles, *Phys. Rev.* **D45**, 2471–2481 (1992).
64. H. -J. He, N. Polonsky and S. -f. Su, *Phys. Rev. D* **64**, 053004 (2001), [hep-ph/0102144](#).
65. F. Mahmoudi and O. Stål, *Phys. Rev. D* **81**, 035016 (2010), [arXiv:0907.1791 \[hep-ph\]](#).
66. A. Pich and P. Tuzón, *Phys. Rev.* **D80**, 091702 (2009), [arXiv:0908.1554 \[hep-ph\]](#); M. Jung, A. Pich and P. Tuzón, *JHEP* **11**, 003 (2010), [arXiv:1006.0470 \[hep-ph\]](#); A. J. Buras, M. V. Carlucci, S. Gori and G. Isidori, *JHEP* **10**, 009 (2010), [arXiv:1005.5310 \[hep-ph\]](#);
67. D. López-Val and J. Solà, *Phys. Rev.* **D81**, 033003 (2010), [arXiv:0908.2898 \[hep-ph\]](#).
68. R. A. Jiménez and J. Solà, *Phys. Lett.* **B389**, 53–61 (1996), [arXiv:hep-ph/9511292](#); J. A. Coarasa, R. A. Jimenez and J. Solà, *Phys. Lett.* **B389**, 312–320 (1996), [arXiv:hep-ph/9511402](#).
69. M. S. Carena and H. E. Haber, *Prog. Part. Nucl. Phys.* **50**, 63–152 (2003), [arXiv:hep-ph/0208209](#).
70. S. Heinemeyer, *Acta Phys. Polon.* **B39**, 2673–2692 (2008), [arXiv:0807.2514 \[hep-ph\]](#).
71. A. Djouadi, *Phys. Rept.* **459**, 1–241 (2008), [arXiv:hep-ph/0503173 \[hep-ph\]](#).
72. H. Flacher et al., *Eur. Phys. J.* **C60**, 543–583 (2009), [arXiv:0811.0009 \[hep-ph\]](#); S. R. Juárez, D. Morales and P. Kielanowski, (2012), [arXiv:1201.1876 \[hep-ph\]](#).
73. F. Mahmoudi, *Comput. Phys. Commun.* **178**, 745–754 (2008), [arXiv:0710.2067 \[hep-ph\]](#); F. Mahmoudi, *Comput. Phys. Commun.* **180**, 1579–1613 (2009), [arXiv:0808.3144 \[hep-ph\]](#).
74. A. W. El Kaffas, P. Osland and O. M. Ogreid, *Phys. Rev. D* **76**, 095001 (2007), [arXiv:0706.2997 \[hep-ph\]](#); A. W. El Kaffas, P. Osland and O. M. Ogreid, *Nonlin. Phenom. Complex Syst.* **10**, 347–357 (2007), [arXiv:hep-ph/0702097](#).
75. A. Azatov, S. Chang, N. Craig and J. Galloway, (2012), [arXiv:1206.1058 \[hep-ph\]](#); D. Carmi, A. Falkowski, E. Kuflik, T. Volansky and J. Zupan, (2012), [arXiv:1207.1718 \[hep-ph\]](#).
76. D. Eriksson, J. Rathsman and O. Stål, *Comput. Phys. Commun.* **181**, 189–205 (2010), [arXiv:0902.0851 \[hep-ph\]](#).
77. P. Bechtle, O. Brein, S. Heinemeyer, G. Weiglein and K. E. Williams, *Comput. Phys. Commun.* **181**, 138–167 (2010), [arXiv:0811.4169 \[hep-ph\]](#); P. Bechtle, O. Brein, S. Heinemeyer, G. Weiglein and K. E. Williams, *Comput. Phys. Commun.* **182**, 2605–2631 (2011), [arXiv:1102.1898 \[hep-ph\]](#).
78. G. Ferrera, J. Guasch, D. López-Val and J. Solà, *Phys. Lett.* **B659**, 297–307 (2008), [arXiv:0707.3162 \[hep-ph\]](#); G. Ferrera, J. Guasch, D. López-Val and J. Solà, *PoS RAD-COR2007*, 043 (2007), [arXiv:0801.3907 \[hep-ph\]](#).
79. A. Arhrib, R. Benbrik and C.-W. Chiang, *Phys. Rev.* **D77**, 115013 (2008), [arXiv:0802.0319 \[hep-ph\]](#).
80. R. N. Hodgkinson, D. López-Val and J. Solà, *Phys. Lett.* **B673**, 47–56 (2009), [arXiv:0901.2257 \[hep-ph\]](#).
81. N. Bernal, D. López-Val and J. Solà, *Phys. Lett.* **B677**, 39–47 (2009), [arXiv:0903.4978 \[hep-ph\]](#); D. López-Val and J. Solà, *Phys. Lett.* **B702**, 246–255 (2011), [arXiv:1106.3226 \[hep-ph\]](#); J. Solà and D. López-Val, *Nuovo Cim.* **C34S1**, 57–67 (2011), [arXiv:1107.1305 \[hep-ph\]](#).
82. F. Cornet and W. Hollik, *Phys. Lett.* **B669**, 58–61 (2008), [arXiv:0808.0719 \[hep-ph\]](#); E. Asakawa, D. Harada,

- S. Kanemura, Y. Okada and K. Tsumura, *Phys. Lett.* **B672**, 354–360 (2009), [arXiv:0809.0094 \[hep-ph\]](#); A. Arhrib, R. Benbrik, C.-H. Chen and R. Santos, *Phys. Rev.* **D80**, 015010 (2009), [arXiv:0901.3380 \[hep-ph\]](#); E. Asakawa, D. Harada, S. Kanemura, Y. Okada and K. Tsumura, *Phys. Rev.* **D82**, 115002 (2010), [arXiv:1009.4670 \[hep-ph\]](#).
83. A. Arhrib and G. Moultaka, *Nucl. Phys.* **B558**, 3–40 (1999), [arXiv:hep-ph/9808317](#); J. Guasch, W. Hollik and A. Kraft, *Nucl. Phys.* **B596**, 66–80 (2001).
84. D. López-Val and J. Solà, *PoS RADCOR2009*, 045 (2010), [arXiv:1001.0473 \[hep-ph\]](#); J. Solà and D. López-Val, *Fortsch. Phys.* **58**, 660–664 (2010).
85. M. Consoli, W. Hollik and F. Jegerlehner, *Phys. Lett.* **B227**, 167 (1989).
86. A. Freitas, W. Hollik, W. Walter and G. Weiglein, *Nucl. Phys.* **B632**, 189–218 (2002), [arXiv:hep-ph/0202131](#).
87. M. Awramik and M. Czakon, *Phys. Rev. Lett.* **89**, 241801 (2002), [arXiv:hep-ph/0208113](#); M. Awramik, M. Czakon, A. Onishchenko and O. Veretin, *Phys. Rev.* **D68**, 053004 (2003), [arXiv:hep-ph/0209084](#); M. Awramik and M. Czakon, *Phys. Lett.* **B568**, 48–54 (2003), [arXiv:hep-ph/0305248 \[hep-ph\]](#); M. Awramik, M. Czakon, A. Freitas and G. Weiglein, *Phys. Rev.* **D69**, 053006 (2004), [arXiv:hep-ph/0311148 \[hep-ph\]](#).
88. M. Awramik, M. Czakon, A. Freitas and G. Weiglein, *Phys. Rev.* **D69**, 053006 (2004), [arXiv:hep-ph/0311148 \[hep-ph\]](#).
89. A. Onishchenko and O. Veretin, *Phys. Lett.* **B551**, 111–114 (2003), [arXiv:hep-ph/0209010](#).
90. J. J. van der Bij, K. G. Chetyrkin, M. Faisst, G. Jikia and T. Seidensticker, *Phys. Lett.* **B498**, 156–162 (2001), [arXiv:hep-ph/0011373](#).
91. W. Grimus, L. Lavoura, O. M. Ogreid and P. Osland, *J. Phys.* **G35**, 075001 (2008), [arXiv:0711.4022 \[hep-ph\] \[hep-ph\]](#); W. Grimus, L. Lavoura, O. Ogreid and P. Osland, *Nucl. Phys.* **B801**, 81–96 (2008), [arXiv:0802.4353 \[hep-ph\]](#).
92. T. Hahn, *Comput. Phys. Commun.* **140**, 418 (2001) [[hep-ph/0012260](#)].
93. A. Djouadi and C. Verzegnassi, *Phys. Lett.* **B195**, 265 (1987); A. Djouadi, *Nuovo Cim.* **A100**, 357 (1988); B. A. Kniehl, *Nucl. Phys.* **B347**, 86–104 (1990); F. Halzen and B. A. Kniehl, *Nucl. Phys.* **B353**, 567–590 (1991); B. A. Kniehl and A. Sirlin, *Nucl. Phys.* **B371**, 141–148 (1992); B. A. Kniehl and A. Sirlin, *Phys. Rev.* **D47**, 883–893 (1993); S. Fanchiotti, B. A. Kniehl and A. Sirlin, *Phys. Rev.* **D48**, 307–331 (1993), [arXiv:hep-ph/9212285 \[hep-ph\]](#); A. Djouadi and P. Gambino, *Phys. Rev.* **D49**, 3499–3511 (1994), [arXiv:hep-ph/9309298 \[hep-ph\]](#); L. Avdeev, J. Fleischer, S. Mikhailov and O. Tarasov, *Phys. Lett.* **B336**, 560–566 (1994), [arXiv:hep-ph/9406363 \[hep-ph\]](#); K. Chetyrkin, J. H. Kuhn and M. Steinhauser, *Phys. Rev. Lett.* **75**, 3394–3397 (1995), [arXiv:hep-ph/9504413 \[hep-ph\]](#); K. Chetyrkin, J. H. Kuhn and M. Steinhauser, *Nucl. Phys.* **B482**, 213–240 (1996), [arXiv:hep-ph/9606230 \[hep-ph\]](#).
94. B. W. Lee, C. Quigg and H. B. Thacker, *Phys. Rev. Lett.* **38**, 883–885 (1977); B. W. Lee, C. Quigg and H. Thacker, *Phys. Rev.* **D16**, 1519 (1977).
95. A. Arhrib, (2000), [arXiv:hep-ph/0012353](#); A. G. Akeroyd, A. Arhrib and E.-M. Naimi, *Phys. Lett. B* **490**, 119 (2000) [[hep-ph/0006035](#)]; S. Kanemura, T. Kubota and E. Takasugi, *Phys. Lett.* **B313**, 155–160 (1993), [arXiv:hep-ph/9303263](#);
- J. Maalampi, J. Sirkka and I. Vilja, *Phys. Lett.* **B265**, 371–376 (1991); A. G. Akeroyd, A. Arhrib and E.-M. Naimi, *Phys. Lett.* **B490**, 119–124 (2000), [arXiv:hep-ph/0006035](#); I. F. Ginzburg and I. P. Ivanov, *Phys. Rev.* **D72**, 115010 (2005), [arXiv:hep-ph/0508020](#); P. Osland, P. N. Pandita and L. Selbuz, *Phys. Rev.* **D78**, 015003 (2008), [arXiv:0802.0060 \[hep-ph\] \[hep-ph\]](#).
96. G. 't Hooft and M. Veltman, *Nucl. Phys.* **B44**, 189–213 (1972).
97. T. Hahn and M. Pérez-Victoria, *Comput. Phys. Commun.* **118**, 153–165 (1999), [arXiv:hep-ph/9807565](#); T. Hahn and M. Rauch, *Nucl. Phys. Proc. Suppl.* **157**, 236–240 (2006), [arXiv:hep-ph/0601248 \[hep-ph\]](#).
98. M. Frank et al., *JHEP* **02**, 047 (2007), [arXiv:hep-ph/0611326](#); G. Degrossi, S. Heinemeyer, W. Hollik, P. Slavich and G. Weiglein, *Eur. Phys. J.* **C28**, 133–143 (2003), [arXiv:hep-ph/0212020](#); S. Heinemeyer, W. Hollik and G. Weiglein, *Eur. Phys. J.* **C9**, 343–366 (1999), [arXiv:hep-ph/9812472](#); S. Heinemeyer, W. Hollik and G. Weiglein, *Comput. Phys. Commun.* **124**, 76–89 (2000), [arXiv:hep-ph/9812320](#).
99. A. Arbey, M. Battaglia, A. Djouadi and F. Mahmoudi, (2012), [arXiv:1207.1348 \[hep-ph\]](#).
100. Tevatron Electroweak Working Group and CDF and D0 Collaborations, FERMILAB-TM-2504-E, CDF-NOTE-10549, D0-NOTE-6222 [arXiv:1107.5255 \[hep-ex\]](#).
101. M. Awramik and M. Czakon, *Nucl. Phys. Proc. Suppl.* **116**, 238–242 (2003), [arXiv:hep-ph/0211041 \[hep-ph\]](#).
102. A. Freitas, W. Hollik, W. Walter and G. Weiglein, *Phys. Lett.* **B495**, 338–346 (2000), [arXiv:hep-ph/0007091 \[hep-ph\]](#).
103. M. Faisst, J. H. Kuhn, T. Seidensticker and O. Veretin, *Nucl. Phys.* **B665**, 649–662 (2003), [arXiv:hep-ph/0302275](#).
104. R. Boughezal, J. B. Tausk and J. J. van der Bij, *Nucl. Phys.* **B713**, 278–290 (2005), [arXiv:hep-ph/0410216](#); Y. Schroder and M. Steinhauser, *Phys. Lett.* **B622**, 124–130 (2005), [arXiv:hep-ph/0504055](#); K. G. Chetyrkin, M. Faisst, J. H. Kuhn, P. Maierhofer and C. Sturm, *Phys. Rev. Lett.* **97**, 102003 (2006), [arXiv:hep-ph/0605201](#); R. Boughezal and M. Czakon, *Nucl. Phys.* **B755**, 221–238 (2006), [arXiv:hep-ph/0606232](#).
105. O. Buchmüller, R. Cavanaugh, A. De Roeck, J. Ellis, H. Flacher et al., *Phys. Rev.* **D81**, 035009 (2010), [arXiv:0912.1036 \[hep-ph\]](#).
106. J. A. Evans and M. A. Luty, *Phys. Rev. Lett.* **103**, 101801 (2009), [arXiv:0904.2182 \[hep-ph\]](#).
107. J. A. Coarasa, D. Garcia, J. Guasch, R. A. Jiménez and J. Solà, *Eur. Phys. J.* **C2**, 373–392 (1998), [arXiv:hep-ph/9607485](#).
108. M. S. Carena, D. Garcia, U. Nierste and C. E. M. Wagner, *Nucl. Phys.* **B577**, 88–120 (2000), [arXiv:hep-ph/9912516](#); J. Guasch, J. Solà and W. Hollik, *Phys. Lett.* **B437**, 88–99 (1998), [arXiv:hep-ph/9802329](#); A. Belyaev, D. Garcia, J. Guasch and J. Solà, *Phys. Rev.* **D65**, 031701 (2002), [arXiv:hep-ph/0105053](#); S. Béjar, J. Guasch, D. López-Val and J. Solà, *Phys. Lett.* **B668**, 364–372 (2008), [arXiv:0805.0973 \[hep-ph\]](#); *Phys. Rev.* **D81**, 113005 (2010), [arXiv:1003.4312 \[hep-ph\]](#).